Mechanisms of MLL Fusion Protein-Mediated Leukemic Transformation

by

Sara C. Monroe

A dissertation submitted in partial fulfillment
of the requirements for the degree of
Doctor of Philosophy
(Molecular and Cellular Pathology)
in the University of Michigan
2010

Doctoral Committee:

    Professor Jay L. Hess, Chair
    Professor Gregory R. Dressler
    Professor James Douglas Engel
    Professor Gabriel Nunez
    Assistant Professor Daniel A. Bochar

To children with cancer.

Acknowledgments

I would like to thank my mentor Jay Hess for his guidance, encouragement, and undying patience throughout the ups, downs, and stumps of my graduate school career and for also recruiting a lab team full of friendly, helpful, thoughtful, and knowledgeable people. I thank all the current and past members of the Hess lab for their feedback and kind gestures including Joel Bronstein, Corrado Caslini, Jim Connelly, Brendan Crawford, Monisha Dandekar, Diane Giannola, Eric Granowicz, Yongsheng Huang, Stephanie Jo, Andrew Muntean, Surya Nagaraja, Daniel Sanders, Kajal Sitwala, Jane Tan, and Jingya Wang. I am grateful to Lynn McCain for help with manuscript preparations and Dave Austin, Todd Kandow, Tom Peterson, and Tim Sikora of Pathology Data Systems for the computer help. I also thank my committee members, Drs. Doug Engel, Greg Dressler, Dan Bochar, and Gabriel Nunez for all of their valuable insight and suggestions. Thank you to our enthusiastic student service representative Laura Hessler, who has been my go-to for every issue or question I have had during graduate school. Thank you to our former and current program directors, Drs. Sem Phan and Nick Lukacs, respectively for helping me develop my scientific career by establishing a comprehensive graduate program. I thank Drs. Yali Dou, Zaneta Nikolovska-Coleska, Jolanta Grembecka, Tomasz Cierpicki, and their labs for sharing their input at lab meetings and the

Preface

Leukemia is responsible for the majority of cancer-related deaths among people under the age of 20 [1]. A subset of particularly aggressive leukemias carry genomic rearrangements of the *Mixed Lineage Leukemia* (*MLL*) gene, and these leukemias are generally associated with poor clinical outcome [2]. *MLL* rearrangements are mainly found in the form of internal gene amplifications and chromosomal translocations, which result in the in-frame fusion of the N-terminus of MLL with one of a variety of different fusion partners. Although significant progress has been made towards understanding how different domains of MLL and its fusion partners contribute to leukemogenesis, there is still much to understand in order to effectively treat patients that are afflicted with *MLL* rearrangements. The aim of this project was to further elucidate the mechanisms of MLL fusion protein-mediated leukemogenesis with a focus on the contribution of the fusion partners.

Table of Contents

List of Figures

List of Tables

List of Abbreviations

CDK, cyclin dependent kinase; ChIP, chromatin immunoprecipitation; CtBP, C-terminal Binding Protein; CTD, carboxy-terminal domain; EAP, Elongation Assisting Proteins or ENL-associated Proteins; HAT, histone acetyl transferase; HD, homeodomain; HLMT, histone lysine methyl transferase; MLL, Mixed Lineage Leukemia; NPM, Nucleophosmin; PMA, phorbol 12-myristate 13-acetate; AEP, AF4 family/ENL family/pTEFb; HMBA, hexamethylene bisacetamide; PHD, plant homeodomain; MOF, males absent on the first; G-CSF, granulocyte colony-stimulating factor; RBbP, Rb binding protein; IL, interleukin; LPS, lipopolysaccharide; DNMT, DNA methyl transferase; HDAC, histone deacetylase; CBP, Creb-binding protein; SET, Su(var), Enhancer of zeste, Trithorax; NURF, nucleosome remodeling factor; TAF, template activating factor; TIF, transcription intermediary factor; YEATS, (Yaf9, ENL, AF9, Taf14, Sas5); FMR2, fragile x mental retardation 2; FLT, FMS-like tyrosine kinase; DRB, 5,6-Dichloro-1-β-D-ribofuranosylbenzimidazole; NuRD, nucleosome remodeling and deacetylase; PAFc, polymerase associated factor complex

Abstract

Leukemogenic MLL fusion proteins, including MLL-AF4, MLL-AF9, and MLL-ENL, transform through up regulated expression of *HOX* genes and the HOX cofactor *MEIS1*. How they lead to the aberrant activation of these genes is not completely understood. In this study, we identified proteins recruited by one of the most common MLL fusion proteins, MLL-AF9, through purification of proteins that interact with the transforming domain of AF9 in myeloblastic M1 cells. Consistent with earlier purifications of ENL and AF4 from 293 cells, the 90 amino acid C-terminal domain associates with many of the most common MLL translocation partners including Enl, Af4, Laf4, Af5q31 and Af10. This complex, previously termed EAP for Elongation Assisting Proteins, contains the RNA polymerase II C-terminal domain kinase Cdk9/Cyclin T1/T2 (pTEFb), the histone H3 lysine 79 methyltransferase Dot1l, and the Polycomb proteins Pc3 and Ring1b. Chromatin immunoprecipitation (ChIP) studies show that myeloid cells transformed by MLL fusion proteins show higher levels and a broader distribution of EAP components at leukemogenic loci. Inhibition of EAP components pTEFb and Dot1l show that both contribute significantly to activation of *Hoxa9* and *Meis1* expression. EAP is dynamically associated with the *Hoxa9* and *Meis1* loci in hematopoietic cells and rapidly dissociates during induction of differentiation. However, in the presence of MLL fusion proteins, EAP dissociation from target loci is prevented. These data suggest that MLL fusion proteins deregulate key target genes by excessive recruitment and impaired dissociation of EAP from target loci.

Chapter 1

Introduction

Chromatin Structure in the Regulation of Transcription

DNA is spooled around histone octamers, known as nucleosomes, which contain two copies of histone 2A, 2B, 3, and 4 [3]. Nucleosomal structure is modified in different ways in order to compact or loosen DNA during transcriptional repression or activation, respectively. It may be altered through ATP-dependent processes, such as nucleosome sliding, eviction, and histone dimer exchange [4], or through post-translational modifications (PTMs) of the protruding histone tails and globular domain [5].

The level of transcriptional control conferred by the structure of chromatin accounts for how cells with the same DNA sequence can form complex organisms. It has also become clear over the past decade that the aberrant regulation of chromatin remodeling processes has critical roles in the development of cancer and many other pathological conditions [6,7,8,9,10,11]. There are several different enzymes that act on histones, including methyl transferases, kinases, ubiquitin ligases, and acetylases, and their activities serve as indicators of transcriptional status [5]. For instance, histone acetylation is generally associated with transcriptional activation, while histone deacetylation is associated with transcriptional repression. Histone lysine methyl transferases

(HLMTs), which are the primary focus of the work presented herein, methylate specific residues on histones. Histone methylation marks are associated with expressed or silenced genes, depending on which residue is methylated [5]. Mixed Lineage Leukemia is among the HLMTs, with many other roles in regulating chromatin structure.

Mixed Lineage Leukemia

Mixed Lineage Leukemia (MLL) is a 3,969 amino acid transcription factor that has multiple functional domains (Fig. 1). At its N-terminus, MLL has DNA binding domains, including three AT hooks and a DNA methyl transferase homology region that binds unmethylated DNA [12,13] and transcriptional repressors such as Bmi1, histone deacetylases (HDACs) 1 and 2, and C-terminal Binding Protein (CtBP) [14]. Downstream are three canonical plant homeodomain (PHD) fingers, a bromodomain, and one extended PHD. PHD3 of MLL binds trimethylated lysine 4 of histone 3 (H3K4me3) [15] as well as the transcriptionally repressive proline isomerase Cyp33 [16,17]. Downstream is a transcriptional transactivation domain that interacts with the acetyl transferase Creb-binding protein (CBP) [18]. The C-terminus interacts with the histone acetyl transferase (HAT) MOF, which acetylates lysine 16 of histone 4 to activate transcription [19]. MLL has a highly conserved SET domain at its C-terminus that confers MLL with an enzymatic ability to methylate the lysine 4 residue of histone 3 (H3K4) [20]. The SET domain also interacts with INI1, a component of the SWI/SNF chromatin remodeling complex [21]. The SWI/SNF complex is comprised of 8 to14 subunits, with the ATPase BRG1 or hBRM at its core [22].

Although BRG1 and hBRM are sufficient to disrupt nucleosomal structure, associating proteins such as INI1 enhance their enzymatic activity and contribute to gene specificity [22]. Thus, MLL operates on many different levels to regulate transcription.
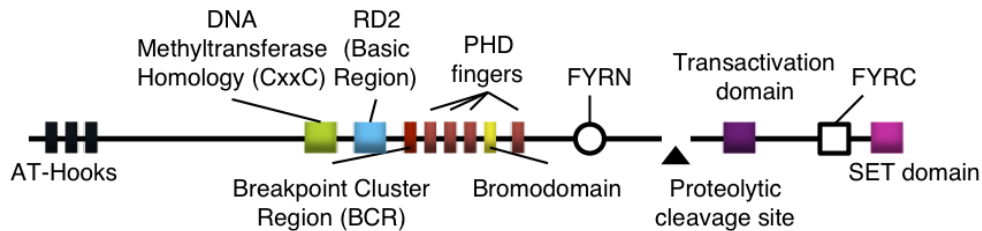
Figure 1 Schematic of wild-type MLL protein

Although there are reports that MLL represses transcription through its DNMT domain and third PHD finger [16,23,24,25,26], it is largely characterized as a transcriptional activator. In fact, the DNMT domain and third PHD finger also have roles in MLL-mediated transcriptional activation [13,15]. MLL regulates the expression of many genes, but some of the most notable in the context of both embryonic development and leukemogenesis are *Hox* genes and Hox cofactors [20,27,28].

HOX genes

HOX genes encode a conserved family of transcription factors that are critical in axis specification during embryonic development [29]. In mammalian cells, they exist in four clusters, *A*, *B*, *C*, and *D*, on four different chromosomes. HOX proteins contain homeodomains that bind DNA with poor sequence

3

specificity; further DNA specificity is conferred by their cofactors MEIS and PBX, which also have homeodomains. HOX proteins can activate or repress transcription, depending on the ternary structure that is created with its cofactors and DNA [30]. They also bind DNA replication origins and are thought to be involved in the deregulation of DNA replication in cancers [31].

The *A* cluster *HOX* genes such as *HOXA7*, *HOXA9*, and *HOXA10* are over-expressed in many cases of acute leukemia, and *HOXA* over-expression is a poor prognostic factor [32,33,34]. Normally, the expression of these genes is tightly controlled at the transcriptional, post-transcriptional, and post-translational levels. They are highly transcribed in primitive hematopoietic cells, and transcription levels decrease with differentiation [29]. HOX transcripts are targeted by microRNAs [35], and the proteins are subjected to proteasomal degradation [36] and post-translational modifications that modulate DNA binding [37,38]. The necessity for all these layers of regulation may be explained by the potency of these proteins, which is demonstrated by the fact that over-expression of *Hoxa9* and its cofactor, *Meis1*, is sufficient to transform hematopoietic cells and lead to leukemia in mice [39]. The combination of Hoxa9 and Meis1 induces a stem-cell like gene expression program that enhances proliferation and imposes a differentiation block [39,40,41].

Mll and *Hox* gene expression

The importance of Mll in regulating *Hox* expression is demonstrated in *Mll*-knockout mice [28]. Homozygous mice die at day ten of embryogenesis, and heterozygous mice display skeletal and hematopoietic defects. These

4

phenotypes are associated with severe deficiencies in *Hox* expression. Subsequent studies have shown that MLL directly binds to the *Hox* and *Meis* loci and activates their transcription through its methyl transferase activity [20].

Mice expressing truncated Mll, which lacks the SET domain and hence its methyl transferase activity display a phenotype mildly reminiscent of the *Mll* knockout mice [42]. These mice are viable, with slight skeletal malformations. They have decreased *Hox* expression that correlates with decreases in H3K4 monomethylation and increases in DNA methylation at their loci. Thus, while the methyl transferase domain of MLL is important for transcription, it is dispensable for viability. Not surprisingly, MLL has roles beyond its methyl transferase activity that are critical to survival.

MLL fusion proteins in leukemia

Rearrangements of the *MLL* gene in the form of translocations is found in up to 10% of human leukemia cases. These events are associated with acute lymphocytic, myeloid, and therapy-related leukemias that generally have a poor prognosis [2,43]. The translocations lead to the production of an in-frame fusion protein where a small portion of the N-terminus of MLL is fused to one of over fifty possible fusion partners. The most common fusion proteins are MLL-AF4, MLL-AF9, and MLL-ENL. Knock-in murine and other transformation models have shown that all three of these fusion proteins are leukemogenic, with characteristic over-expression of *Hox* genes [44,45,46,47,48,49,50]. This accurately portrays the human disease, where leukemias carrying MLL fusions have distinctly high levels of *HOX* and the HOX cofactor *MEIS1* [51]. Furthermore, *Hoxa9* and *Meis1*

are essential for leukemic transformation by MLL-AF9 and MLL-ENL in murine leukemogenesis assays [52], and HOXA9 is also critical to human leukemia cell lines that carry these translocations [40].

There are many interesting aspects of MLL fusion proteins that contribute to transformation. The N-terminus interacts with menin and the polymerase associated factor complex (PAFc). These interactions are important for targeting MLL and MLL fusion proteins to genes and for MLL fusion protein-mediated leukemogenesis [53,54,55,56,57]. Menin, originally identified as a tumor suppressor in multiple endocrine neoplasias [58] also recruits LEDGF, a chromatin-associating protein with roles in transcriptional activation [54]. PAFc, which is composed of five subunits, has roles in both the initiation and elongation stages of RNA polymerase II activity [59]. PAFc is critical for histone 2B monoubiquitination, which is a prerequisite for H3K4 and H3K79 methylation [60,61,62]. The DNMT domain of N-terminal MLL has been shown to bind CpG rich regions in DNA, physically protecting *Hox* genes from DNA methylation-mediated gene silencing [13]. The C-terminal fusion partners have little homology between each other but have been grouped into two categories: nuclear and cytoplasmic partners.

The cytoplasmic partners, such as AF1p and GAS7, are found only in a minority of *MLL* rearrangements. These proteins, which do not have known nuclear functions, appear to cause dimerization of the fusion protein, which is sufficient to cause leukemic transformation [63,64]. The dimerization-based mode of transformation is illustrated in a transgenic mouse that expresses MLL

fused to beta-galactosidase, an arbitrary, tetramerizing protein, and develops leukemia [65]. However, dimerization-based leukemia has a long latency and low penetrance compared to leukemia induced by MLL fusions with nuclear partners.

The nuclear fusion partners, AF4, AF9, and ENL are by far the most common and are transcriptional activators [66,67,68]. MLL-ENL and MLL-AF9 have been shown to require the transactivation domains of their respective partners for transformation [66]. These fusion proteins result in acute lymphocytic and myeloid leukemias that develop within three months, with most mice succumbing to the disease within a year [44,46].

MLL fusion proteins bind across transcriptionally active genes and are associated with chromatin modifications indicative of active transcription, such as H3 and H4 acetylation, H3K4 methylation, and H3K79 methylation [69]. These marks are induced by the dimerization and transactivation-based modes of transcription. However, MLL fusion proteins do not possess the transactivation and SET domains of wild-type MLL that are associated with some of these chromatin modifications. The following studies explored whether these domains are important to MLL fusion protein activity and how MLL fusion proteins establish or compensate for them.

Chapter 2

The Role of Wildtype Mll in MLL Fusion Protein-Mediated Leukemogenesis

Introduction

Both MLL fusion proteins and wild-type MLL function as transcriptional activators of *Hox* expression. In almost all cases of leukemia with *MLL* translocations, the expression of wild-type *MLL* is retained. In fact, increased levels of wild-type Mll co-localize with MLL fusions at target genes such as *Hoxa9* and *Meis1* [69]. This suggests that wild-type MLL may have a role in MLL fusion-mediated leukemogenesis. Wild-type MLL has H3K4 methyltransferase activity through its SET domain [20] as well as the ability to interact with the HATs CBP and MOF [19], and these activities are associated with transcriptional activation of *Hox* genes. MLL fusion proteins have lost these domains in the translocation event. Thus, one possibility is that wild-type Mll is critical to MLL fusion protein-induced transformation through its HAT and HMT functions. Another possibility is that MLL fusion proteins implement alternative mechanisms to recruit HMT, HAT, or other chromatin modifying-activities. We first explored the role of wild-type Mll in MLL-AF9-transformed myeloblasts, and in our experimental system, found that loss of wild-type Mll does not have a discernable effect on the phenotype of MLL-AF9 transformed cells.

Materials and Methods

Cell Lines MLL-AF9 and HOXA9/MEIS1 transformed myeloblast cell lines that have exons three and four of both *Mll* alleles flanked by *loxp* sites (Fig. 2.1, *Mll-loxp* cells from Patricia Ernst) were obtained from Mary Ellen Martin in Jay Hess's lab (UPenn).
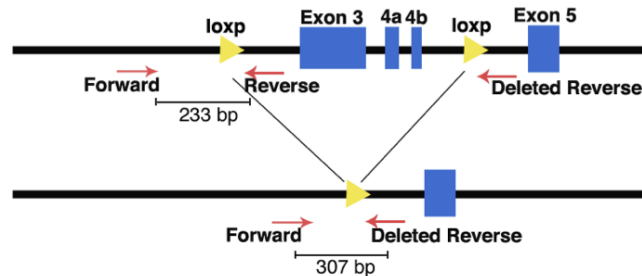
Figure 2.1 Schematic of floxed *Mll* alleles Red arrows indicate primers used for genotyping. Size of amplified fragment is indicated below.

MSCV-*Cre-ER*-puro (from Charles Roberts) was packaged into retrovirus using the Plat-E cell line. The *Mll*-floxed hematopoietic progenitor cells were then transduced by spinoculation with *Cre-ER* retrovirus for 90 minutes at 2500 RPM, 25°C in an Eppendorf 5810 R centrifuge. *MLL-AF9, Cre-ER* transduced cells were selected with 625 nM puromycin and then single-cell sorted to obtain monoclonal cell lines. *HOXA9/MEIS1, Cre-ER* transduced cells were single cell sorted and screened by genotyping (see below) after 4-hydroxytamoxifen treatment, as *MEIS1* is in the MSCV-puro vector. MLL-AF9 and HOXA9/MEIS1 transformed cells were treated with 25 nM and 100 nM 4-hydroxytamoxifen (Sigma), respectively, in order to activate Cre recombinase. All cells were grown

in IMDM (Invitrogen) with 15% FBS (Stem Cell Technologies) and 10 ng/mL IL-3. 293 cells were maintained in DMEM with 10% FBS.

Genotyping Primers used for detection of *Mll* after Cre-mediated excised are 5'-GATTGGCCAATGTCTCGTAGTAGGC-3' (forward) and 5'-CAGTGGACATTCCAACTCTTCAA-3' (reverse). Primers used for detection of in tact *Mll* use the same forward primer, but the reverse primer 5'-CACCCAGCATTGCAGAGTCAG-3'. All three primers were used in the same PCR reaction using an annealing temperature of 58°C. Products were run on 3% agarose (Invitrogen) gels and visualized with ethidium bromide.

Chromatin Immunoprecipitation Chromatin immunoprecipitation (ChIP) was performed according to Upstate's protocol using their recommended lysis, dilution, and wash buffers. In brief, cells were fixed in 1% formaldehyde for 15 minutes at room temperature. Cells were pelleted, PBS-rinsed, and snap frozen. After thawing, cells were lysed and sonicated at high intensity 30 second on-off cycles for 15 minutes in the Diagenode Bioruptor XL. These conditions generated an average DNA fragment size of 500 bp as determined by DNA electrophoresis. Protein-DNA complexes were collected using anti-MLL[C] (from Yali Dou), anti-trimethyl-H3K4 (Millipore, 04-745), or anti-AF9 (Bethyl, A300-597A)-conjugated Protein G Dynabeads. After washing the beads, DNA was eluted by incubation with SDS buffer (1% SDS, 100 mM sodium bicarbonate) for 30 minutes at 42ºC. DNA-protein cross-links were reversed overnight in 0.2 M NaCl at 65°C. DNA was purified using the QIAquick PCR Purification Kit (Qiagen) and subjected to qPCR.

Morphology Staining After 4-hydroxytamoxifen treatment, cells were stained with HEMA-3 stain kit (Fisher Scientific) according to the manufacturer's instructions.

Cell Growth Cells were seeded at a density of 10^5 cells/mL in 8 mL of growth media and counted each day using Trypan blue (Invitrogen) exclusion.

Flow Cytometric Analysis Cells were harvested, washed with PBS, and stained for 30 minutes with anti-c-Kit-FITC (BD Pharmingen), anti-Mac1-PE, and anti-Gr-1-FITC (BD Pharmingen. Cells were washed with PBS two times, filtered into flow cytometry polystyrene tubes with strainer caps, and flow cytometry was performed at the University of Michigan Flow Cytometry Core. Data were analyzed using WinList 3.0 software.

qPCR *Hoxa9* and *Meis1* expression and ChIPed DNA were detected using Taqman primers (Applied Biosystems) using Applied Biosystems 7500 Real-Time PCR system. Expression was normalized to *Gapdh* (Applied Biosystems). and analyzed using the ΔC^t method [70]. Data is expressed as percent of total input using the formula % Total Input = 2^-[Ct (IP)-Ct (Input)] [71]. Primer and probe sequences used in ChIP experiments are provided in Table 2.1.

Primer	Taqman Probe	Forward	Reverse
1	CCTGCGGTGGCAACCTCAGATCC	GCCATCAAGGCCTAATCGTG	AAGACCCGAAGCTCCTCCTG
2	CCCACATCGAGGGCAGGAAACACT	CACCCGCGGCGTCTT	CGAACCAATGGATCTGGCA
3	TGAATTTTCCCCCTTTTGGGCCAC	TAGACTCACAAGGACAATATCTCCTTTT	AGGTACTGAGTATTAAGCAGCTGTTTACA
4	CCACCGCCCCTCCCATTAACAACA	CTGTTGCTTTGTGTTCCAGATTG	AAGTGAGAAGGCCACAGCCA
5	CCTCTTGATGTTGACTGGCGATTTTCCC	TGACCCCTCAGCAAGACAAAC	TCCCGCTCCCCAGACTG
6	AAGCGCCTGGCTGGCTTTCCA	AGGGTGATCTGGCCGATGT	AAAATGGGCTACCGACCCTAGT
7	TGTTGGTCGCTCCTGACTTTCCACC	CACAGCGAGGCAAACGAAT	TTATTGTTTCGGAAGCCACACA
8	ATTATGACTGCAAAACACCGGGCCATT	CGCGATCCCTTTGCATAAAA	CGTAAATCACTCCGCACGCT
9	CTTCAGTCCTTGCAGCTTCCAGTCCAA	CAGCTCTGGCCGAACACC	TTCCACGAGGCACCAAACA
10	TACCCTCCAGCCGGCCTTATGGC	GGTGCGCTCTCCTTCGC	GCATAGTCAGTCAGGGACAAAGTGT
11	CCAACTGGCTACATGCTCGCTCCA	TCTCTCTCCCTCCGCAGATAAC	GGGCATCGCTTCTTCCG
Meis1 (Promoter)	CGATTTATTTCAAGCGTCC	TCTGCCTGCCCTACGTTTATTC	TTCCAGCCTCTCTTCCCAAA
Meis1 (Coding)	ACCGGTCCACCACCTGAACCACG	GCATGCAGCCAGGTCCAT	TAAAGCGTCATTGACCGAGGA
hHoxa9-1	N/A	CAAATCGCATTGTCGCTCTA	CCGCAGGGATTATTTACAGG
hHoxa9-2	N/A	CGACCCACGGAAATTATGAA	TGCAAAACATCGGACCATTA

Table 2.1 Primers and Probes for ChIP

Results

Disruption of wild-type *Mll*

Conditional *Mll* knock-out cells that have exons three and four of both *Mll* alleles flanked by *loxp* sites (Fig. 2.1) have previously been utilized to study the role of wild-type Mll in normal hematopoeisis [27,72]. After Cre recombinase-mediated excision of exons three and four of *Mll*, the gene encodes a hypomorphic Mll protein that lacks 1000 residues at the N-terminus, including the AT hooks and subnuclear and nuclear targeting motifs. Hematopoietic cells with *Mll* disrupted by this method have reductions in *Hox* expression and lose the ability to reconstitute blood and bone marrow in recipient mice.

We transformed hematopoietic progenitor cells isolated from these conditional *Mll*-/- mice with MLL-AF9 or a combination of HOXA9 and MEIS1 to test the importance and specificity of wild-type Mll to MLL fusion protein-mediated leukemic transformation. Complete excision of wild-type *Mll* could not be achieved in the polyclonal pool of drug-selected Cre-ER positive cells. Thus, four monoclonal cell lines stably expressing Cre-ER were established and treated with 4-hydroxytamoxifen. To follow Cre activity, the cells were genotyped after ethanol or 4-hydroxytamoxifen treatment using PCR primers that amplify in tact or disrupted *Mll* (Fig. 2.1). In the HOXA9/MEIS1 transformed cells, complete excision of *Mll* was detected after 24 hours of treatment with 100 nM 4-hydroxytamoxifen (Fig. 2.2, bottom). Non-floxed MLL-AF9 transformed cells were sensitive to the toxicity of 4-hydroxytamoxifen, and complete disruption of *Mll* in

these cells was achieved after five days of treatment with 25 nM 4-

hydroxytamoxifen (Fig. 2.2, top).

MLL-AF9-transformed Clones

Clone Number	1	2	7	C
Tamoxifen	- +	- +	- +	- +

307 →
233 →

Hoxa9/Meis1-transformed Clones

Clone Number	56	58	60
Tamoxifen	- +	- +	- +

307 →
233 →
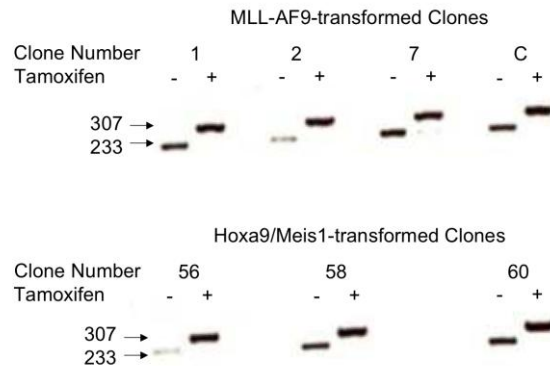
Figure 2.2 Genotyping results after 4-hydroxytamoxifen treatment Monoclonal MLL-AF9-transformed (top) or Hoxa9/Meis1-transformed (bottom) cell lines treated with ethanol (-) or 4-hydroxytamoxifen (+).

To ensure that *Mll* disruption resulted in loss of functional Mll protein,

chromatin immunoprecipation (ChIP) followed by q-PCR was performed to detect

wild-type Mll and its associated chromatin modification, H3K4 trimethylation, at

target loci in MLL-AF9 transformed cells (Fig. 2.3). In cells with the wild-type *Mll*

alleles disrupted, a three-fold reduction of Mll binding was observed at the *Hoxa9*

locus. However, no changes in H3K4 trimethylation were seen after two weeks of

excision.

Using an AF9 antibody that recognizes both endogenous Af9 and MLL-

AF9, we looked at binding of AF9 and MLL-AF9 after *Mll* disruption (Fig. 2.4).

Interestingly, a decrease in binding by one or both of these proteins was

detected, suggesting there may be a link between wild-type Mll and the fusion

protein and/or the fusion partner.
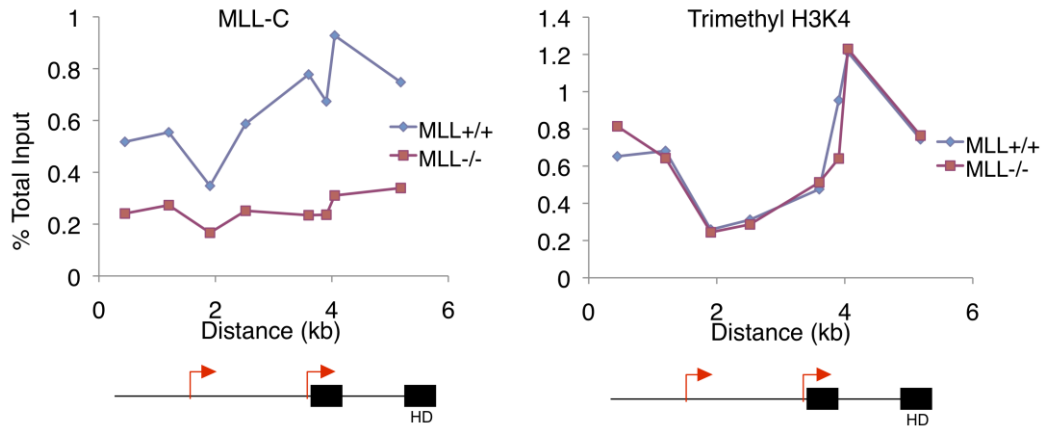
Figure 2.3 Effects of *Mll* disruption on Mll and H3K4 trimethylation levels at *Hoxa9* ChIP-qPCR for Mll (left) and H3K4 trimethylation in *Mll+/+* and *Mll-/-* cells. Schematics of *Hoxa9* are depicted below the graphs, with red arrows indicating transcription start sites and black boxes indicating exons. HD is the homeodomain-encoding exon. This experiment was performed once.
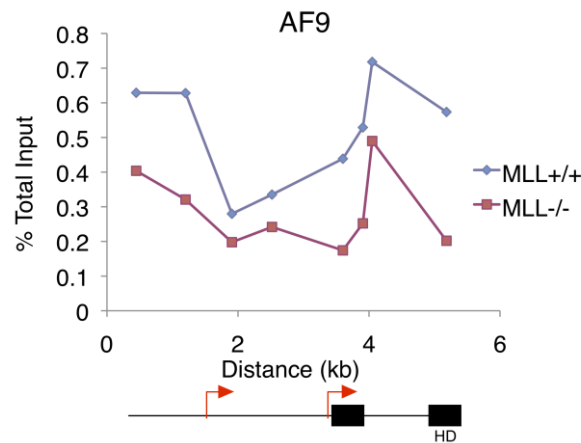
Figure 2.4 Effects of *Mll* disruption on Af9 at *Hoxa9* ChIP-qPCR for Af9 at *Hoxa9* in *Mll+/+* and *Mll-/-* cells Schematics of *Hoxa9* are depicted below the graphs, with red arrows indicating transcription start sites and black boxes indicating exons. HD is the homeodomain-encoding exon. This experiment was performed once.

We also looked at another target of Mll, *Meis1*, and similar results were observed, with decreases in Mll and Af9 binding, but no change in H3K4 trimethylation (Fig. 2.5).

15
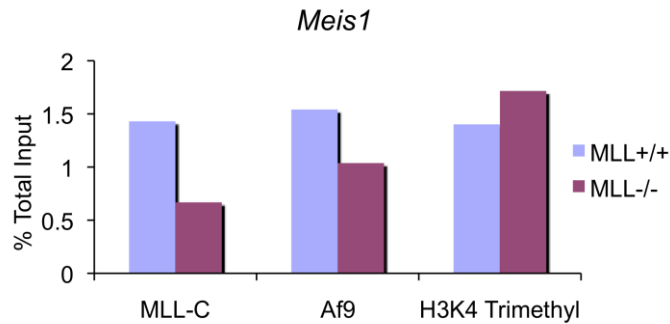
Figure 2.5 Mll-C, Af9, and trimethylated H3K4 levels at *Meis1* ChIP-qPCR in the coding region of *Meis1* in *Mll+/+* and *Mll-/-* cells. Antibodies used for ChIP are indicated below the graph. This experiment was performed once.

MLL-AF9 transformed cells do not require wild-type MLL

Both the HOXA9/MEIS1 and MLL-AF9 transformed cells continued to grow in the presence of 4-hydroxytamoxifen, and a dramatic effect of disrupting wild-type *Mll* was not observed. However, we continued to analyze the cells to determine whether loss of wild-type MLL had an effect on any aspect of the leukemic phenotype. The morphology, growth, cell surface markers, and gene expression levels of cells with and without functional wild-type Mll were compared in four monoclonal cell lines. As shown below in representative experiments, no significant differences were observed in the morphology, growth, immunophenotype, or gene expression of the monoclonal cell lines after *Mll* disruption (Fig. 2.6A-D). The only exception was an increased expression of *Meis1* found in Clone 1 (Fig. 2.6, right). Since this was not observed in the other three clones, it is thought to be a quirk of Clone 1 rather than a representative result of *Mll* loss.

16
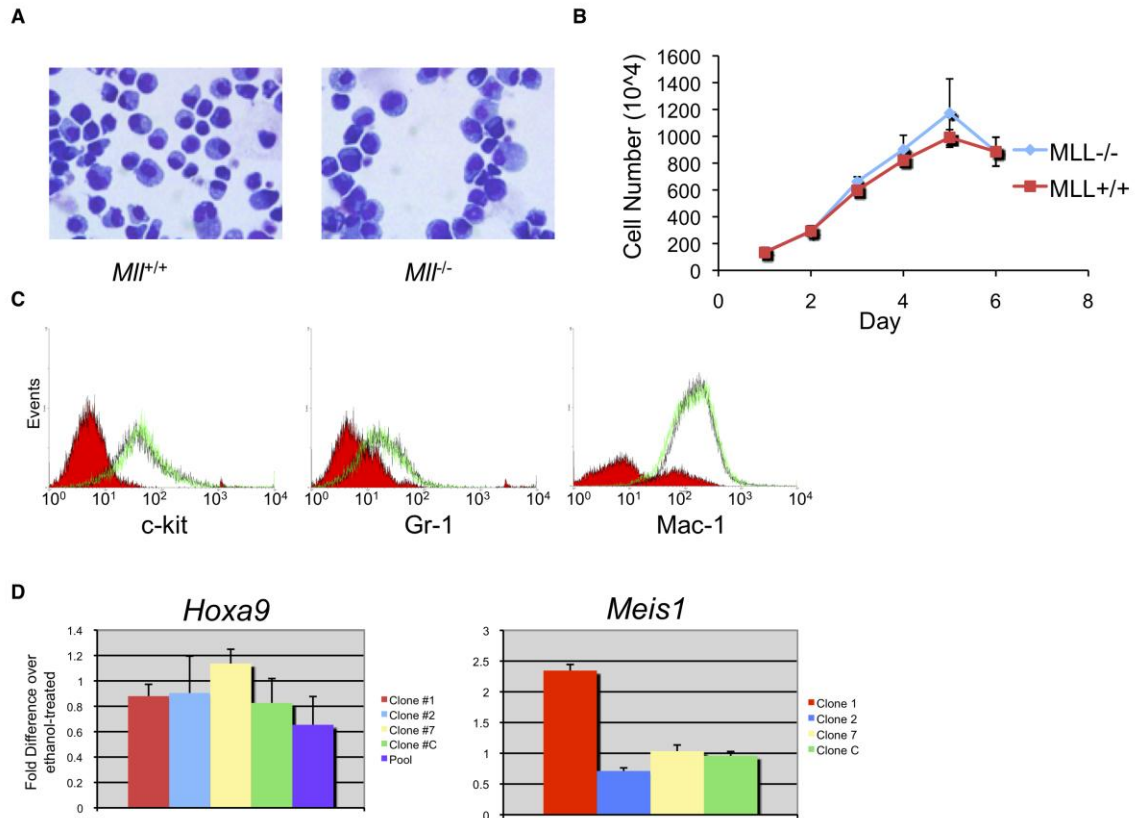
Figure 2.6 Effects of wild-type *Mll* disruption in MLL-AF9 transformed cells A) Wright-Giemsa stained cell with (left) or lacking (right) functional wild-type Mll. B) Growth curves of MLL-AF9 transformed cells with *Mll*-/-or *Mll*+/+. C) Immunophenotype after *Mll* disruption. Red graphs are isotype controls. Black graphs represent *Mll*+/+ cells. Green graphs represent *Mll*-/- cells. D) *Hoxa9* (left) and *Meis1* (right) expression in four monoclonal cells lines or the polyclonal pool of Cre-ER-expressing cells.

Discussion

According to these experiments, disrupting wild-type Mll function does not have a significant effect on leukemic myeloblasts. However, Thiel et al. recently published that wild-type Mll is needed for MLL fusion protein-mediated leukemogenesis [57]. This was concluded based on the same conditional knock-out cells used here and knock-down experiments in murine and human leukemia cells. Another recent report suggests that wild-type MLL is needed for MLL fusion protein binding to target loci [73].

The most likely explanation for the discrepancy between our results and those of other groups is that the monoclonal cell lines used in our experiments represent a fraction of cells that have acquired additional genetic events that contribute to transformation. Even though dramatic reductions in wild-type Mll binding were observed after *Mll* excision, no changes in H3K4 trimethylation were detected. This is in contrast to the study by Thiel et al. where decreases in di and trimethylated H3K4 were observed after shRNA-mediated knockdown of *MLL* in the human leukemia THP-1 cell line, which expresses MLL-AF9. Thus, the monoclonal cell lines utilized in this study may have found ways to adapt, for example, by recruiting another H3K4 methyl transferase, or although unlikely given the half-life of wild-type MLL [74,75], residual wild-type Mll protein may be stabilized by the MLL fusion protein or some other mechanism. Of note, one acute myeloid leukemia cell line with the MLL-AF6 translocation lacks expression of the other *MLL* allele [76].

In retrospect, it appears that the polyclonal cell line may indicate a role of wild-type Mll in MLL-AF9 mediated-leukemic transformation as *Hoxa9* levels decreased to approximately 60% after *Mll* disruption (Fig. 2.6D). These cells were not used for further study since complete excision of wild-type MLL could not be achieved, again perhaps indicating the importance of wild-type Mll to many of the cells. Testing the leukemogenicity of polyclonal and monoclonal MLL-AF9-transformed *Mll*+/+ and *Mll*-/- cells by transplantation in irradiated mice may reconcile our data with those of Thiel et al.

Based on the results of these initial experiments, we focused our efforts on identifying what additional proteins and activities are recruited by one of the most common MLL translocation partners, AF9.

Chapter 3

The Role of the Fusion Partner in MLL Fusion Protein-Mediated

Leukemogenesis

Introduction

AF4, AF9, and ENL

AF9 and ENL share 80% sequence homology and further structural

homology in their C-terminal transactivation domains that is critical to gene

activation [66]. The 90 C-terminal amino acids of AF9 and ENL are sufficient and

necessary for leukemic transformation when fused to the N-terminus of MLL

[44,82]. Through two-hybrid, GST pull-down, and overexpression systems, AF4,

AF5q31, and PC3 have been shown to interact with these 90 residues. ENL also

binds histone 1 and histone 3 through its N-terminal YEATS domain, which is

shared with AF9 [77,78,79].

AF4, AF5q31, and LAF4 are members of the fragile X mental retardation

(FMR2) family of proteins, all four of which have been identified as MLL fusion

partners in leukemia. These proteins have three characterized domains,

including a DNA binding domain at the N-terminus, a transactivation domain, and

a conserved C-terminal domain [80]. Early studies revealed that AF4 colocalizes

with AF9 in leukemia cells, and although the MLL-AF4 fusion protein maintains

this association, it alters the subnuclear localization of AF9 [81]. Altogether, these

initial experiments suggested a mechanistic link between the various MLL fusion proteins in leukemia.

In this study, we focused on defining the mechanisms of transactivation by one of the most common MLL fusion proteins, MLL-AF9, and explored possible therapeutic targets. We first identified proteins that interact with the C-terminal 90 amino acids of AF9, the minimal domain required for transformation when fused to the N-terminal fragment of MLL [44,82]. We found that, in myeloblastic cells, a complex that includes several other MLL fusion partners and key transcriptional regulators associates with the transforming domain of AF9 and the MLL-AF9 fusion protein. These proteins have been named Elongation Assisting Proteins (EAP). ChIP studies for EAP components show that they are localized to leukemogenic genes in cells with and lacking MLL fusion proteins. Notably, in cells transformed by MLL fusion proteins, increased amounts of EAP are localized to the *Hox* loci and the complex is more broadly distributed. Furthermore, while EAP recruited independently of MLL fusion proteins dissociates from target loci in response to differentiation cues, MLL fusion protein-associated EAP remains at target genes, maintaining *Hox* and *Meis* expression. These findings suggest that a key activity of MLL fusion proteins is to prevent the normal dissociation of elongation machinery from loci critical for leukemogenesis.

Materials and Methods

Cloning and Transduction of AF9$^{C\text{-}term}$ into M1 cells Bases 1691-1963
encoding residues 478-568 of human *AF9* (Accession NP_004520) were PCR-
amplified from an MLL-AF9 expression vector and cloned into the Xho1 and Not1
sites of a modified murine stem cell virus (MSCV) vector. This vector contains
two N-terminal FLAG tags, three nuclear translocation signals, and two C-
terminal MYC tags and expresses GFP off of an internal ribosome entry site
(MIGR1-2XFLAG-3XNLS-2XMYC). MIGR1-2XFLAG-AF9-3XNLS-2XMYC and
the control MIGR1-2XFLAG-3XNLS-2XMYC were packaged into viruses using
the 293-derived Plat-E cell line [83]. One ml of viral supernatant and 5 μg/ml
polybrene was added to three million M1 cells (from ATCC) in a six-well tissue
culture dish. Cells were spin-infected for 90 minutes at 2500 RPM in an
Eppendorf 5810 R centrifuge. The next day the media was changed. Cells were
GFP sorted at the University of Michigan Flow Cytometry Core one week after
transduction.

Cell lines M1 (ATCC), M1-control, M1-AF9$^{C\text{-}term}$, RS4;11 (ATCC), KOPN-8
(DSMZ), REH (ATCC), Raji (ATCC), 697 (DSMZ), NALM-1 (DSMZ), HAL-01
(DSMZ), and NALM-6 (DSMZ) cells were maintained in RPMI media containing
10% fetal bovine serum. MV4:11 (ATCC) cells were maintained in IMDM with
15% FBS and 10 ng/mL IL-3. 293 cells (ATCC) were grown in Dulbecco's
Modified Eagle's Medium (DMEM) supplemented with 10% fetal bovine serum
(Gibco). E2A-HLF, MLL-AF9, and MLL-ENL transformed bone marrow cells were
established in our lab. In brief, 6-8 week old C57/BL6 mice were injected with

150 mg/kg 5-fluorouracil. Bone marrow was harvested after four days and placed in a pre-stimulation IMDM media containing 100 ng/ml SCF, 10 ng/ml IL-3, and 10 ng/ml IL-6. The next day, cells were transduced with pMSCV-E2A-HLF (a generous gift from Dr. Michael Cleary), pMSCV-MLL-AF9, or pMSCV-MLL-ENL that was packaged into retroviruses using Plat-E cells as described above for the MIGR1 constructs. Forty-eight hours post-transduction, cells were placed in selection media containing 1 mg/ml G418 (Invitrogen). Fusion protein-transformed cells were maintained in IMDM media containing 15% FBS and 10 ng/ml IL-3.

LC-tandem MS Protein Identification of EAP by LC-tandem MS Samples were resolved by SDS-PAGE and visualized with MS-compatible silver stain (PROTSIL-2, Sigma). Whole lanes corresponding to control and AF9 IP were cut into 16 slices each and destained following the manufacturer's protocol. Cysteines were reduced with 150 ml of 10 mM DTT followed by alkylation with 50 mM iodoacetamide (in 0.1M ammonium bicarbonate, pH 8.0) at RT for 30 min each. Gel slices were crushed, dried using a vacufuge, and re-swollen in 30 μl of ammonium bicarbonate buffer containing 500 ng of sequencing grade, modified trypsin (Promega). After 5 minutes incubation on ice, another 40 μl of ammonium bicarbonate buffer was added and digestion was carried out at 37°C overnight. An additional 250 ng of trypsin was added 2 hours prior to the extraction of peptides. Peptides were extracted once each with 150 μl of 60% acetonitrile containing 0.1% TFA and acetonitrile containing 0.1% TFA. All extracts were pooled and concentrated using a vacufuge to a final volume of 30 μl.

Ten μl of the digest was separated on a reverse phase column (Aquasil C18, 15 mm tip x 75 mm i.d. x 15 cm, Picofrit column, New Objectives, Woburn MS) using acetonitrile/1% acetic acid gradient system (5-75% acetonitrile over 40 minutes followed by 95 % acetonitrile wash for 5 minutes) at a flow rate of ~300 nl/min. Eluted peptides were directly introduced into an ion-trap mass spectrometer (LTQ-XL, ThermoFisher) equipped with a nano-spray source. The mass spectrometer operated in data-dependent MS/MS mode to acquire a full MS scan (400-2000 m/z) followed by MS/MS on the top 5 ions from the full MS scan (relative collision energy ~35%). Dynamic exclusion was set to collect 2 MS/MS spectra on each ion and exclude it for an additional 2 minutes. Raw files were converted to mzXML format and searched against mouse IPI database (V 3.31, 67,611 entries) + reverse database using X!Tandem [84] with *k-score* plug-in, an open-source search engine developed by the Global Proteome Machine. Search parameters included a precursor peptide mass tolerance window of 3 Da and fragment mass tolerance of 0.8 Da. Oxidation of methionine (+16 Da) and carbamidomethylation of cysteines (+57 Da) were considered as variable modifications. Search was restricted to tryptic peptides with one missed cleavage. X!Tandem outputs were subjected to PeptideProphet [85] and ProteinProphet [85] analysis using default parameters of each program. All proteins with a ProteinProphet probability of >0.9 (error rate <3%) were considered for further analysis. MS/MS spectra corresponding to proteins that were unique to the experimental sample were manually verified.

Immunoprecipitation and Western blots Nuclei were isolated from 200 ml to

1000 ml of M1 suspension culture by douncing cells in hypotonic buffer (10 mM

KCl, 10 mM Tris-Cl, pH 7.9) and spinning at 4000 rpm for 15 minutes, 4°C.

Nuclei were then lysed in BC-300 lysis buffer: 0.1% NP40, 10% glycerol, 300-500

mM KCl, 100 uM PMSF, 1 protease inhibitor cocktail tablet (Roche), 1 mM

EDTA, 50 mM Tris-CL pH 7.9 for 30 minutes at 4ºC. Some immunoprecipitations

were done in the presence of 100 μg/ml ethidium bromide or after treatment with

2500 units of Benzonase (EMD Biosciences) in the presence of 2 mM $MgCl_2$.

Cell lysate was spun at maximum speed in an Eppendorf 5424 microcentrifuge

for 15 minutes and supernatant was pre-cleared with protein-G-agarose (Roche)

beads for 1 hour at 4ºC. After pre-clearing, the lysate was incubated with 100 μl

anti-FLAG M2 agarose beads (Sigma) for 1 hour rocking at 4ºC. Beads were

subjected to six five-minute washes with lysis buffer (excluding protease

inhibitors). For mass spectrometry analysis, the purified proteins were eluted with

2X FLAG peptide (Sigma, Sequence: DYKDDDDDYKDDDDK) two times for

fifteen minutes each at 4ºC, resolved by SDS-PAGE, visualized with

ProteoSilver2 kit (Sigma) according to the manufacturer's instructions, and

submitted to the University of Michigan Mass Spectrometry Core. For Western

blotting, the beads were heated at 90ºC Celsius for 5 minutes in SDS Tris-

Glycine sample buffer (Invitrogen). The supernatant was loaded onto 4-20% Tris-

Glycine gels (Invitrogen), and proteins were transferred to a nitrocellulose

membrane for 1 hour. Membranes were blocked in 5% non-fat dry milk (Bio-Rad)

and then incubated with the appropriate primary antibody overnight. Goat anti-

rabbit or goat anti-mouse secondary antibodies (Santa Cruz) were used at 1:2000 for 30 minutes. Proteins were detected using SuperSignal West Pico Chemiluminescent Substrate (Pierce). Whole cell lysate was used for IPs in human leukemia cell lines and antibodies conjugated to Protein G Dynabeads (in PBS with 5% BSA) (Invitrogen), prepared by overnight incubation, were used for overnight IP (antibodies listed below).

Gradient Centrifugation FLAG-AF9$^{C\text{-term}}$ from M1 cells was immuno-purified as described above. The 2X FLAG peptide eluate was loaded onto a 15-45% glycerol or 5-20% sucrose gradient and ultracentrifuged at 23,000 rpm, 4°C for 16 hours in the TH-660 rotor of a Sorvall WX Ultra 80 centrifuge. Protein standard, supplemented with Dextran blue (Sigma) for a 2 megadalton marker, was run in parallel (GE Healthcare). 200 uL fractions were collected and proteins were either concentrated at 14,000 RPM for 2 hours (Millipore, YM-3) for Western blot analsysis of sucrose gradient or precipitated with tricholoracetic acid (TCA) for mass spectrometry-based analysis. For TCA precipitation, samples were first incubated with 2% sodium deoxycholate for 30 minutes on ice, then with10% TCA for 1 hour on ice. Samples were spun for 10 minute at 14,000 rpm, 4°C in an Eppendorf 5424 microcentrifuge, washed with 1 mL cold acetone for 10 minutes, and spun again at 14,000 rpm, 4°C for 10 min. After air-drying, samples were dissolved in urea buffer (9 M urea, 20 mM HEPES, pH 7.5) for mass spectrometric analysis.

Transient Transfections 10^5 human embryonic kidney 293 cells were seeded in 10 cm or 15 cm (for mass spectrometry) dishes overnight. Cells were transfected

with 10 µg empty vector, 10 µg pMYC-MLL$^{1116-1397}$-AF9, 5 µg empty vector and 5 µg pcDNA-HA-Dot1l, 5 µg pcDNA-HA-Dot1l and 5 µg pFLAG-HA-MLL$^{1116-1397}$, or 5 µg pcDNA-HA-Dot1l and 5 µg pFLAG-MLL-AF9, harvested after 48 hours for whole cell lysis in BC-300 buffer, and immunoprecipitated overnight with anti-FLAG M2 (Sigma) or anti-MYC (Clontech) affinity resin. After five five-minute washes with lysis buffer, beads were boiled in SDS Tris-Glycine loading buffer, loaded onto 6% or 4-20% Tris-Glycine gels, and transferred to nitrocellulose membranes. After 1 hour blocking in 5% non-fat milk, blots were incubated with anti-HA (Covance), anti-FLAG (Sigma), or anti-CDK9 (Santa Cruz) overnight, with secondary antibody for 30 minutes, and subjected to enhanced chemiluminescence with SuperSignal West Pico Chemiluminescent Substrate. A gel with empty vector and pMYC-MLL$^{1116-1397}$-AF9 IP'ed samples was silver stained with Sigma's ProteoSilver2 kit and submitted to the University of Michigan Mass Spectrometry Core for analysis.

Chromatin Immunoprecipitation Chromatin immunoprecipitation (ChIP) was performed according to Upstate's protocol using recommended lysis, dilution, and wash buffers. In brief, cells were fixed in 1% formaldehyde for 15 minutes at room temperature. Cells were pelleted, PBS-rinsed, and snap frozen. After thawing, cells were lysed and sonicated at high intensity 30 second on-off cycles for 15 minutes in the Diagenode Bioruptor XL. These conditions generated an average DNA fragment size of 500 bp as determined by DNA electrophoresis. Protein-DNA complexes were collected using antibody-conjugated Protein G Dynabeads that were prepared as described above for standard

immunoprecipitations (antibodies listed below). After washing the beads, DNA was eluted by incubation with SDS buffer (1% SDS, 100 mM sodium bicarbonate) for 30 minutes at 42ºC. DNA-protein cross-links were reversed overnight in 0.2 M NaCl at 65°C. DNA was purified using the QIAquick PCR Purification Kit (Qiagen) and subjected to qPCR as described below. Primer and probe sequences are provided in Table 2.1. For the human MonoMac6 leukemia cell line, DNA samples were run on an agarose (Invitrogen) gel, amplified by standard PCR on an Eppendorf Mastercycler, and visualized with ethidium bromide. Primers are listed in Table 2.1.

Knockdown of DOT1L Knockdown experiments were performed by Stephanie Jo of Jay Hess's lab. MV4:11 cells at a concentration of 10 million cells/ml were transfected with a 500 nM mixture of 2 siRNA oligonucleotides targeting DOT1L (Dharmacon) by electroporation using a Bio-Rad GenePulser MXcell. RNA was extracted and reverse-transcribed (described below) for qPCR 48 hours post-transfection. Gene expression was normalized to 5S ribosomal RNA.

Flavopiridol Experiments MLL-AF9, MLL-ENL, or E2A-HLF cells were seeded at 10^5 cells/ml in growth media. The following day, cells were treated with 0 nM-200 nM flavopiridol, which was generously provided by Sanofi-Aventis and the National Cancer Institute, NIH. Gene expression was analyzed after 24 hours of treatment as described below. Viability was assessed by cell counting with Trypan blue exclusion at 48 hours. Viability curves were generated using Prism 5.0 software.

Screening of human ALL cell lines was performed by Daniel Sanders of

Jay Hess's lab with assistance from the University of Michigan Center for Chemical Genomics (CCG). Cells were seeded at a density of 1250 cells/well in a 384-well plate overnight in RPMI-1640 medium containing 10% FBS. 200 nl of flavopiridol (stock concentrations of 0.04mM – 5mM) was added using a Beckman Biomek FX with a HDR (Beckman Coulter, Fullerton,CA) to give a final concentrations of 0.2 -25µM. 10 µM of staurosporine (BIOMOL) was used as a positive control for complete cell death and DMSO was used as a negative control. The plates were incubated in a 37° C, 5% CO_2 incubator for 48 hours. Viability was assessed using CellTiter-Glo Luminescent Cell Viability Assay (Promega). 25µl of CellTiter-Glo reagent was added to each well using a Multidrop (Thermo Scientific) and luminescence was read (gain 3600, 0.76 sec/well read) with a PHERAstar plate reader (BMG Labtech). pIC_{50} curves were generated using gretl software.

Treatment with Differentiation Agents MLL-AF9, MLL-ENL, or E2A-HLF cells were seeded at 10^5 cells/ml in growth media. The next day, cells were treated with 100 ng/ml IL6 (R&D Systems), 10 nM PMA (Sigma) 5 µg/ml LPS (Sigma), 10 ng/mL G-CSF (R&D Systems) or an equal volume of PBS, ethanol (for PMA), or DMSO as a control. 24-72 hours after treatment, cells were counted using Trypan blue exclusion or RNA was isolated for gene expression analysis.

Il-6/LPS-induced Differentiation of Myeloblastic Cells M1-AF9^{C-term}, MLL-AF9, MLL-ENL, or E2A-HLF cells were seeded at 10^5 cells/ml in growth media. The next day, cells were treated with 100 ng/ml IL6, 5 µg/ml LPS, or an equal volume of PBS as a control. At different time points following treatment, cells were

collected for morphologic staining with the HEMA-3 stain kit (Fisher Scientific).

Additional aliquots were prepared for gene expression analysis for *Hoxa9*, *Meis1*,

Gapdh, and *beta-actin* (described below), standard immunoprecipitation and

Western blot (described above), or chromatin immunoprecipitation (described

above).

Luciferase Reporter Assay 293 cells were seeded in 12 well plates in triplicate.

The next day the growth media was replaced with OptiMEM (Gibco) media

supplemented with 0.5% FBS and cells were co-transfected with MIGR1 or

pMLL-AF9,100 ng Hoxa9-Luc, 15 ng CMV-Renilla and combinations of pCMV-

NPM (from Dr. Sheng-Hao Chao), pCMV-HEXIM (from Dr. Sheng-Hao Chao),

and pCMV-NPMC+ (from Dr. Sheng-Hao Chao) using Fugene 6 (Roche). Total

amount of DNA transfected per well was 0.5 μg. 48 hours post-transfection cells

were lysed and assayed for luminescence using Promega's Dual Luciferase

Reporter Kit according to the manufacturer's instructions. Luminescence was

monitored using a Monolight 3010 luminometer (BD Biosciences).

Methyl Cellulose Assays Virus was prepared and transduced into murine bone

marrow as described above, except using MSCV-HA-NPM, MSCV-HA-NPMC+,

MSCV-FLAG-MLLAF9-IRES-GFP, MSCV-FLT3-ITD. Bone marrow cells were

plated in Methyl Cellulose (Stem Cell Technologies) with 100 ng/ml SCF (R&D

Systems), 10 ng/ml IL-3 (R&D Systems), 10 ng/mL GM-CSF (R&D Systems), 10

ng/ml IL-6 (R&D Systems), and 1 mg/mL neomycin (Gibco) 3 days after

transduction. Colonies were counted and replated weekly for three weeks. Cells

were also collected for RNA and morphology analysis at these time points.

qPCR qPCR for ChIPed samples was performed with Taqman primers and Taqman Universal Master Mix (Applied Biosystems) using the Applied Biosystems 7500 Real-Time PCR system. Primers are listed in Table 2.1. Data is expressed as percent of total input using the formula % Total Input = 2^-[Ct (IP)-Ct (Input)] [71].

For expression analysis, RNA was extracted from cell lines with Trizol reagent (Invitrogen) according to the manufacturer's protocol. Reverse-transcription was performed using Superscript II (Invitrogen) according to the manufacturer's protocol. FAM-labeled *Hoxa9*, *Meis1*, *Af9*, *Enl*, *Cyclin T2*, *Dot1L*, *c-Jun*, *Hexim1*, *Hexim2*, *Npm1*, *Gapdh*, *β-Actin*, and *U2 snRNA* Taqman primers (Applied Biosystems) Primer/Probe set number 9 and 11 in Table 2.1 (for detecting abortive and full-length *Hoxa9* transcripts) were used in expression analysis of murine cell lines. The qPCR reactions were carried out with Taqman Universal Master Mix (Applied Biosystems) using Applied Biosystems 7500 Real-Time PCR system. SYBR Primers detecting FLAG-tagged MLL constructs have been previously reported and were obtained from Dr. Andrew Muntean [55]. Sequences are provided in Table 3.1. Gene expression was normalized to *Gapdh* for all experiments except the flavopiridol, HMBA, and DOT1L knockdown experiments. In the flavopiridol and HMBA experiments, gene expression was normalized to *U2 snRNA*, which is transcribed independently of pTEFb CTD kinase activity [86]. For DOT1L knockdown experiments, primers for qPCR were designed with MacVector sequence analysis program. Single product formation was confirmed by running PCR products on a 1% agarose gel. SYBR Universal

Master Mix (Applied Biosystems) was used for qPCR. Data were normalized to

5S ribosomal RNA. Primer sequences are provided in Table 3.1. Analysis was

performed using the comparative Ct method [70].

Gene	Forward Primer	Reverse Primer
HOXA9	CCACGCTTGACACTCACACTTTG	TTGGCTGCTGGGTTATTGGG
MEIS1	CAGCACAGGTGACGATGATGAC	AAGGATGGTGAGTCCCGTGTCTTG
DOT1L	ATGACCGACGACGACCTGTTTGTG	CGACGCCATAGTGATGTTTGC
5S rRNA	TCTACGGCCATACCACCCTGA	GCCTACAGCACCCGGTATTCC
FLAG-MLL	GGACTACAAGGACGACGATGA	ACAGCTGTGCGCCATGTT

Table 3.1 SYBR green primer sequences for gene expression analysis

Flow Cytometric Analysis E2A-HLF, MLL-AF9, and MLL-ENL cells were

treated with LPS or PBS as described above. After 24 hours, cells were

harvested, washed with PBS, and stained for 30 minutes with anti-c-KIT (BD

Pharmingen) and anti-Gr-1 (BD Pharmingen) conjugated to FITC and PE,

respectively. Cells were washed with PBS two times, filtered into flow cytometry

polystyrene tubes with strainer caps, and flow cytometry was performed at the

University of Michigan Flow Cytometry Core. Data was analyzed using FlowJo

software.

CTD Kinase Assay 400 milliion M1-control or M1- AF9$^{\text{C-term}}$ cells were lysed in

the same conditions described above. Anti-FLAG beads (Sigma) were added to

whole cell lysate for overnight IP as described above. After washes, 100 ng of

recombinant PolII-CTD (Calbiochem), 100 μM ATP, 5 mM $MgCl_2$, and 1 mM

DTT, were added to the beads. Reaction mixture was incubated for 1 hour at room temperature with rocking. Supernatant was removed, the reaction was stopped by addition of SDS loading buffer, and samples were loaded onto a gel for SDS-PAGE and Western blotting as described above.

Antibodies ChIP antibodies include Dot1L (Bethyl, A300-953A, A300-954A mixture), ENL (from Dr. Robert Slany), Ring1b (MBL, D139-3), PC3 (Santa Cruz, sc-23591) AF4 (from Dr. John Kersey), AF5q31 (from Dr. Robert Roeder), Laf4 (Abcam, ab-38318), monomeH3K79 (Abcam, ab-2886), dimeH3K79 (Abcam, ab-3594), trimeH3K79 (Abcam, ab-2621), trimeH3K9 (Abcam, ab-8898), trimeH3K27 (Millipore, 07-449), RNA polymerase II (Covance, MMS-126R), pSer2-CTD (Covance, MMS-129R), pSer5-CTD (Covance, MMS-134R), Cyclin T2 (Santa Cruz, sc-12421), MLL-C (from Dr. Yali Dou), trimeH3K4 (Millipore, 04-745), NPM1 (Abcam, ab-10530), HEXIM1 (Santa Cruz, sc-48871), HEXIM2 (Santa Cruz, sc48874), CDK1 (Abcam, ab-18), mouse and rabbit IgG (Santa Cruz, sc-2025, sc-2027), IgM (Abcam, ab-9175). Standard IP and Western blot antibodies: Cdk9 (Santa Cruz, sc-8338), Cyclin T1 (Santa Cruz, sc-10750), AF4 (from Dr. John Kersey), Laf4 (Abcam, ab-38318), AF5q31 (from Dr. Robert Roeder), ENL (from Dr. Robert Slany), AF9 (Bethyl, A300-597A), Ring1b (MBL, D139-3), CBX8 (Abcam, ab-70796), HA (Covance, MMS-101P) Dot1L (Bethyl, A300-953A, A300-954A mixture), MLL (Bethyl, A300-086A, A300-087A mixture), MLL-C (from Dr. Yali Dou) FLAG (Sigma, F-3165), mouse and rabbit IgG (Santa Cruz, sc-2025, sc-2027), CDK1 (Abcam, ab-18), pSerine (Qiagen, 37430), pThreonine (Qiagen, 37420), pSer5-CTD (Covance, MMS-134R).

Results

MLL[1116-1397]-AF9 associates with histone-associated proteins and the COP9 signalosome in 293 cells

We began our study of MLL fusion partner associations by transiently transfecting 293 cells with the transforming domain of AF9 fused to a small portion of N-terminal MLL (MLL[1116-1397]). In this experiment, mass spectrometry-based analysis identified the histone-associated proteins, SET (TAF-1), TIF-1beta, and RBBP4 and 7. SET is a nuclear oncogene that is important in the activation of genes through its role as a histone chaperone [87]. SET also interacts with CBP and enhances its HAT activity [87,88]. Notably, SET is found in translocations with the nucleoporin, NUP214, in pediatric cases of acute T-cell lymphocytic leukemias that are characterized by *HOXA* overexpression [89]. SET-associated proteins, TIF-1beta (KAP-1), which is mainly characterized as a repressor but serves as a transcriptional activator in embryonic stem cells [90] and Protein Phosphatase 2 were also identified in this experiment (Table 3.2). Finally, two components of the nucleosome remodeling and deacetylase (NuRD) complex [91], RBBP4 (small subunit of CAF-1/RBAP48, p48) and 7 (RBAP46/p46), were identified in association with MLL[1116-1397]-AF9. These RBBPs were originally identified by their interactions with the Rb tumor suppressor, and have since been found to have roles in binding histones and stimulating HAT1 activity [92]. The finding that MLL[1116-1397]-AF9 associates with the aforementioned proteins, which have roles in transcriptional activation and repression [91,93,94], suggests a couple of possibilities. One is that in the

presence of MLL fusion proteins, SET, TIF-1beta, and NuRD components serve as transcriptional activators. The other possibility is in line with the ability of MLL fusion proteins to repress transcription [16,23,24,25,26], where MLL-AF9 may coordinate with transcriptional repressors to suppress the expression of tumor suppressors.

Many subunits of the COP9 signalosome were identified as well (Table 3.2). Certain COP9 subunits have roles in binding histones and acting as transcriptional coactivators at target genes [95], but the COP9 signalosome is widely recognized for its role in mediating proteasomal degradation. Given that we identified nearly all of the subunits including the ubiquitin-conjugating enzyme UBC3B suggests that their function in this MLL$^{1116-1397}$-AF9-associated complex is to degrade substrates, likely MYC- MLL$^{1116-1397}$-AF9, which is massively over-expressed. Thus, these results may not reflect physiological interactions with AF9.

Protein	Total Peptides	Unique Peptides	Protein Probability
MLL	190	17	1
AF9	20	2	1
TIF-1beta	6	4	1
SET	7	4	1
Rbbp4/7	5	2	1
Myb binding protein 1A	10	7	1
Protein Phosphatase 2c	46	22	1
NPM1	9	3	1
Rad18	3	2	1
UBC3B	4	2	1
COP9 subunit 2	5	3	1
COP9 subunit 3	4	3	1
COP9 subunit 4	15	10	1
COP9 subunit 5	8	5	1
COP9 subunit 6	8	4	1
COP9 subunit 7a	4	3	1
COP9 subunit 7b	4	3	1
COP9 subunit 8	10	5	1

Table 3.2 Summary of mass spectrometry-based analysis of proteins associating with MYC-MLL[1116-1397]-AF9 in 293 transfectants Summary of mass spectrometry-based identification of the COP9 signalosome as MYC-MLL[1116-1397]-AF9-associating proteins. Protein probability, total number of peptides, and number of unique peptides are indicated. This experiments was performed once.

The transforming domain of AF9 (AF9$^{\text{C-term}}$) associates with other MLL fusion partners and key transcriptional regulators in hematopoietic cells

Using another approach, we stably-transduced the C-terminal 90 amino acids of AF9 into leukemic M1 cells. To ensure efficient nuclear targeting and protein purification, we included two N-terminal FLAG-epitope tags, three nuclear translocations signals, and two C-terminal MYC tags in this AF9 construct (Fig. 3.1). Cell extracts were immunopurified with FLAG affinity resin and resolved by polyacrylamide gel electrophoresis (PAGE) followed by silver staining (Fig. 3.2A).

A protein expressing only the tags and nuclear translocation signals served as a negative control. Proteins specifically interacting with AF9$^{\text{C-term}}$ identified by mass spectrometry include MLL fusion partners Af4, Laf4, Af5q31, Af10, Ell, and Enl, in addition to Cdk9, Cyclin T1/T2 (pTEFb), Dot1l, Pc3 and Ring1b (Fig. 3.2B). A more detailed list, with the number of peptides identified for each protein is summarized in Table 3.3. None of the proteins identified in 293 cells were identified with significance in these experiments. This may be because those proteins associate exclusively with MLL$^{1116\text{-}1397}$, they require the tertiary structure formed by MLL$^{1116\text{-}1397}$-AF9, they are cell type-specific associations, or because they were an artifact of over-expression. We proceeded to characterize the proteins that associate with AF9$^{\text{C-term}}$ as they are largely characterized as transcriptional activators [96,97,98] and thus have important implications in *Hox* regulation and deregulation by MLL fusion proteins. This group of proteins has been named Elongation Assisting Proteins (EAP).
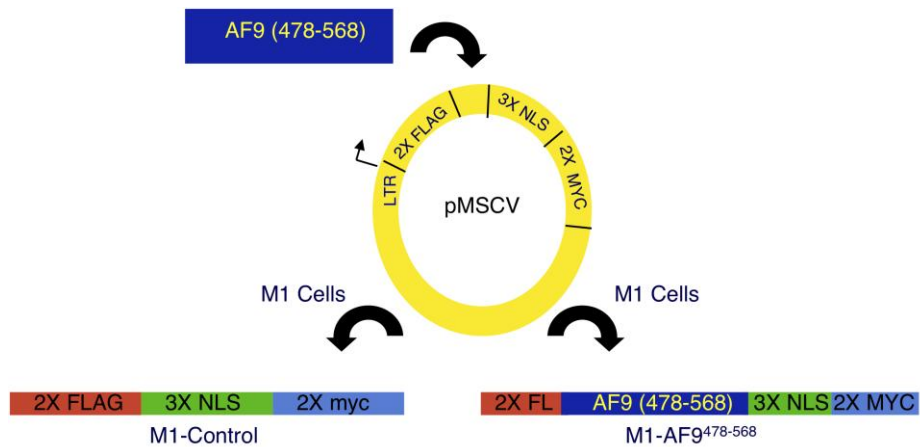
Figure 3.1 Schematic of AF9$^{C\text{-term}}$ and control constructs
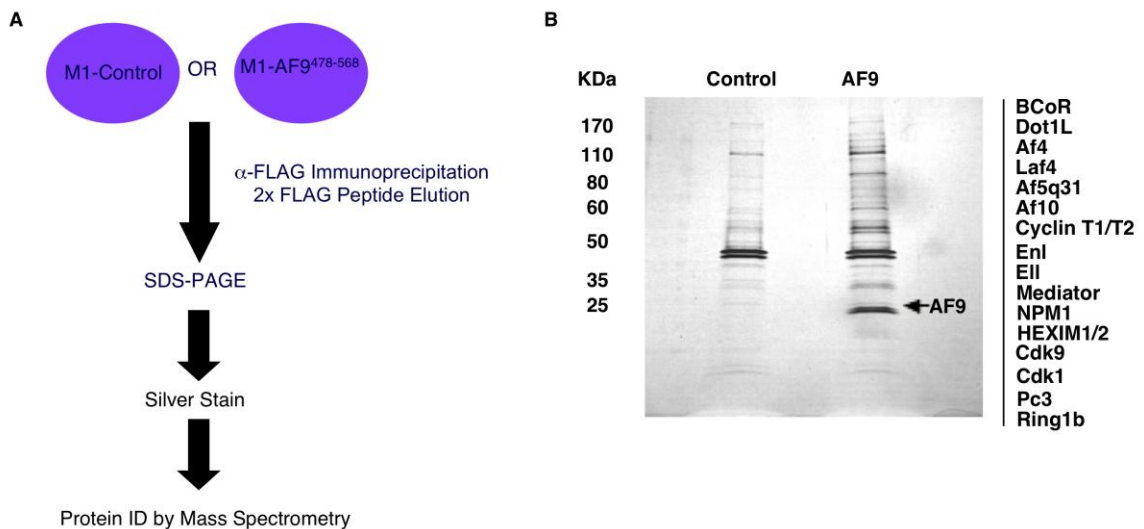
Figure 3.2 Mass spectrometry-based identification of AF9$^{C\text{-term}}$-associating proteins A) Schematic of experimental design. B) Representative silver-stained gel with a list of proteins associating with AF9$^{C\text{-term}}$ identified by mass spectrometry to the right. Proteins immunoprecipitating with the control fragment were subtracted in the analysis in order to identify proteins differentially associating with AF9$^{C\text{-term}}$.

Protein	Total Peptides	Unique Peptides	Protein Probability	Number of Experiments
BCoR	23	15	1	5
Dot1L	9	6	1	6
Af4	51	24	1	7
Laf4	126	39	1	11
Af5q31	213	53	1	10
Af10	15	9	1	6
CyclinT1	46	17	1	8
Cyclin T2	5	2	1	4
Enl	14	6	1	1
Ell	37	19	1	5
Med4	5	3	1	2
Med6	2	1	1	1
Med8	3	2	1	1
Med9	2	2	1	1
Med18	4	3	1	1
Med19	2	1	.96	1
Crsp2	9	6	1	1
Crsp6	8	5	1	1
Crsp7	9	5	1	1
Crsp8	16	8	1	1
Thrap4	13	9	1	2
Thrap5	12	6	1	2
Crsp9	1	1	.93	1
NPM	2	1	.85	3
HEXIM1	28	8	1	4
HEXIM2	21	7	1	5
MePCE	59	8	1	5
Larp7	59	8	1	5
Cdk9	14	6	1	9
Cdk1	2	2	1	1
PRMT5	9	3	1	5
Pc3	1	1	.93	1
Ring1b	5	3	1	3

Table 3.3 List of AF9$^{C\text{-term}}$-associating proteins identified by mass spectrometry Protein probability, total number of peptides, number of unique peptides, and number of experiments in which the proteins were identified are indicated.

Associations with Af5q31, Laf4, Cdk9, and Pc3 were verified by Western

blot (Fig. 3.3A). BCoR, AF5q31, Laf4, Cdk9, Cyclin T1/T2, Dot1L, and Af10 were

identified by mass spectrometric-based analysis after the immunoprecipitations

were carried out in 500 mM KCl and 100 µg/mL ethidium bromide, suggesting

that they are strong and are not mediated through DNA interactions. Benzonase

treatment was tested on Dot1l, AF5q31, and Cdk9 associations to confirm the

ethidium bromide results (Fig. 3.3B). Mass spectrometric analysis identified

Ring1b and Pc3 after AF9$^{C\text{-term}}$ immunoprecipitation in up to 500 mM KCl, but not

when ethidium bromide was present. Enl, Ell, and Af4 were identified by mass

spectrometry after immunoprecipitation in 300 mM salt, and whether these

interactions are DNA-dependent was not tested.
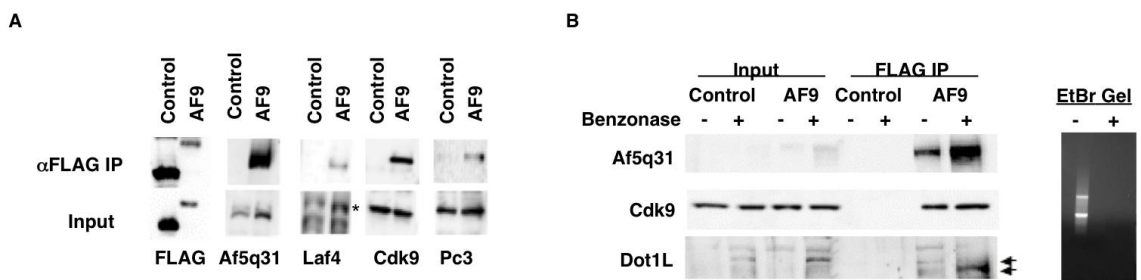
Figure 3.3 Western blot verification of protein associations A) Western blots after FLAG IP from M1-Control and M1-AF9$^{C\text{-term}}$ cell lines. Antibodies used for detection are indicated below blots. B) Detection of associations after nuclease treatment. Antibodies used for detection are indicated to the left of the blots. On the right, is an ethidium bromide stained agarose gel of DNA present at the beginning of the immunoprecipitation in the presence or absence of Benzonase.

To test whether the associations are preserved in the context of the MLL

fusion protein, we performed immunoprecipitations in 293 transfectants and

human leukemia cell lines (Fig. 3.4A, C). These experiments showed that like

MLL-ENL and MLL-AF4 [99,100], MLL-AF9 retains the ability to associate with

key EAP subunits, including pTEFb, DOTL, and RING1b. Furthermore, chromatin

immunoprecipitation of different EAP components shows that many of them

localize to the *HOXA9* locus in MonoMac6 cells, which express the MLL-AF9

fusion protein (Fig. 3.4B).
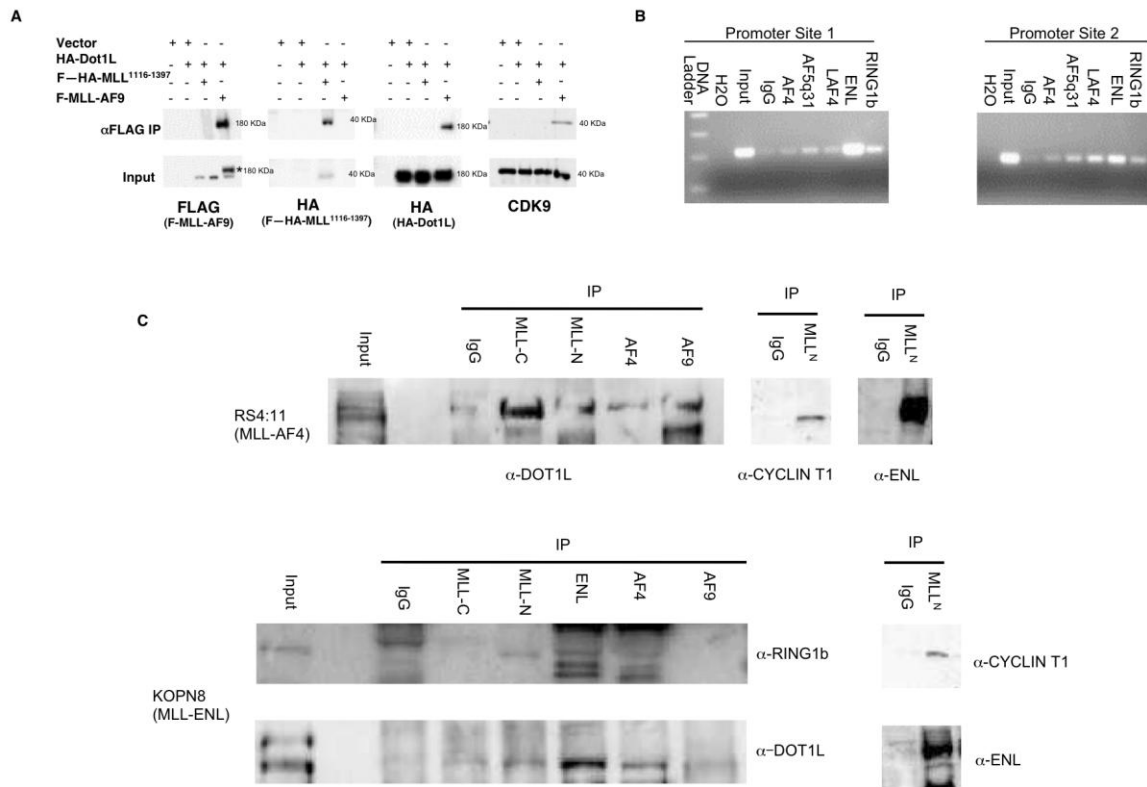
Figure 3.4 MLL fusion proteins associate with EAP A) Transient co-transfections of 293 cells with an N-terminal fragment of MLL (FLAG-HA-MLL[1116-1397]) or FLAG-MLL-AF9 with HA-Dot1L. B) ChIP for different EAP components (indicated above the gels) in MonoMac6 cells at two promoter sites of *HOXA9* detected by conventional PCR. C) Immunoprecipitation of EAP components from the RS4:11 and KOPN8 human leukemia cell lines that express the MLL-AF4 and MLL-ENL fusion proteins, respectively. Antibodies used in immunoprecipitations are indicated above the blots. Proteins were detected using antibodies indicated below the blots in the RS4:11 cells and to the right of the blots in the KOPN8 cells.

In order to address the heterogeneity of EAP, we performed a preliminary

gradient centrifugation experiment where 2X FLAG eluate after FLAG-AF9[C-term]-

immunoprecipitation from M1-AF9[C-term] cells was loaded onto a glycerol gradient

and ultracentrifuged to separate AF9[C-term]-containing complexes based on

differences in size. Fractions were collected, and proteins were TCA precipitated

and dissolved in a minimal volume for mass spectrometric-based identification of

proteins. Detection of the 90 amino acid AF9 fragment was limited by mass

spectrometry since this technique was only able to identify one peptide of this

small construct. Stably over-expressed AF9$^{C\text{-term}}$ was only detected in the low

density fractions, suggesting that most of the AF9$^{C\text{-term}}$ may be extraneous (Table

3.4). Western blot analysis on other gradient centrifugation experiments shows

that AF9$^{C\text{-term}}$ is found throughout the gradient, again, with the highest levels in

the low-density fractions (Fig. 3.5). Western blot analysis of other EAP subunits

was limited by a combination of low protein levels and poor antibodies.

Results from glycerol gradient centrifugation suggest that the EAP

complex is heterogeneous with an approximately 2 Megadalton RNA polymerase

II-associated EAP complex, containing FMR2 members, pTEFb, and pTEFb-

associated factors such as the inhibitory HEXIM proteins, LARP7, and MEPCE

(Table 3.4). Chromatin-associated proteins such as Dot1L and the Polycomb

proteins were difficult to detect in these experiments, with Dot1l and Af10 present

in low abundance in the high-density fractions. This finding supports the model

proposed by Yokoyama et al. who describe physically distinct pTEFb and Dot1l-

associated complexes that functionally coordinate to regulate transcription [100].

Further, purification of Dot1L from stable 293 transfectants led to the

identification a 2 Megadalton complex termed DOTCom [101]. DotCom consists

of a few EAP components, including AF9, ENL, and AF10, along with

components of the WNT signaling pathway, and does not include pTEFb.

Fraction #	1	2	3	4	5	6	7	8	9	10	11	12	13	14	15	16	17	18	19	20	21
AF4	0	0	0	3	2	5	0	0	4	5	0	4	0	0	0	0	0	0	0	0	0
LAF4	0	0	0	1	0	0	1	0	1	1	0	1	1	0	0	0	0	0	0	0	0
AF5q31	0	3	2	21	16	14	8	8	11	9	3	9	3	4	3	1	1	4	2	0	0
Cyclin T1	0	0	0	0	0	1	5	9	10	11	7	6	4	3	3	2	3	1	2	0	1
Cdk9	0	0	0	1	0	1	4	7	11	7	5	8	3	4	4	2	3	2	2	0	1
Dot1l	0	0	0	0	0	0	0	0	0	0	0	0	0	0	0	0	0	0	1	0	0
AF10	0	0	0	0	0	0	0	0	0	0	0	0	0	0	0	0	0	0	1	0	0
HEXIM1	0	0	0	0	0	0	0	2	1	0	0	2	0	0	0	0	0	0	0	0	0
HEXIM2	0	0	0	0	0	0	0	1	1	1	0	0	0	0	0	0	0	0	0	0	1
LARP7	0	0	0	0	0	0	8	7	11	5	3	8	2	0	1	3	1	1	0	0	0
MEPCE	0	0	0	0	0	1	4	3	3	5	3	4	1	2	0	1	2	0	1	0	2
AF9	4	3	2	1	0	0	0	0	0	0	0	0	0	0	0	0	0	0	0	0	0

(2 MDa marked at fraction 9; Density increases with fraction number. Number of Peptides indicated at right.)

Table 3.4 Mass spectrometry-based analysis of AF9^{C-term}-associated proteins after glycerol gradient centrifugation Gradient fractions collected from a 15-45% glycerol gradient are indicated above the table, with increasing fraction number corresponding to increasing density. Proteins identified are listed on the left, with the number of peptides identified in each fraction highlighted in pink.
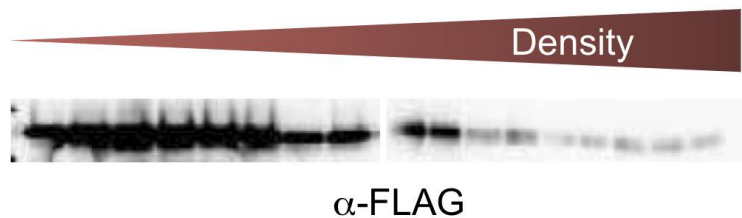

α-FLAG

Figure 3.5 Western blot analysis of FLAG-AF9^{C-term} after sucrose gradient centrifugation 2X FLAG eluate was loaded onto a 5-20% sucrose gradient, which was ultracentrifuged for 16 hours. Fractions were collected, concentrated, and subjected to SDS-PAGE followed by Western blot for FLAG-AF9^{C-term}.

MLL fusion proteins increase the amount of pTEFb and Dot1L at target loci

A key question for understanding mechanisms of transformation by MLL fusion proteins is how the amount and distribution of EAP subunits at target loci differs between cells transformed by MLL fusion proteins versus those transformed by other mechanisms. To address this, we established leukemia cell

lines by expression of MLL-ENL, MLL-AF9, or E2A-HLF in murine hematopoietic

progenitor cells and analyzed EAP component expression levels and binding at

Hoxa9. E2A-HLF transformed cells are not dependent on *Hox* expression for

growth [52]. These cells express *Hoxa9* at 5-10-fold lower levels than MLL

fusion-transformed cell lines and have barely detectable expression of *Meis1*

(Fig. 3.6). The cells express comparable levels of the EAP components *Enl*,

Cyclin T2, and *Dot1L* while *Af9* expression is significantly lower in the MLL fusion
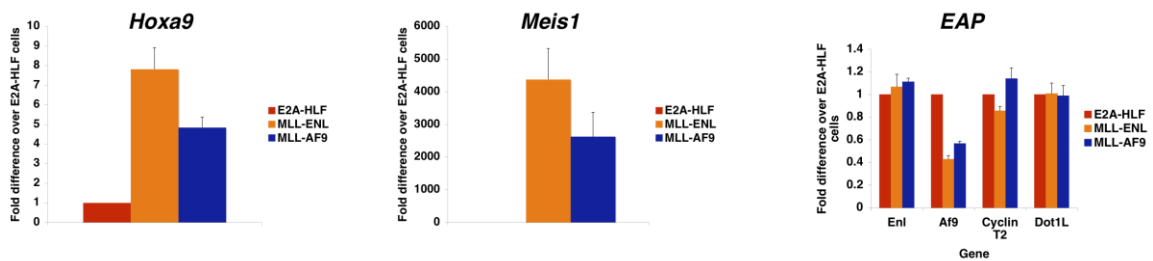
transformed cells (Fig 3.6).

Figure 3.6 Gene expression in fusion-transformed cell lines qPCR analysis of *Hoxa9* (left), *Meis1* (middle), and *EAP* (right) expression in the fusion-transformed cell lines expressed as the fold difference over E2A-HLF-transformed cells. Data are normalized to *Gapdh.*

Although the fusion proteins expressed in these cell lines have N-terminal

FLAG epitope tags, ChIP experiments using different FLAG antibodies were

unsuccessful. Hence, AF9 and ENL antibodies were used to detect fusion protein

binding at target loci. ChIP-qPCR experiments using these antibodies show a

pattern of binding similar to that we previously reported for a conditional form of

MLL-ENL [69] or for MLL-AF4 [102] (Fig. 3.7), with peaks in both the promoter

and coding region of *Hoxa9* that contrast with the distribution of MLL, which is

concentrated at the promoter in cells lacking MLL rearrangements [69]. This

pattern of binding is not found after ChIP-qPCR for endogenous Enl and Af9 in

cell lines that lack MLL fusion proteins (Fig. 3.15 and Fig. 3.18, top panel). An

interesting note is that while MLL-AF9 appears to recruit wild-type Enl, wild-type

Af9 levels are minimal at target loci in cells transformed with MLL-ENL. This is

possibly due to the lower levels of *Af9* expression in the MLL fusion-transformed

cell lines compared to the E2A-HLF-transformed cells.
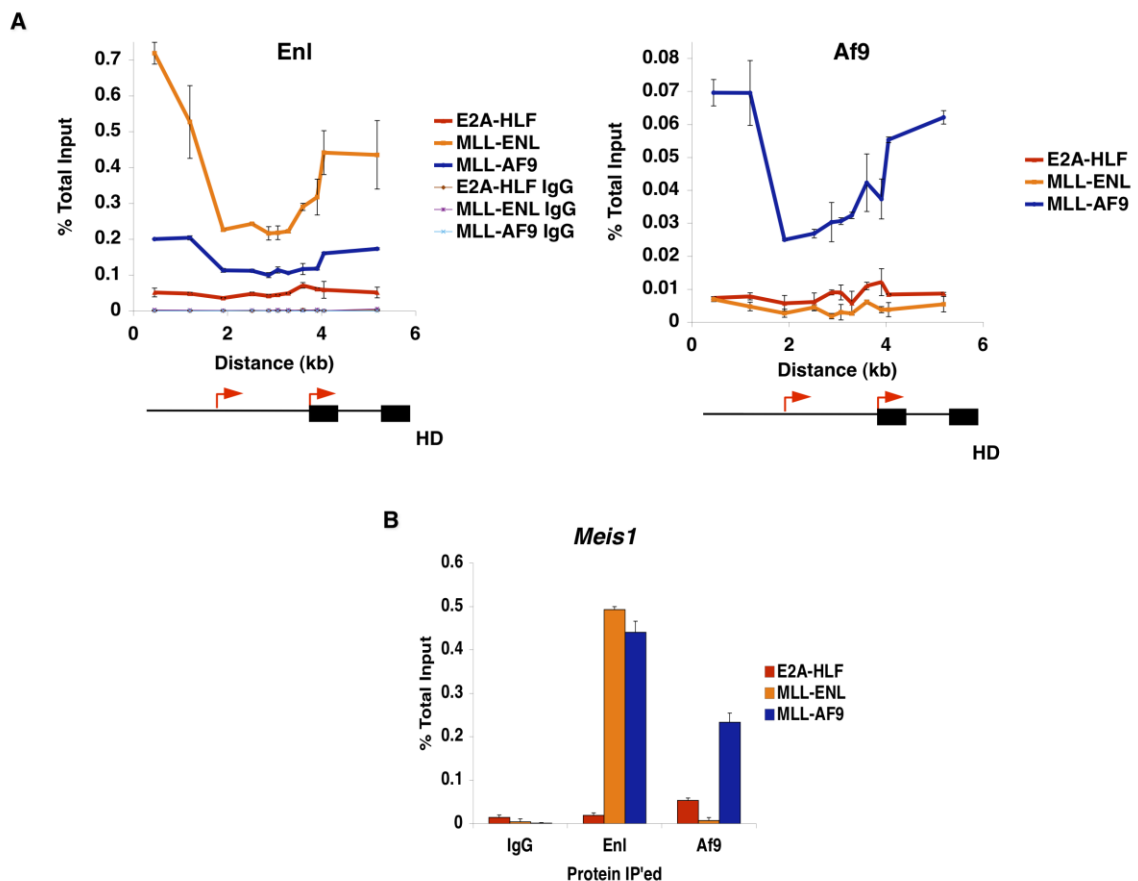
Figure 3.7 Localization of ENL/MLL-ENL and AF9/MLL-AF9 to target loci A)
ChIP-qPCR analysis of binding at *Hoxa9* locus. Schematics of *Hoxa9* are
depicted below the graphs, with red arrows indicating transcription start sites and
black boxes indicating exons. HD is the homeodomain-encoding exon. B) ChIP-
qPCR in the coding region of the *Meis1* locus after immunoprecipitation of the
proteins indicated along the x-axis.

Until recently, pTEFb has mainly been studied in the context of HIV [103].

It is a crucial co-factor to the viral protein, Tat, which recruits pTEFb to TAR

elements of nascent viral transcripts in order to overcome abortive transcription. Tat-mediated transactivation is absolutely dependent on pTEFb activity, and the importance of pTEFb in the development of other diseases, such as cardiac hypertrophy and cancer, is being established, as well [103].

pTEFb phosphorylates Serine 2 of the RNA polymerase II (Pol II) CTD as well as the 5,6-Dichloro-1-β-D-ribofuranosylbenzimidazole (DRB) sensitivity inducing factor DSIF, thereby releasing RNA pol II from elongation inhibition [104]. One possibility is that MLL fusion proteins deregulate *Hox* expression through recruitment of excessive pTEFb to target loci thereby resulting in unregulated transcriptional elongation. We tested for evidence of RNA polymerase II stalling at the *Hoxa9* locus in the fusion-transformed cell lines. We used qPCR primers within the first 100 bases of the transcriptional start site of *Hoxa9* as an indicator of abortive transcription and within the last exon of *Hoxa9* as an indicator of complete transcription. The amount of short transcripts greatly exceeds that of mature transcripts in the E2A-HLF transformed cells, with only 20% of the initiated transcription developing into mature transcripts. There are higher levels of full-length transcripts in the MLL fusion transformed cells, with full-length transcripts comprising 40 to 80% of all transcripts (Fig. 3.8).

In keeping with this, ChIP for the pTEFb component Cyclin T2 showed that more Cyclin T2 is localized to the coding regions of *Hoxa9* and *Meis1* in cells with MLL fusion proteins than in those lacking MLL rearrangements (Fig. 3.9A, B). In cells transformed by E2A-HLF, ChIP for Pol II showed that it is present at *Hoxa9* and *Meis1* similar to levels in MLL-AF9-transformed cells (Fig. 3.9A, B).

Serine 5 CTD phosphorylation, a modification associated with Pol II

transcriptional initiation, is also present at levels similar to MLL-AF9-transformed

cells at *Hoxa9*. However, cells expressing MLL fusion proteins show 2 to 10-fold

more Serine 2 phosphorylated Pol II at the *Hoxa9* and *Meis1* loci (Fig. 3.9A, B).

These data indicate that, while *Hoxa9* transcription in the E2A-HLF cells is

initiated at levels similar to MLL-AF9-transformed cells, it is lacking in its ability to

progress to transcriptional elongation. However, the MLL fusion transformed cells

are able to overcome this elongation block at the *Hoxa9* promoter, likely due to
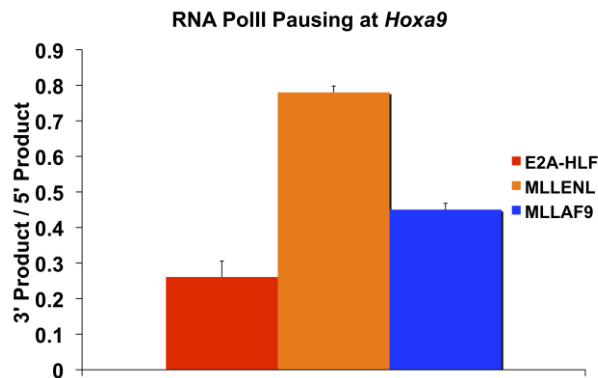
pTEFb recruitment.

Figure 3.8 RNA polymerase II stalling at *Hoxa9* qPCR for mature (3') and abortive (5') *Hoxa9* transcripts in fusion-transformed cell lines with PCR primers that amplified the HD-encoding exon or 100 bp downstream from the transcriptional start site. Data are expressed as the amount of mature transcripts over total initiated transcripts and are normalized to *Gapdh*.
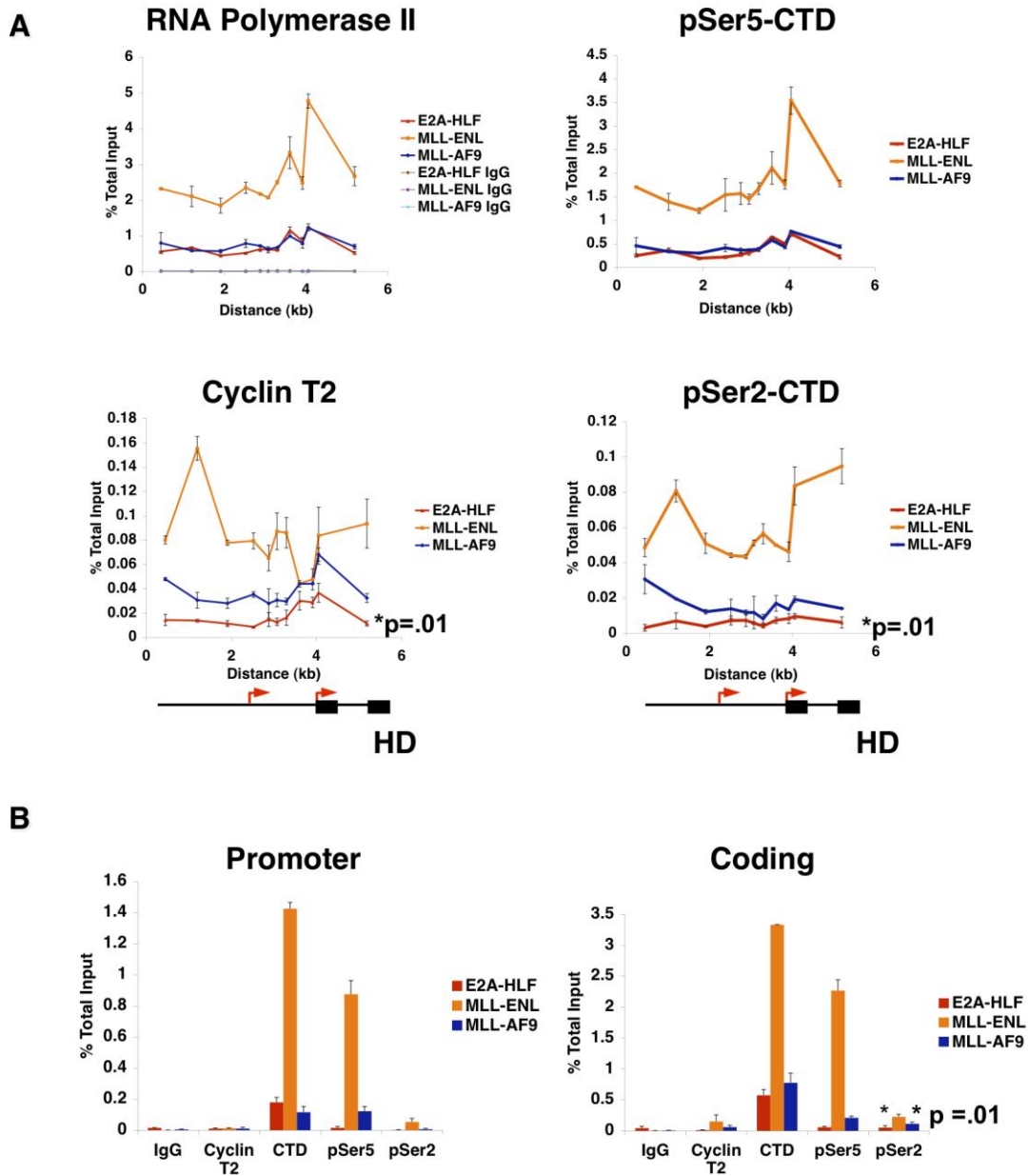
Figure 3.9 Association of MLL fusion proteins with elongating RNA polymerase II ChIP-qPCR experiments for different RNA polymerase II associated factors at *Hoxa9* (A) and *Meis1* (B). Schematics of *Hoxa9* are depicted below the graphs, with red arrows indicating transcription start sites and black boxes indicating exons. HD is the homeodomain-encoding exon. p values are provided for the differences in binding between the MLL-AF9 and E2A-HLF-transformed cells at the most 3' site (HD) in *Hoxa9* and the coding region of *Meis1*.

Assessment of pTEFb as a therapeutic target

Other groups have also reported the importance of transcriptional elongation to MLL fusion protein-mediated transcription. It was shown that knock-down of ENL compromises transcriptional elongation, and that ENL, AF4, and AF5q31 stimulate elongation in an RNA tethering assay. Furthermore, loss of the pTEFb interaction domain in AF4 family members, abrogates the fusion protein's leukemogenicity [99,100,105]. These data altogether suggest that the kinase activity of pTEFb is a potential therapeutic target in leukemias with *MLL* rearrangements. To assess whether cells transformed by MLL fusion proteins are differentially sensitive to CDK9 inhibition, we treated murine AML cell lines transformed by E2A-HLF, MLL-AF9, and MLL-ENL as well as a range of human ALL cell lines harboring different chromosomal translocations (RS4;11, KOPN-8, REH, 697, NALM-1, HAL-01, NALM6, RAJI) with the cyclin-dependent kinase inhibitor, flavopiridol, which has a K_i of 3 nM with CDK9 and weaker inhibition of other CDKs [106], and measured effects on cell viability and gene expression. Viability assays showed that cell lines with MLL fusion proteins are modestly more sensitive to flavopiridol than those lacking MLL fusion proteins (Fig. 3.10A, B).
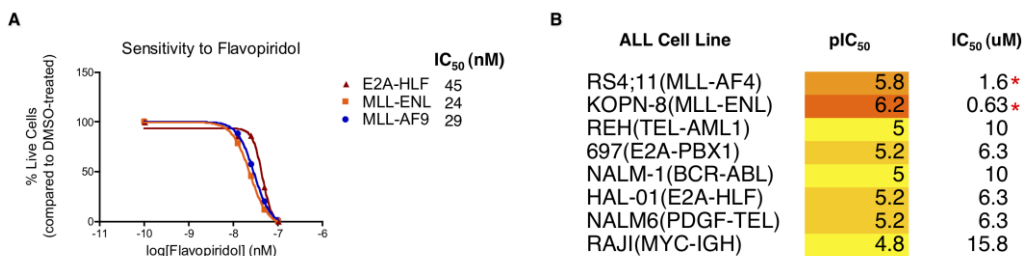
Figure 3.10 Sensitivity of leukemic cell lines to flavopiridol A) Viability assay in murine fusion-transformed cell lines. B) Viability assay (contributed by Daniel Sanders) in human leukemia cell lines carrying various chromosomal aberrations.

Flavopiridol treatment results in decreased *Hoxa9* and *Meis1* expression, but other constitutively expressed genes such as *Gapdh* and *beta-actin* are also affected in the MLL-ENL-transformed cells (Fig. 3.11), a finding that is consistent with the general role of pTEFb in transcriptional regulation [107,108]. Thus, the MLL fusion transformed-cell lines are not more sensitive to flavopiridol due to selective inhibition of *Hoxa9* transcription. In fact, at higher concentrations, flavopiridol more effectively inhibits *Hoxa9* expression in low-expressing E2A-HLF transformed cells, even more so than the house-keeping genes (Fig. 3.11). It is also possible that the inhibition of other cyclin-dependent kinases may be leading to the toxicity and gene expression decreases observed in these assays. Of note, flavopiridol is currently in clinical trials for the treatment of leukemia and other cancers, and its potency is attributed to inhibiting many CDKs. Nonetheless, in combination with other drugs, it is showing promise as a therapeutic as it targets cycling cells and recruits quiescent leukemic cells into a proliferative state [109,110,111]. However, it is largely protein-bound and the dosage is limited by diarrhea and other side effects.
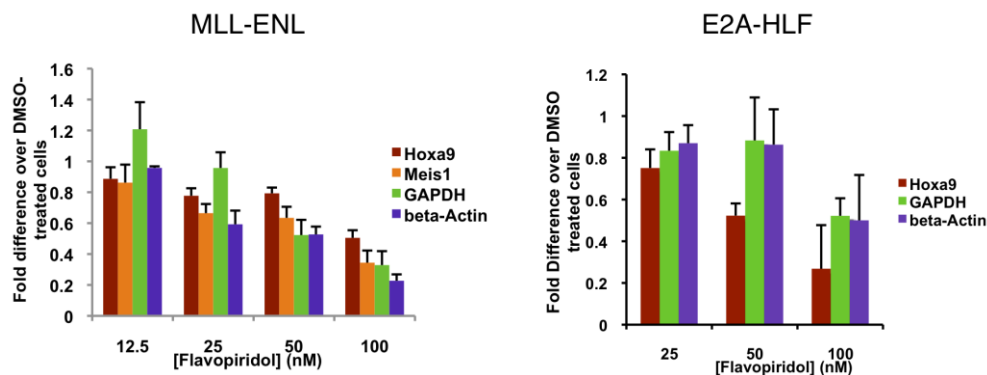
Figure 3.11 Effects of flavopiridol on gene expression qPCR analysis of gene expression in MLL-ENL (left) and E2A-HLF (right) transformed cells after 24 hour treatment with flavopiridol. Data are normalized to *U2 snRNA*.

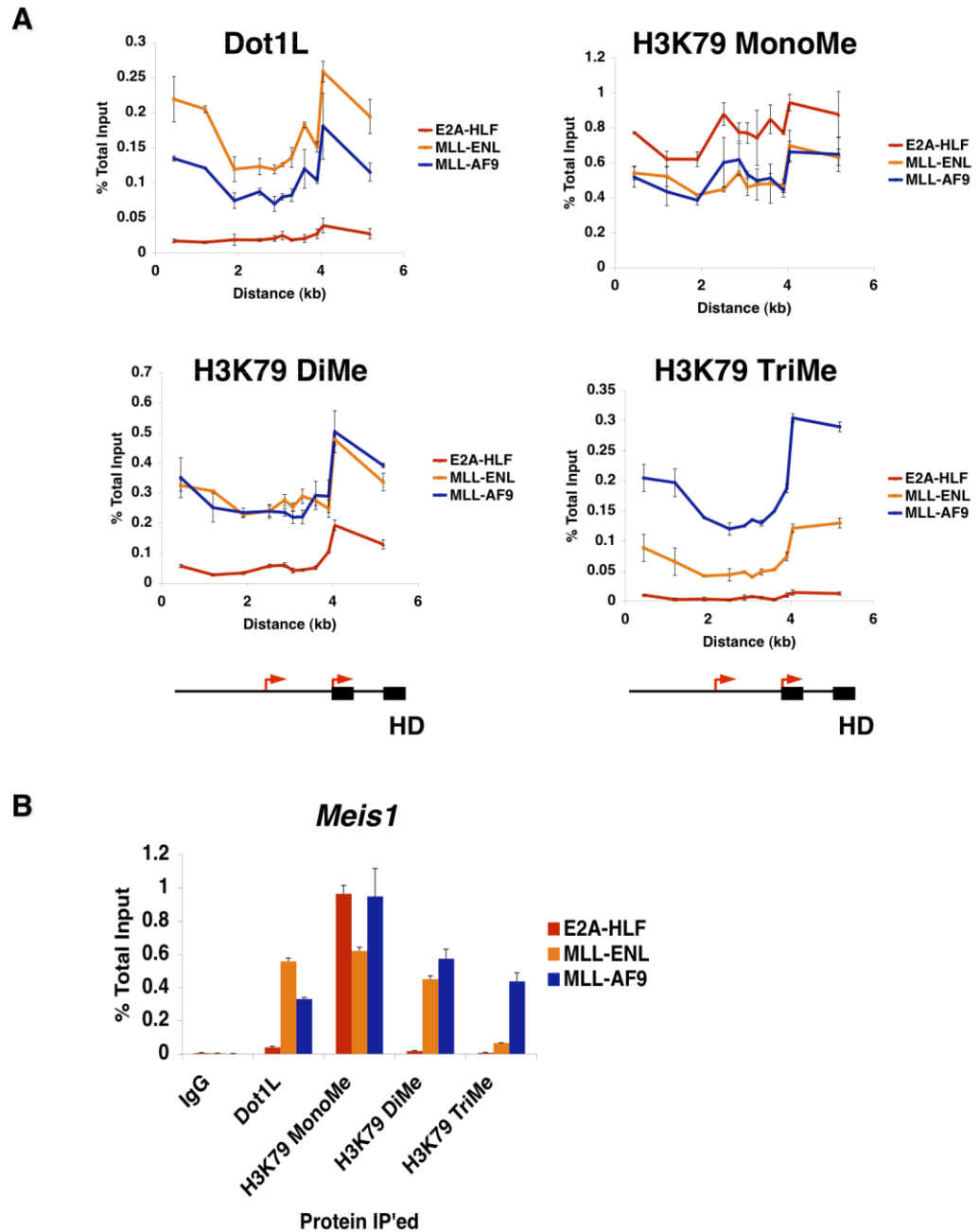**Assessment of Dot1L as a therapeutic target**

Dot1L is different from other histone lysine methyl transferases in that it does not have a SET domain, and it methylates H3 in the globular domain of the nucleosome [112]. Furthermore, it is the only known H3K79 methyl transferase. Characterizing this enzyme in normal and pathological conditions has been an active area of research for the past several years. Although Dot1L is necessary for mammalian development [113], loss of Dot1L is relatively well-tolerated in adult mice (Jo et al, in preparation). This, along with its unique catalytic activity, makes it an attractive candidate as a therapeutic target.

ChIP studies performed for Dot1l show that the enzyme is present at elevated levels at MLL fusion target loci in a pattern similar to the MLL fusion proteins (Fig. 3.12A, B). While monomethylation of H3K79, a regulatory mark [96], is higher in the E2A-HLF cells, di and trimethylation of H3K79, marks associated with active transcription [96], are higher in cells transformed by MLL fusion proteins, showing a broad distribution across the locus. These findings are consistent with recent ChIP experiments performed on human ALL cell lines

[102] and primary ALL blasts [50], which show that precursor B ALLs with MLL rearrangements show large blocks of histone H3 lysine 79 di-methylation at the *HOXA9* locus compared to leukemic cells lacking MLL rearrangements. Elevated levels of Dot1L and its associated H3K79 di and trimethyl marks are also seen in the coding region of the *Meis1* locus (Fig. 3.12B). Trimethylated H3K79 is consistently higher at *Hoxa9* and *Meis1* in MLL-AF9 transformed cells compared to MLL-ENL transformed cells even though MLL-ENL transformed cells express higher levels of these genes. This may be because MLL-AF9, which contains the 90 C-terminal amino acids of AF9, is capable of recruiting positive regulators of Dot1L-mediated trimethylation, while MLL-ENL, which contains most of the ENL protein, is not able to perhaps due to the presence of regulatory domains. In regards to the association of H3K79 trimethylation with expressed genes, the C-terminus of AF9 may not be sufficient for optimal transcriptional activity [100]. MLL-AF9 transformed cells lag behind MLL-ENL transformed cells in their levels of RNA polymerase II-associated factors at target loci (Fig. 3.9), which may be why they express lower levels of target genes.

Knockdown of Dot1L in cells with MLL rearrangements show decreased *Hoxa9* and *Meis1* expression, demonstrating the importance of Dot1L to MLL fusion protein-mediated gene activation (Fig. 3.13, contributed by Stephanie Jo) [50]. Remarkably, our initial studies with *Dot1L* conditional knockout mice show that transformation by MLL-AF9 is absolutely dependent on Dot1L, while other oncoproteins, such as E2A-HLF or the combination of HOXA9 and MEIS1, are

not (Stephanie Jo, Hess lab), suggesting that loss of Dot1L function is not generally toxic to myeloid cells.

Figure 3.12 Association of MLL fusion proteins with Dot1L ChIP-qPCR performed for Dot1L and its associating H3K79 methylation marks at *Hoxa9* (A) and *Meis1*. (B). Schematics of *Hoxa9* are depicted below the graphs, with red arrows indicating transcription start sites and black boxes indicating exons. HD is the homeodomain-encoding exon. IgG controls are shown in Figure 3.9.
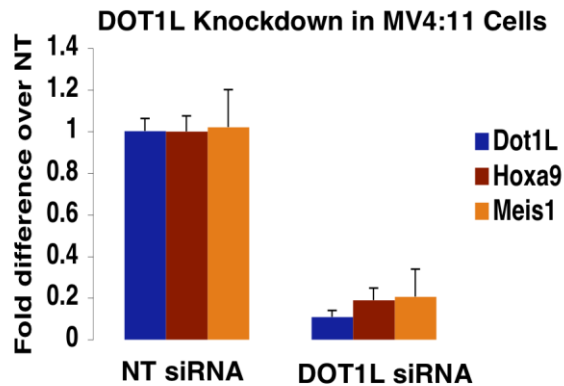
DOT1L Knockdown in MV4:11 Cells

Figure 3.13 Knockdown of Dot1L in MV4:11 Cells qPCR detection of *Dot1L*, *Hoxa9*, and *Meis1* after siRNA-mediated knockdown of *DOT1L* expression in the MV4:11 human leukemia cell line.

EAP association with target loci is dynamic and is altered by recruitment via MLL fusion proteins

Previous studies in 293 cells, as well as the work reported here, indicate that the EAP complex regulates *Hoxa9* and *Meis1* transcription both in cells with and lacking MLL rearrangements [105]. Since the composition of the complex appears to be similar, the question arises how regulation of the complex is altered by MLL fusion proteins so that this does not allow for down-regulation of target genes. One attractive possibility is that through fusion with MLL, EAP association with target loci becomes dependent not only on interactions mediated by EAP subunits, but also on the amino terminal MLL sequences. The presence of a number of DNA binding motifs including the AT hooks, DNMT domain, as well as interactions with menin, PAFc, or wild-type MLL [55,57,73], could result in

tighter association with target loci, making dissociation of the complex resistant to normal physiologic differentiation cues.

To explore this further, we first developed a model system in which we could study the association of EAP with target loci during the induction of myeloid differentiation. Myeloblastic M1 cells and our stably-transduced M1-AF9$^{C\text{-term}}$ cell line differentiate into macrophages in response to IL-6 (Fig. 3.14A, [114]), with dramatic down-regulation of *Hoxa9* and *Meis1* evident after 24 and 4 hours of treatment, respectively (Fig. 3.14B). An interesting note is that the stably over-expressed AF9$^{C\text{-term}}$ localizes to *Hoxa9* and *Meis1*. To date, Af9 has not been shown to directly regulate *Hoxa* cluster genes [115]. This result may be due to over-expression of AF9$^{C\text{-term}}$. Another possibility is that the retroviral integration that occurred upstream of *Hoxa9* and *Meis1* in the M1 cell line [116,117], may recruit Af9 as a means to *Hoxa9* and *Meis1* overexpression.
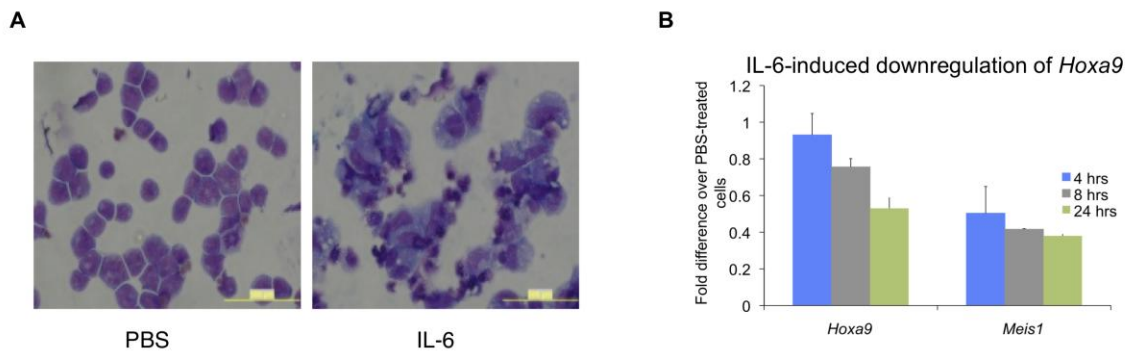

Figure 3.14 IL-6-induced differentiation of M1 cells A) Wright-Giemsa stained cells after 48 hours of IL-6 treatment. B) Gene expression of *Hoxa9* and *Meis1* after 4, 8, or 24 hours of IL-6 treatment.

The decreases in *Hoxa9* and *Meis1* expression are accompanied by rapid dissociation of EAP subunits including Af9, Cyclin T2, and Dot1 from the *Hoxa9*

locus, which is evident as early as 4 hours (Fig. 3.15B, C). Notably, with the

exception of endogenous Af9, decreases in *EAP* expression are not detected

until 8 hrs post-treatment (Fig. 3.15A), indicating that the dissociation precedes

EAP down-regulation in differentiating cells. The MYC-AF9 is stably expressed

by an MSCV promoter, and its expression is presumably independent of IL-6-

mediated gene regulation. Af9 and Enl were the earliest to dissociate from the

Meis1 locus (Fig. 3.15C), and it remains to be seen whether their dissociation

precedes *Meis1* down-regulation. Thus, there may be differences in regulation

between *Hoxa9* and *Meis1* in this experimental model.
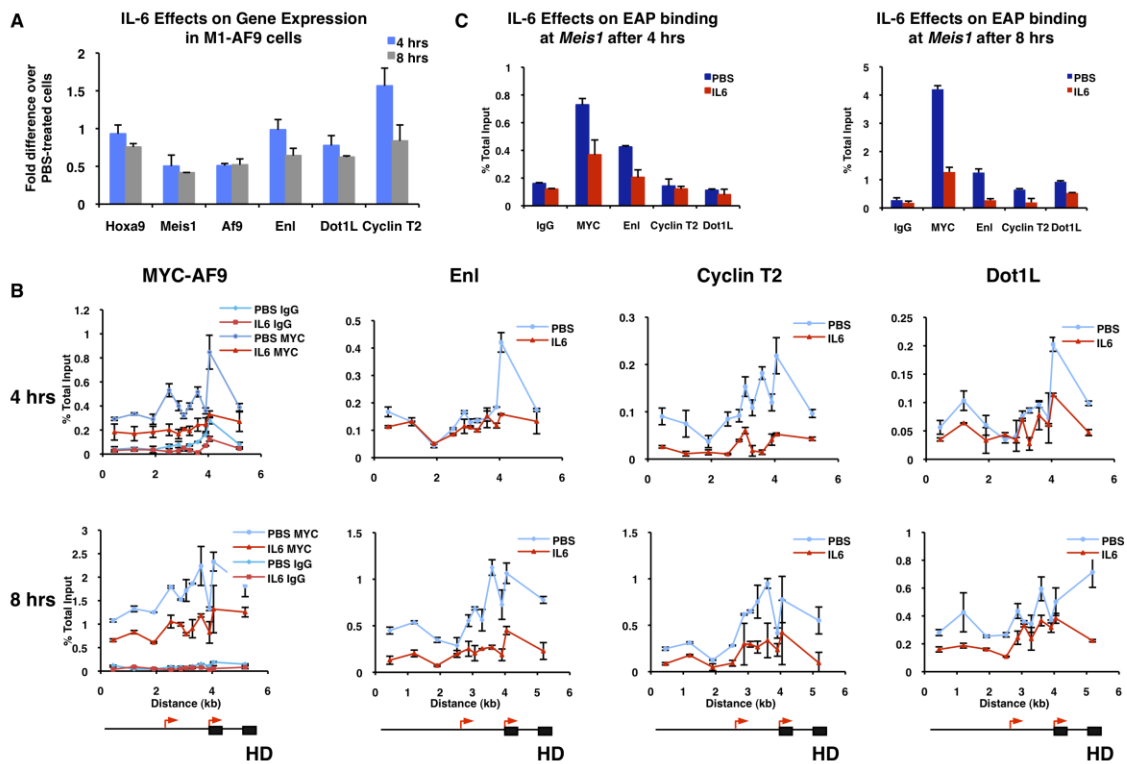
Figure 3.15 Expression and localization of EAP subunits during IL-6-induced differentiation of M1 cells A) Expression of EAP components after 4 and 8 hours of IL-6 treatment. B) ChIP for different EAP subunits indicated above the graphs at 4 and 8 hours. Schematics of *Hoxa9* are depicted below the graphs, with red arrows indicating transcription start sites and black boxes indicating exons. HD is the homeodomain-encoding exon. C) ChIP for EAP components in the coding region of *Meis1*.

We then utilized the E2A-HLF, MLL-ENL, and MLL-AF9 transformed cell lines to test if EAP dissociation is altered by MLL fusion proteins. We screened a panel of differentiation agents to assess the sensitivity of the cell lines as measured by changes in *Hoxa9* expression (Fig. 3.16). These experiments show that LPS down-regulates *Hoxa9* expression by approximately 60% in E2A-HLF transformed cells, but not in MLL fusion transformed cells.
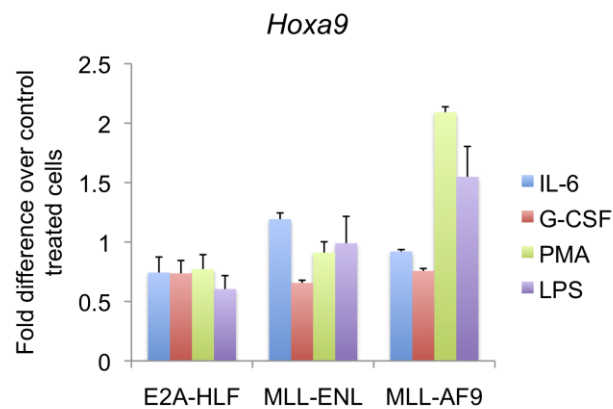

Figure 3.16 *Hoxa9* expression after 48 hour treatment with differentiation-inducing agents qPCR for *Hoxa9* expression after treatment with IL-6, GCSF, PMA, or LPS. Data are expressed as fold difference over PBS (IL-6, G-CSF, LPS) or ethanol (for PMA)-treated cells. Data are normalized to *beta-actin*.

E2A-HLF transformed murine bone marrow cell lines are highly sensitive to induction of differentiation with lipopolysaccharide (LPS) (Fig. 3.17A-C), with dramatic downregulation of *Hoxa9* (*Meis1* is barely detectable in these cells) observed after 24 hours of LPS treatment (Fig. 3.17C). In contrast, cells transformed by MLL-AF9 or MLL-ENL do not show appreciable *Hoxa9* or *Meis1* downregulation or differentiation (Fig. 3.17A-C). To show that LPS signaling is intact in the MLL fusion transformed cell lines, we tested the expression of *c-Jun*,

a target gene of LPS signaling [118]. Both MLL transformed cell lines showed

upregulation of *c-Jun*, although the increase in MLL-AF9 transformed cells is

relatively modest (Fig. 3.17C). It remains possible that E2A-HLF transformed

cells express higher levels of the LPS receptor, co-receptors, or signaling

intermediates or regulators. However, since the proteins involved in the LPS

signaling pathway in myeloblasts is unknown, this possibility could not be tested.

Another explanation for the observed difference in *Hox* expression is that

the MLL fusion protein alters association of EAP with target loci. In support of

this, ChIP shows that in E2A-HLF transformed cells, key EAP subunits, including

Enl, Af9, and Dot1l, dissociate from the *Hoxa9* and *Meis1* loci in response to LPS

(Fig. 3.18A, B). In contrast, cells transformed by either MLL-AF9 or MLL-ENL

show persistent association of these EAP subunits with the loci after LPS

treatment. It is possible that a consequence of EAP dissociation is the

dissociation of RNA polymerase II as we detected decreases in total Pol II

binding at *Hoxa9* and *Meis1* in terminally differentiated E2A-HLF cells, while Pol

II levels at these loci in MLL fusion-transformed cells were unchanged or

elevated (Fig. 3.18A,B).

There are other explanations as to how EAP subunits may be retained at

target loci by MLL fusion proteins. The MLL fusion protein may recruit other

proteins to target loci in order to maintain EAP association, or they may prevent

the recruitment of proteins that displace EAP from target loci. Insight into these

possibilities may be gleaned from the identification of proteins associating with

EAP after LPS treatment in LPS-sensitive E2A-HLF transformed cells versus

LPS-resistant MLL fusion transformed cells.
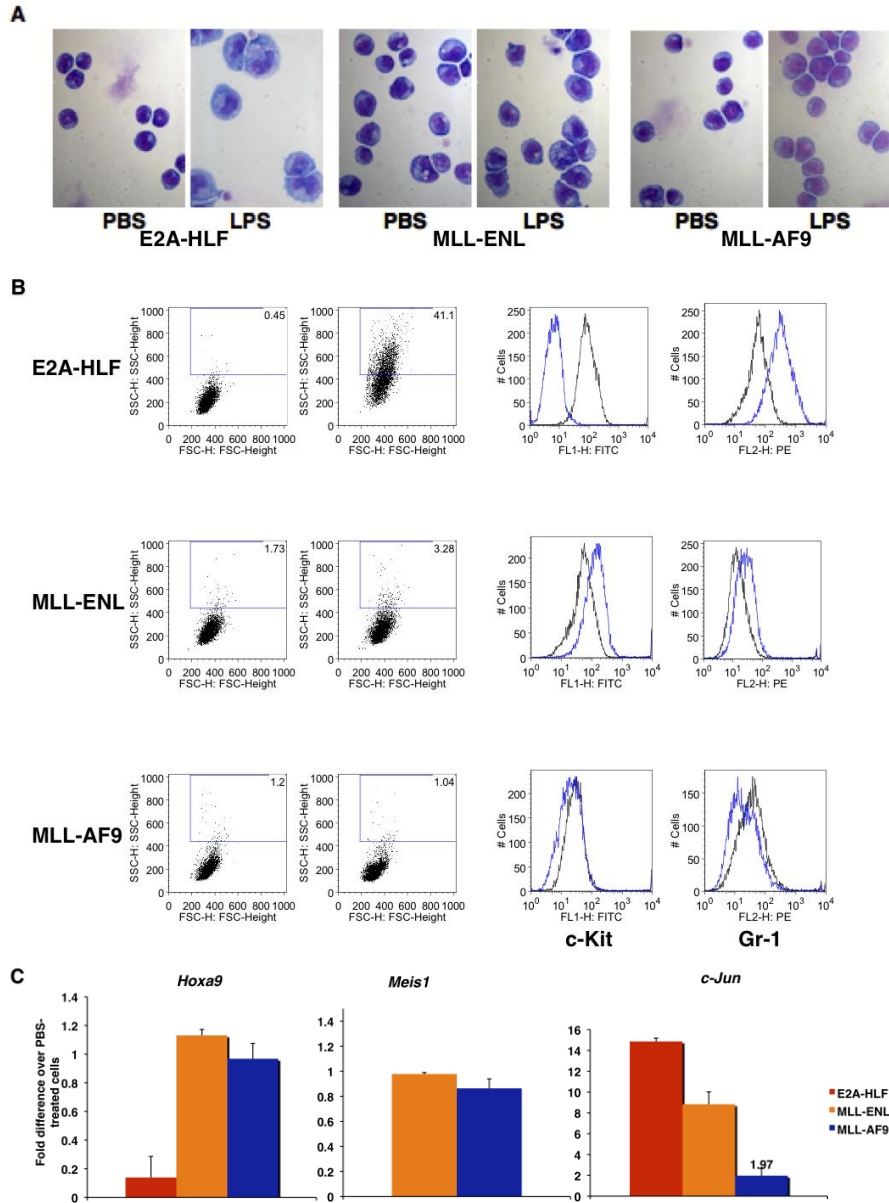
Figure 3.17 MLL fusion transformed cell lines are resistant to LPS-induced differentiation A) Wright-Giemsa staining of cells after 24 hour LPS treatment. B) Flow cytometric analysis on LPS- and PBS-treated cell lines for forward scatter (size), side scatter (granularity), and the cell surface differentiation markers c-Kit and Gr-1. Black and blue graphs represent PBS and LPS treated cells, respectively. Percentage of total cells in the gated region is indicated in the top-right corner of the boxes. C) qPCR for *Hoxa9*, *c-Jun*, and *Meis1* expression.
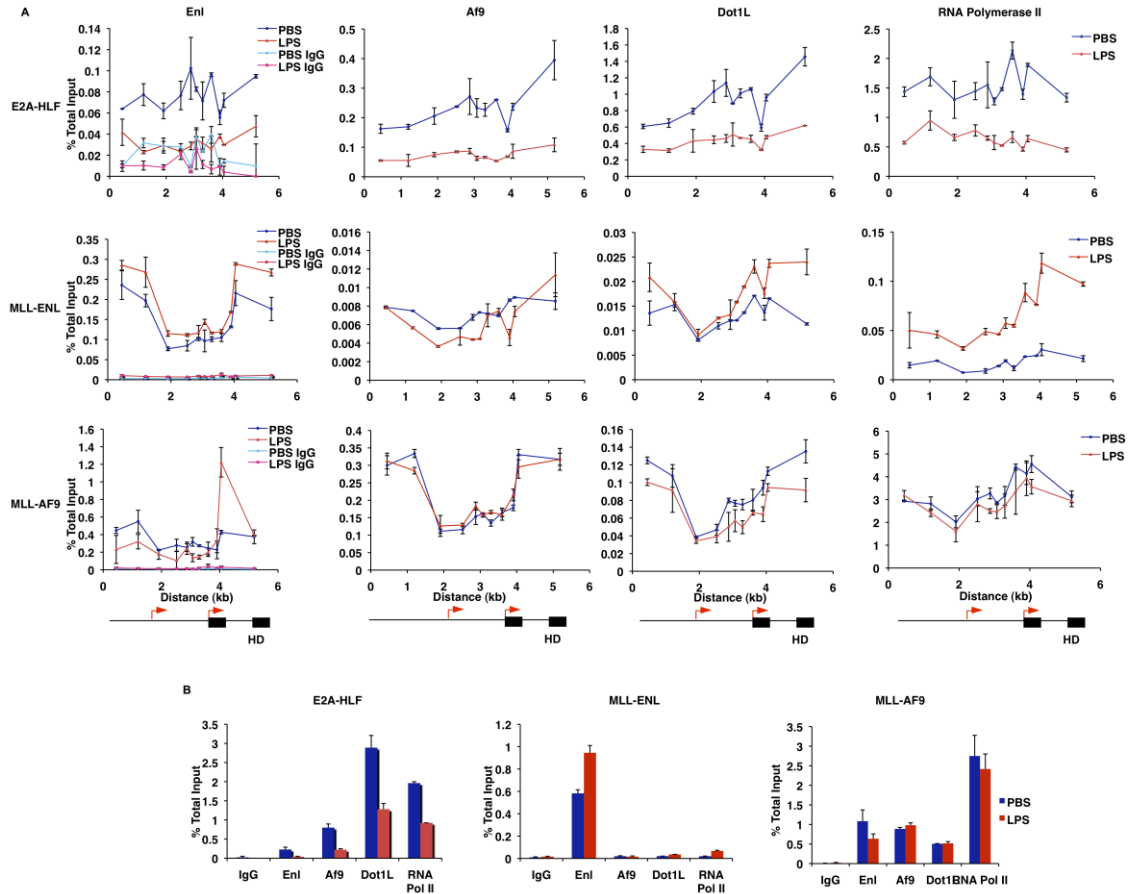
Figure 3.18 Dissociation of EAP from target loci after LPS treatment A) ChIP-qPCR for EAP components across *Hoxa9* in leukemia cell lines after 24 hours of LPS treatment. Schematics of *Hoxa9* are depicted below the graphs, with red arrows indicating transcription start sites and black boxes indicating exons. HD is the homeodomain-encoding exon. B) ChIP-qPCR for binding in the coding region of *Meis1*. Note that each cell line was subjected to experimentation on different days. Thus, % Total Inputs may not be directly comparable between the three cell lines for technical reasons such as differences in antibody and sample preparation.

60

Discussion

Mechanism of the Fusion Partner

The mechanism by which MLL translocation partners deregulate transcription is beginning to be defined. One of the first insights was provided by Bitoun et al. who identified proteins in human embryonic kidney cells that associate with the MLL translocation partner AF4, including ENL, AF5q31, CDK9 and CYCLIN T1 [119]. AF4, in association with ENL and AF9, was found to stimulate activity of the RNA polymerase II (RNA Pol II)-CTD kinase pTEFb and the histone methyltransferase DOT1L. Subsequently, we reported a complex of proteins termed EAP for ENL-associated Proteins or Elongation Assisting Proteins that interacts with the MLL translocation partner ENL in 293 cells [105]. EAP is similar to the complex reported by Bitoun et al. but includes a number of additional interacting proteins such as AF10, PC3, RING1b and others. Importantly, the amino acids in ENL that directly interact with DOT1L were found to be essential for MLL-ENL to transform bone marrow progenitors. This, together with earlier data showing that the MLL-DOT1L fusion is sufficient for leukemic transformation [98], suggested that DOT1L methyltransferase activity is crucial for *HOX* gene deregulation and transformation seen in leukemias with *MLL* rearrangements.

pTEFb, which interacts with AF4 family members [99,100,120] has also been shown to be critical to MLL fusion protein-mediated transformation [100]. Yokoyama et al highlight the importance of pTEFb, which is shown to be part of a core complex termed AEP that is physically distinct from the DOT1L complex.

They show that fusing the pTEFb-interacting domain of AF4 family members to MLL is necessary and sufficient for leukemic transformation, while contrary to a previous report [98], DOT1L is not sufficient. However, the authors do not rule out the importance of DOT1L to transformation. Thus, both CTD kinase and histone methyl transferase activities of MLL fusion protein complexes appear to be critical to their ability to aberrantly activate the expression of leukemogenic genes.

Significance

Deregulation of the *A* cluster *HOX* genes and *MEIS1* is emerging as a very common mechanism of transformation in acute leukemia [34]. It is also becoming apparent that controlling transcriptional elongation plays a central role in regulating transcription at these loci. The *Drosophila Hox* genes *Ultrabithorax* and *Abdominal-B*, for example, have Pol II associated with their proximal promoters, even though they are not expressed [121]. Similarly, Pol II is also present at silenced genes in mammalian cells [122]. Furthermore, mutations in elongation factors elongin A or Cdk9 result in homeotic defects associated with Pol II stalling [123].

Just as transcriptional elongation is regulated in the developing embryo, deregulation of transcriptional elongation is emerging as an important mechanism in growth regulation and oncogenesis. For example, high levels of CDK9 expression are associated with a variety of solid tumors including neuroblastoma, primitive neuroectodermal tumors, prostate cancer and a wide range of lymphomas [124]. The mechanisms regulating CDK9 association with

promoters are incompletely defined. In some cases, recruitment appears to mediated by the bromodomain containing-protein BRD4, while in other cases, specific transcription factors such as MYC recruit pTEFb directly [97]. From work presented here and in previous experiments [105,119], it now is clear that another recruitment mechanism, particularly important for *Hox* gene regulation, involves interactions with the EAP complex.

The amount of evidence showing that deregulated recruitment of DOT1L plays a role in oncogenesis is also increasing rapidly. One of the first connections was that DOT1L interacts with the MLL translocation partner AF10 and that its methyltransferase activity is important for MLL fusion protein-mediated transformation [98]. Subsequent studies and the work reported here implicate DOT1L in transformation by other MLL fusion proteins (MLL-AF4, MLL-ENL, MLL-AF9) as well as by the CALM-AF10 translocation in AML and SET-NUP214 in T-ALL [50,89,105]. As is the case for pTEFb, the mechanisms regulating DOT1L association with target loci are poorly understood.

By association with the EAP complex, both CDK9 and DOT1L would be coordinately recruited to target promoters such as the *HOX* loci. While many mechanisms are possible, one possibility is that EAP is recruited via the YEATs domains in AF9 or ENL, which bind histones H1 and H3 [77], wild-type MLL [15,73], or AF10's PHD finger, a domain that binds trimethylated histone 3 in other proteins [15,125]. The central role of AF9 and ENL in transcriptional regulation of the *HOX* loci is highlighted by the histone H3 lysine 79 demethylation and loss of *HOX* transcription with ENL knockdown [105] and by

63

the finding that Af9 knockout mice show homeotic transformations and posterior

shifts in *Hox* gene expression [115]. Importantly, our experiments show that EAP

association with target loci is dynamic and under active regulation, as the

complex rapidly dissociates from the *Hox* and *Meis* loci within 4 hours of

treatment with differentiation-inducing agents.

A number of possible models can be imagined for how the EAP complex

results in persistent high-level *Hox* transcription in cells with MLL fusion proteins.

The finding of increased levels of EAP subunits in the presence of MLL fusion

proteins and the lack of silencing of the *Hox* and *Meis* loci in these cells in

response to induction of differentiation suggests the model shown in Fig. 3.19. In

this model, fusion of EAP subunits to N-terminal MLL sequences, as occurs in

mixed lineage leukemia, alters association of the EAP complex so that levels of

the complex are increased and dissociation is impaired. This results in persistent

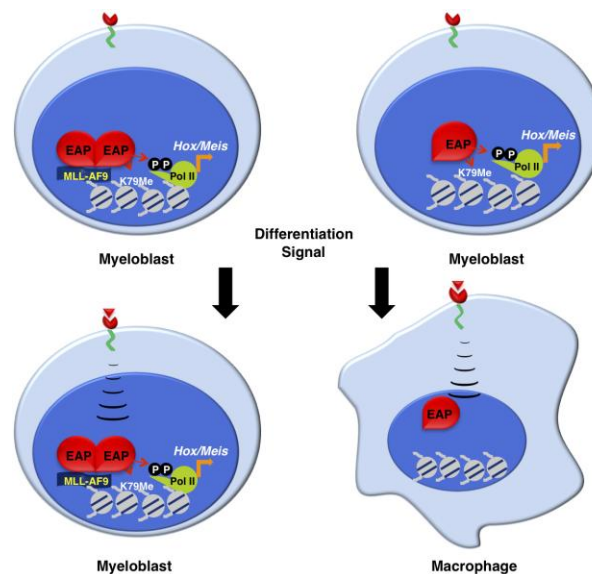*Hox* and *Meis* gene expression in spite of differentiation signaling cues.

Figure 3.19 Model for EAP regulation of *Hox* genes in hematopoietic cells with
and lacking *MLL* rearrangements

Remaining questions

Other activities of EAP

There are other potential activities of the EAP complex that have yet to be explored. A robust phospho-Ser5 activity on RNA polymerase II was detected after immuno-purification of AF9$^{C\text{-term}}$-associated proteins from M1 cells and incubation with recombinant CTD (Fig. 3.20). Interestingly, a higher weight band at the expected size of endogenous hyper-phosphorylated RNA polymerase II was detected as well. This indicates that AF9 $^{C\text{-term}}$ associates with either hyper-phosphorylated RNA polymerase II or hypo-phosphorylated RNA polymerase II that was phosphorylated in the kinase reaction.
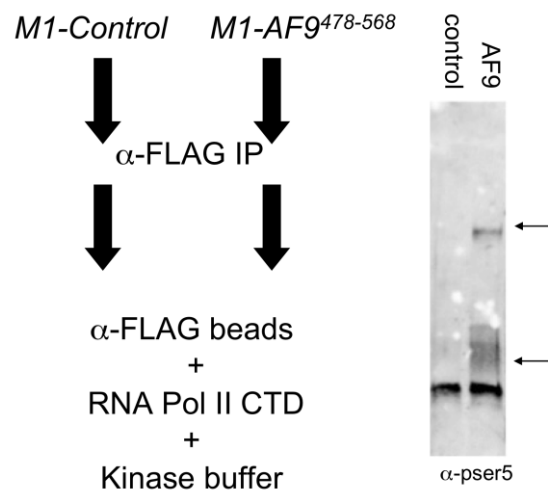

Figure 3.20 phospho-Ser5 CTD kinase activity of EAP A schematic of the experimental design is shown on the left. After immunoprecipitation and washing, FLAG beads were incubated with recombinant RNA polymerase II CTD in a kinase reaction mixture that contains ATP. On the right, is a blot for phospho-Ser5 after the kinase reaction. The arrows indicate Ser 5 phosphorylated recombinant CTD (lower arrow) and hyper-phosphorylated RNA polymerase II (upper arrow).

ChIP data show that MLL fusion protein-transformed cells have elevated levels of phospho-Ser5 (Fig. 3.9) and in the case of MLL-ENL, RNA polymerase II, and

mass spectrometric-based analysis (Table 4) of AF9 $^{C\text{-term}}$ -associating proteins

identified 13 subunits of the Mediator complex (Table 3.3), which is involved in

assembly of the pre-initiation complex and bridges RNA polymerase II to

transcription factors. Altogether, these data implicate EAP in early steps of RNA

polymerase II maturation.

There are many CDKs that are reported to phosphorylate Ser5 of RNA

polymerase II, such as CDK7 and CDK1, the latter of which was identified by

mass spectrometry to associate with AF9 $^{C\text{-term}}$. By Western blot, an association

with the transforming domain of AF9 was weakly detected (Fig. 3.21A). However,

ChIP for CDK1 at the *Hoxa9* locus of MLL-ENL-transformed cells shows that it is

present, while there is barely any CDK1 detectable at *Hoxa9* in the E2A-HLF-
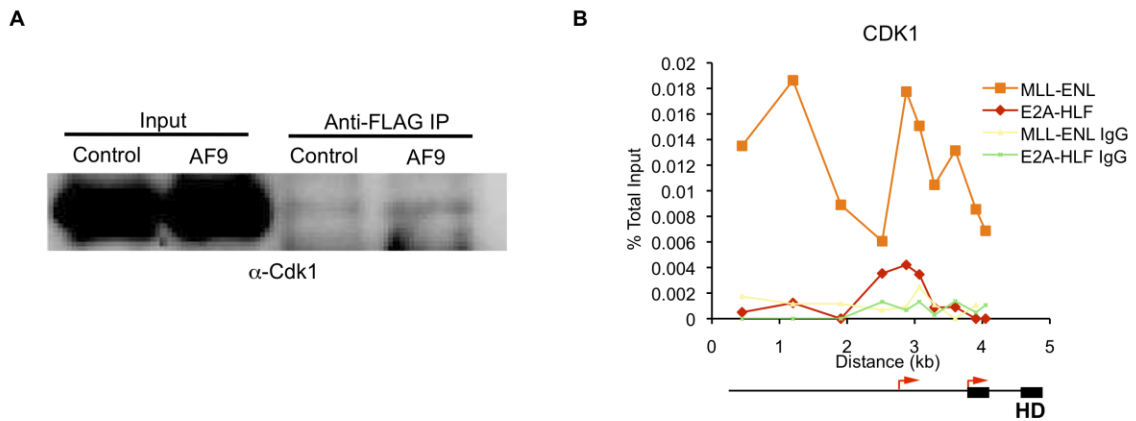
transformed cells (Fig. 3.21B).

Figure 3.21 Association of CDK1 with EAP A) Western blot for CDK1 after AF9 $^{C\text{-term}}$ purification from M1 cells. B) ChIP-qPCR for CDK1 at *Hoxa9* in fusion-transformed cells. Schematics of *Hoxa9* are depicted below the graphs, with red arrows indicating transcription start sites and black boxes indicating exons. HD is the homeodomain-encoding exon.

Thus, CDK1 is associated with the *Hoxa9* locus, however a close connection with the EAP complex is not convincing. It is worth exploring whether other kinases may be responsible for Ser5 phosphorylation of RNA polymerase II seen in the in vitro assay. The other possibility is that pTEFb has the ability to phosphorylate Ser5 in these experimental conditions.

Regulation of EAP

Defining how cell signaling pathways impinge upon EAP's activity and association with DNA is another important topic for future investigation. It is noteworthy in this regard that both Lilliputian, the *Drosophila* homolog of AF4/FMR2, and Dot1 appear to be downstream effectors of the RAS signaling pathway [126]. Dot1L is also linked to the Wnt signaling pathway, which is essential to the development of leukemia cells [101,127]. In our experiments, we identified many phospho-sites in several different EAP components. Interestingly, a motif that is recurrent in many EAP subunits was phosphorylated in LAF4, AF5q31, Cyclin T2, and AF9 (Fig. 3.22).

NELLpSPLKDSDEVR (LAF4)
SSpSPGKPQAVSSLSSSHSR (AF5q31)
HGPAQAVTGTSVTpSPIK (Cyclin T2)
NQILEVKpSPIK (AF9)

Figure 3.22 CDK consensus site in EAP components CDK consensus site is in red. Peptides are from EAP components indicated to the right. "p" indicates phosphorylated serines identified by mass spectrometry.

This motif, SPXK, is a CDK consensus site [128] and is found in critical domains of EAP components, including the transactivation domain of AF9 and the histone methyl transferase domain of Dot1L. It is also found among the AT hooks of MLL and other DNA binding proteins. Furthermore, a study predicting substrates of

CDK1 identifies Dot1L and the MLL homolog ASH1 as potential substrates [129].

In order to explore whether phosphorylation might be an important mode of regulation of the EAP complex, we immunoprecipitated AF9 $^{C-term}$ from M1 cells after PBS or LPS treatment and blotted with phospho-threonine and phospho-serine antibodies (Fig. 3.23, left). Interestingly, we found a downward shift in migration of a band corresponding to the size of AF9 $^{C-term}$ (Fig. 3.23, left), possibly indicating that AF9 $^{C-term}$ is dephoshorylated in response to IL-6 signaling. However, an anti-FLAG blot for FLAG-AF9 $^{C-term}$ is necessary to ensure that these bands are reflecting changes in AF9^{C-term} rather than some other protein.
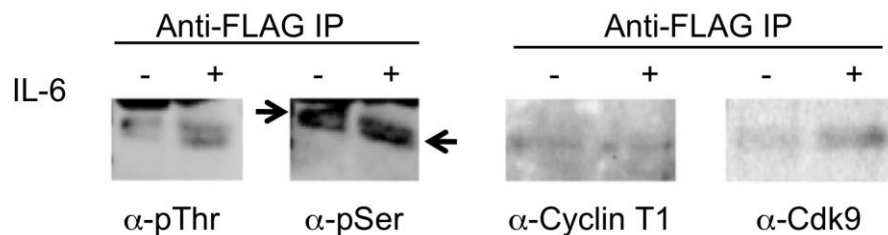

Figure 3.23 Western blot for AF9 $^{C-term}$ -associating proteins after 24 hours of IL-6 treatment FLAG-Control or FLAG-AF9^{C-term} was IP'ed from IL-6-treated M1-AF9 $^{C-term}$ cells. Arrows indicate what are proposed to be the hyper- and hypo-phosphorylated forms of AF9. Antibodies used for detection are indicated below the blots.

To determine if this modification altered AF9 $^{C-term}$'s ability to interact with other EAP subunits, we blotted for Cyclin T1 and Cdk9 as well (Fig. 3.23, right). These two associations were retained in spite of the modifications to AF9^{C-term}. Thus, it could be hypothesized that IL-6 signaling, which induces differentiation through the JAK-STAT pathway in M1 cells [130], leads to the dissociation of AF9 $^{C-term}$ and pTEFb from DNA (Fig. 3.15), possibly through direct or indirect post-

translational modifications (PTMs) of AF9$^{C\text{-term}}$. However, these EAP components

remain associated together. It is possible that they relocate to other genes or are

sequestered away as an inactive complex. Whether other associations such as

those with Dot1L and the Polycomb proteins are maintained in response to

differentiation was not tested. It will be interesting to see to what extent this

complex remains associated in different physiological conditions.

Of further interest is the identification of signaling pathways that maintain

or enhance EAP associations and enzymatic activity. Firstly, it is important to

know which phosphorylation or other PTM sites are critical to localization, protein

and DNA interactions, and enzymatic activities and to identify the enzymes

responsible for them. This may reveal new therapeutic targets, such as kinases,

phosphatases, and other enzymes that are aberrantly activated in *MLL*-

rearranged leukemias.

EAP association with transcriptional repressors

Paradoxically, we and other groups identified transcriptional repressors in

association with AF9 and ENL [78,79,131]. Preliminary experiments show that

the MLL fusion-transformed cells have higher levels of Pc3 and Ring1b at *Hoxa9*

and *Meis1* than the E2A-HLF-transformed cells (Fig. 3.24), which have much

lower levels of expression of these genes (Fig. 3.6). Their binding appears to be

independent of H3K27 and H3K9 repressive marks, which are similar between

the two cell lines (Fig. 3.24). Furthermore, Ring1b dissociates along with

transcriptional activators in response to IL-6-induced *Hoxa9* downregulation (Fig.

3.25). We also assessed binding of Polycomb proteins and associating

repressive marks at the *Hoxa9* locus after LPS treatment. In E2A-HLF

transformed cells that experience reductions in *Hoxa9* after LPS treatment (Fig.

3.17C), Ring1b remains at the locus, while Pc3 dissociates (Fig. 3.26A, top

graphs). There are slight decreases in H3K27 trimethylation and increases in

H3K9 trimethylation, which are histone marks associated with silenced genes

(Fig. 3.26A, bottom graphs). In the MLL fusion protein-transformed cells, which

maintain *Hoxa9* expression after LPS treatment, both Pc3 and Ring1b dissociate

from *Hoxa9* (Fig. 3.26B, C, top panels). H3K9 and H3K27 trimethylation levels

remain unchanged or decrease at *Hoxa9* in these cells (Fig. 3.26B, C, bottom

panels). One explanation is that a proper balance of the Polycomb proteins is

important to maintaining the structural integrity of the EAP complex. However, it

is also possible that they have yet to be discovered roles in transcriptional

regulation. Indeed, ongoing experiments are revealing that Polycomb proteins

have roles in transcriptional activation during leukemogenesis (Jiaying Tan, Hess

lab). Other groups have also implicated Ring1b and other Polycomb proteins in

the activation of *Hox* genes during embryonic development and propose that they

may be required for H3K9 acetylation, a mark associated with transcriptionally
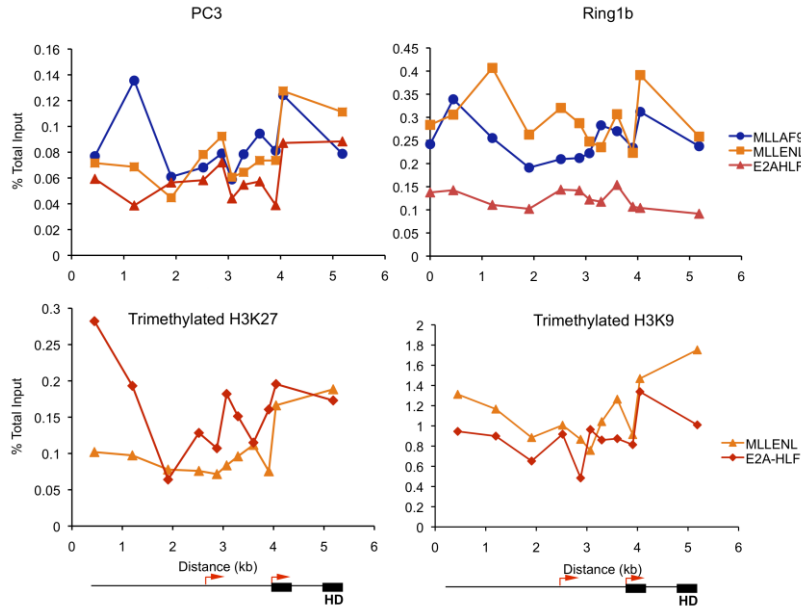
active genes [132,133].

Figure 3.24 Polycomb binding at *Hoxa9* ChIP-qPCR for Polycomb proteins and associating repressive histone marks. Schematics of *Hoxa9* are depicted below the graphs, with red arrows indicating transcription start sites and black boxes indicating exons. HD is the homeodomain-encoding exon. IgG controls are shown in Fig. 3.36 for top panel and Fig. 3.21 for bottom panel.
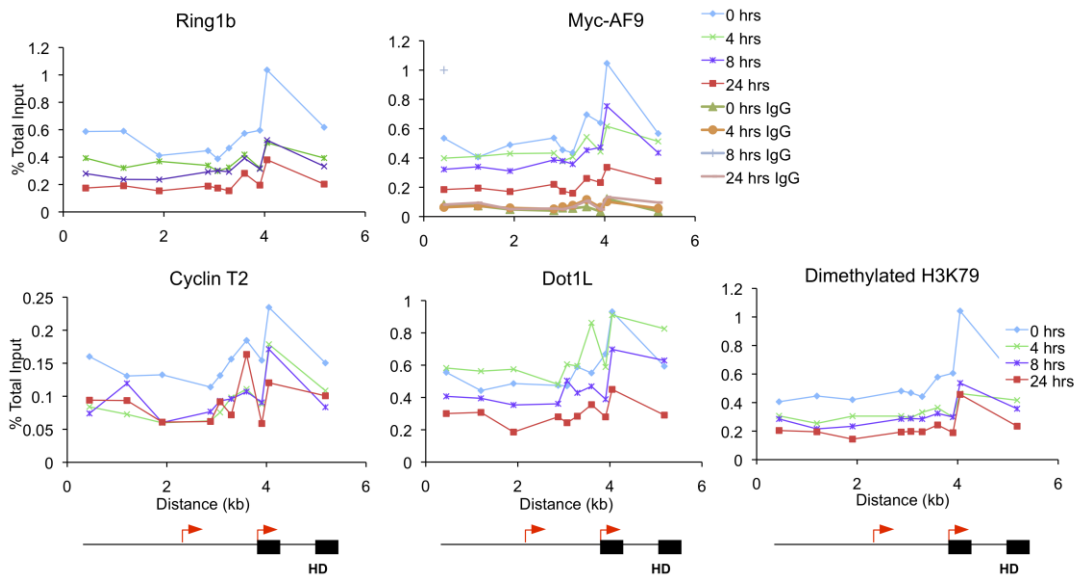

Figure. 3.25 Dissociation of Ring1b from *Hoxa9* locus in differentiating M1-AF9 [C-term] cells ChIP-qPCR for Ring1b and transcriptional activators at *Hoxa9* after 24 hour IL-6 treatment. Schematics of *Hoxa9* are depicted below the graphs, with red arrows indicating transcription start sites and black boxes indicating exons. HD is the homeodomain-encoding exon.

Figure 3.26 Polycomb dissociation from *Hoxa9* after 24 hours of LPS treatment
ChIP-qPCR for Polycomb proteins and associating repressive histone marks.
Schematics of *Hoxa9* are depicted below the graphs, with red arrows indicating
transcription start sites and black boxes indicating exons. HD is the
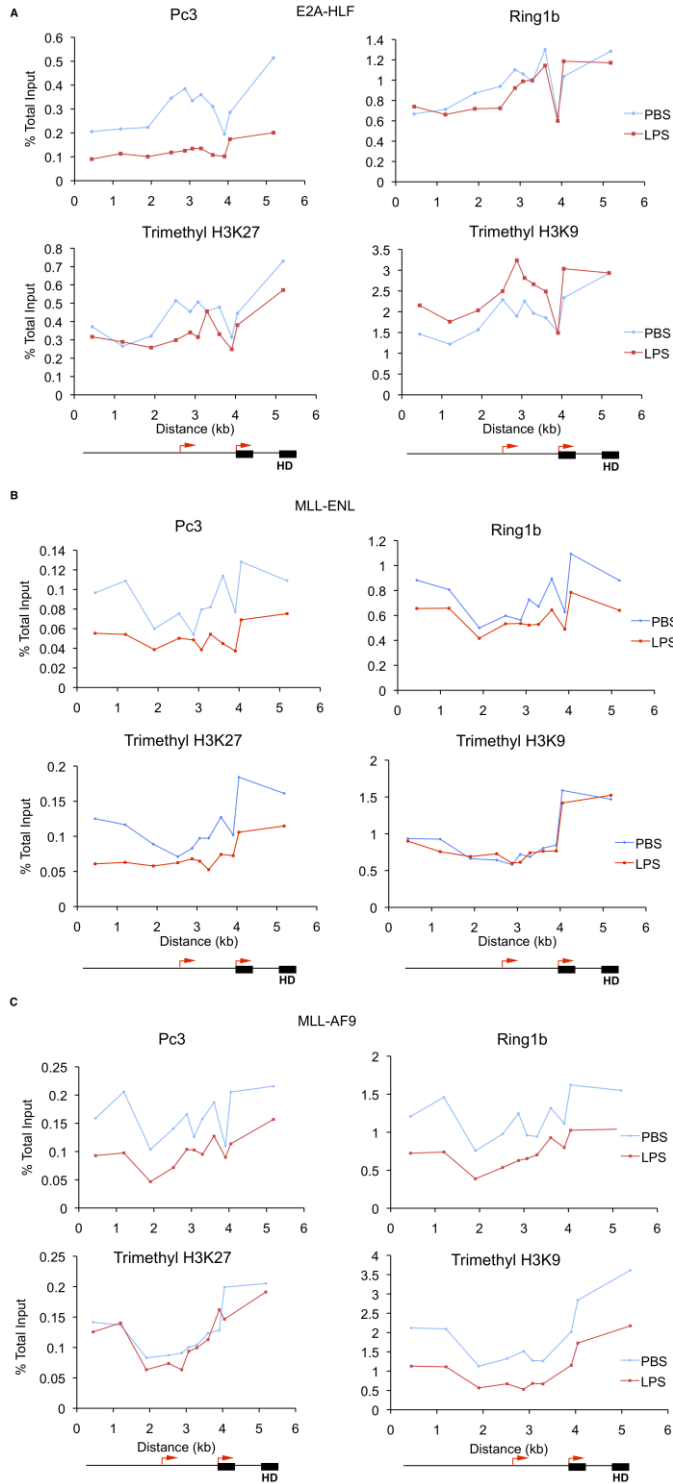homeodomain-encoding exon.

The pTEFb inhibitors HEXIM1 and HEXIM2 were also found to associate with AF9 [C-term]. The HEXIM proteins, in association with 7SK snRNA, inhibit the catalytic activity of CDK9 and are thought to sequester pTEFb away from DNA [103]. Our finding that AF9 [C-term] associates with these inhibitory constituents indicates that there is either a separate EAP inhibitory complex sequestered away from DNA or that HEXIM is at AF9 [C-term] target loci. We performed ChIP to explore whether HEXIM localizes to DNA with the active EAP complex and indeed detected HEXIM1 at *Hoxa9*, with similar amounts between the E2A-HLF and MLL-ENL-transformed cells (Fig. 3.27A). HEXIM1 levels are present at significantly higher levels at *Meis1* in the E2A-HLF cells (Fig. 3.27B), which have barely detectable *Meis1* expression.

We also tested for the presence of the HEXIM-interacting protein Nucleophosmin 1 (Npm1) [134]. NPM1 is a multi-functional protein, with roles in ribosome biogenesis, genomic stability, histone chaperoning, protein stabilization, and transcriptional regulation, among many others [135]. We found that Npm1 also localizes to *Hoxa9* and *Meis1*, with higher levels in the low-expressing E2A-HLF transformed cells (Fig. 3.27A, B). Of note, while MLL fusion proteins express *Hexim1* at levels similar to E2A-HLF-transformed cells, they express less *Hexim2* and *Npm1* (Fig. 3.27C). Thus, the differences in Npm1 levels found by ChIP-qPCR at the *Hoxa9* and *Meis1* loci may be due to differences in expression at the transcriptional level.
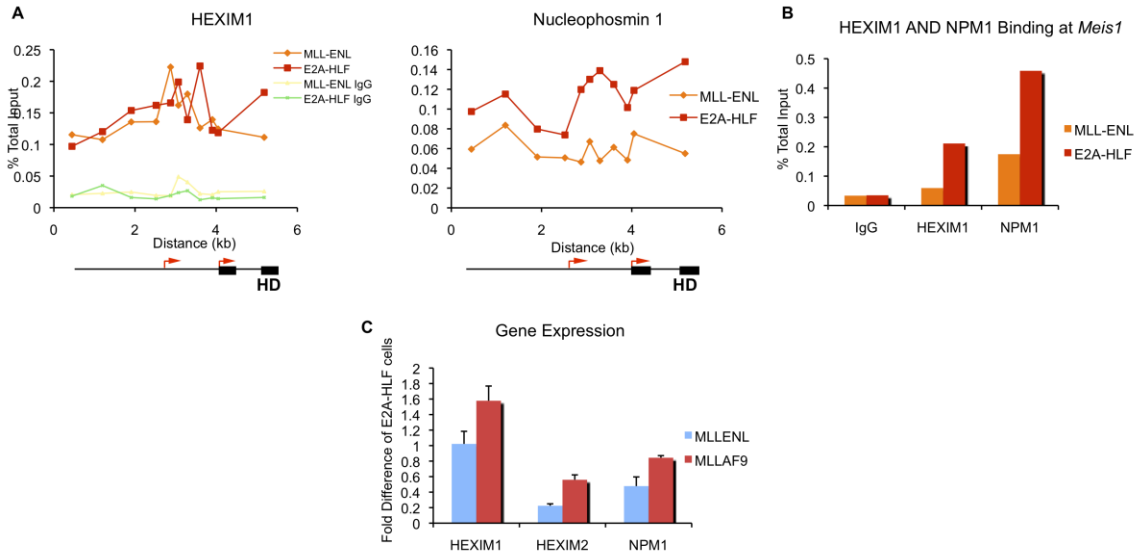
Figure 3.27 HEXIM and NPM1 expression and localization in fusion transformed cell lines A) ChIP for HEXIM1 and NPM1 at *Hoxa9*. Schematics of *Hoxa9* are depicted below the graphs, with red arrows indicating transcription start sites and black boxes indicating exons. HD is the homeodomain-encoding exon. B) Binding at coding region of *Meis1*. C) qPCR for expression of *Hexim1*, *Hexim2*, and *Npm*1 in the fusion-transformed cell lines normalized to *Gapdh*.

We also analyzed Hexim1 and Npm1 localization in M1 cells that express the transforming domain of AF9 or a control fragment with the hypothesis that AF9 may hinder Hexim and Npm1 binding to the active locus. These experiments showed that the M1-AF9 [C-term] cells had approximately two-fold less Hexim1 and Npm1 at the *Hoxa9* and *Meis1* loci (Fig. 3.28A, B).
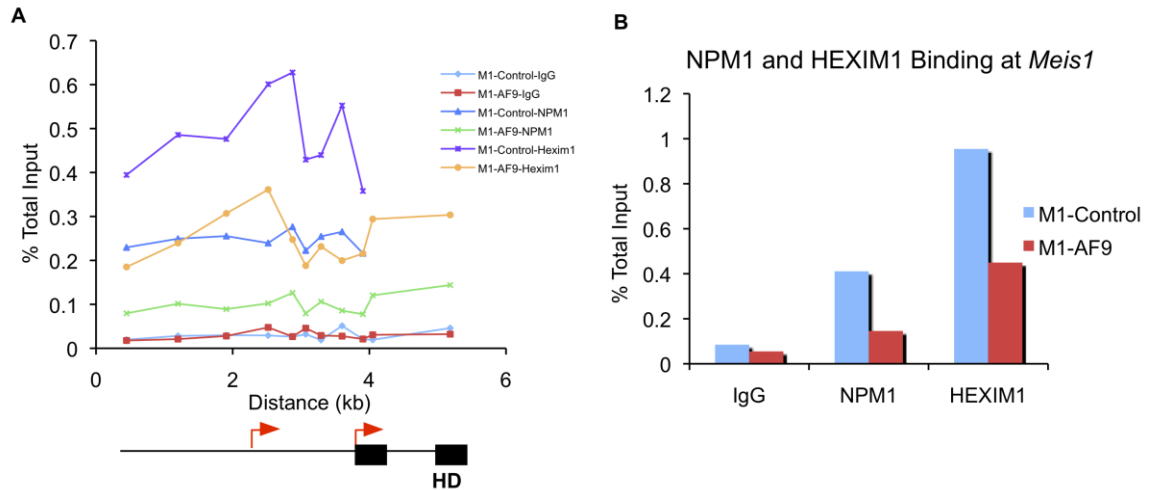
Figure 3.28 Hexim1 and Npm1 localization in M1-control and M1-AF9 $^{C\text{-}term}$ cell lines A) ChIP-qPCR for HEXIM1 and NPM1 at *Hoxa9*. Schematics of *Hoxa9* are depicted below the graphs, with red arrows indicating transcription start sites and black boxes indicating exons. HD is the homeodomain-encoding exon. B) Binding at coding region of *Meis1*.

Interestingly, MLL fusion protein-transformed cells are highly resistant to the chemical HMBA (Fig. 3.29A), which upregulates *HEXIM* expression and leads to the differentiation of myeloid leukemia cells [136]. It will be interesting to determine whether Hexim levels increase at *Hoxa9* in HMBA-treated E2A-HLF cells and whether HMBA-treated MLL fusion protein-transformed cells are able to block this localization. The results obtained thus far indicate that MLL-ENL transformed cells avoid HMBA-induced *Hexim* upregulation at the transcriptional level, while MLL-AF9 and E2A-HLF-transformed cells have increased levels of *Hexim1 or 2* in response to HMBA (Fig. 3.29B). All cell lines experience slight increases in *Npm1* expression (Fig. 3.29B). Thus, this may be a system in which to test for localization of Npm1 and Hexim proteins to *Hox* and *Meis* loci. Forcing the expression of *HEXIM1* and *NPM1* by retroviral transduction in different hematopoietic cell lines is another approach to testing whether these proteins are

75

recruited to *Hoxa9* to inhibit transcription and if MLL fusion proteins block this
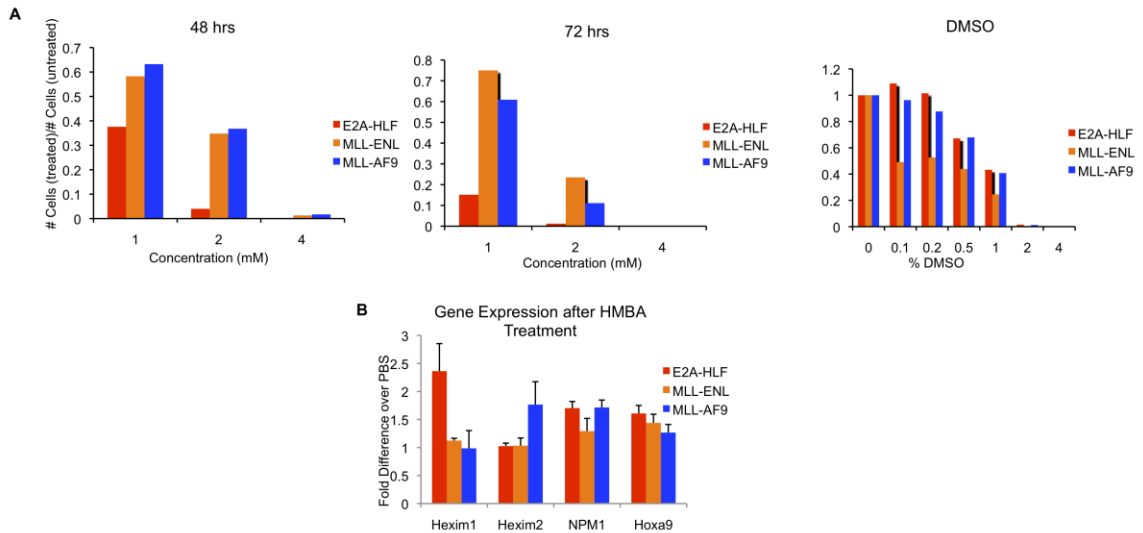
recruitment.

Figure 3.29 Sensitivity of fusion-transformed cell lines to HMBA A) Cell count
after 48 (left) and 72 (middle) hour treatments with HMBA. Control DMSO
treatment (right) was used to assess general sensitivity of the cell lines. B)
Expression of *Hexim1*, *Hexim2*, *Npm1*, and *Hoxa9* after 24 hour HMBA
treatment. Data are normalized to *U2 snRNA*.

We began to explore how Npm1 and Hexim localization are altered during

changes in *Hoxa9* expression in the LPS differentiation system. These

preliminary results do not show changes in the levels of these proteins at the

locus, but rather a possible change in the distribution that may impact *Hox*a9

expression (Fig. 3.30). Upon LPS treatment of E2A-HLF-transformed cells and

Hoxa9 down-regulation, Npm1 and Hexim1 appear to occupy the coding region

of the gene. In the MLL fusion transformed cells, which do not show decreases in

Hoxa9 expression in response to LPS, Npm1 and Hexim1 appear to be confined

to the promoter region. Thus, Npm1 and Hexim1 may exert their inhibitory

functions on the elongation machinery, as would be expected from the role of

pTEFb in transcriptional elongation.

76
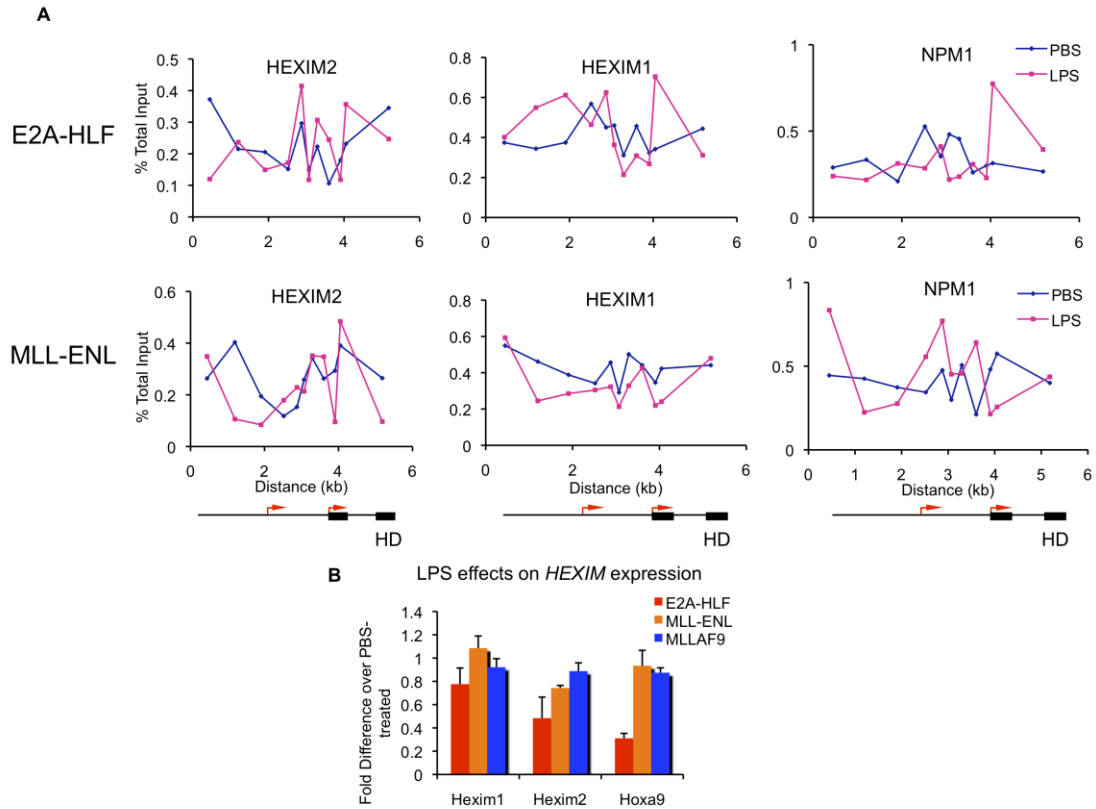
Figure 3.30 Hexim and Npm1 expression and localization after 24 hours of LPS treatments A) ChIP for HEXIM1 and NPM1 at *Hoxa9* Schematics of Hoxa9 are depicted below the graphs, with red arrows indicating transcription start sites and black boxes indicating exons. HD is the homeodomain-encoding exon. B) Expression of *HEXIM1*, *HEXIM2*, and *Hoxa9* after LPS treatment. Data are normalized to *Gapdh*.

Further studies show that NPM1 represses *Hoxa9* expression. In luciferase reporter assays using 293 cell transfectants, NPM1 was shown to repress MLL-fusion protein-mediated transactivation (Fig. 3.31), and this effect was potentiated by co-transfection with HEXIM1. In addition, a mutant of NPM1, NPMC+, that localizes to the cytoplasm and sequesters HEXIM1 [134] leads to activation of *Hoxa9* promoter activity. Importantly, NPMC+ is the most common mutation found in leukemia, present in one third of all adult leukemias, and it is

77

associated with the upregulation of *HOX* genes [137,138]. Thus, it appears that

NPM1 may have important roles in directly regulating *HOX* expression.

Effects of HEXIM1 and NPM on *Hoxa9* Promoter Activity
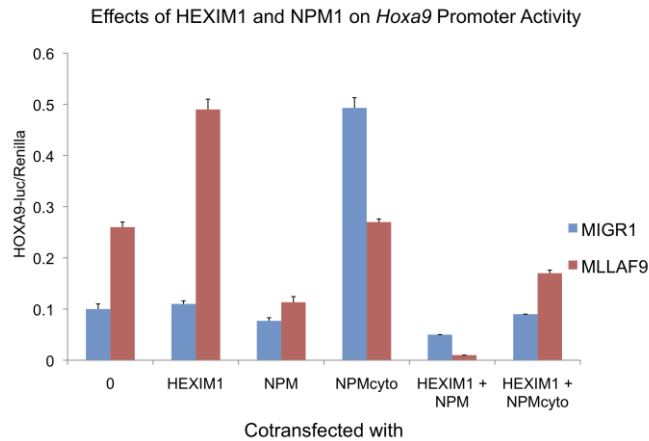
Figure 3.31 Effects of NPM1 and HEXIM1 on MLL fusion protein-mediated *Hoxa9* activation Luciferase reporter assay expressing luciferase from a *Hoxa9* promoter after transfection with the plasmids indicated below.

   We moved into a hematopoietic system to test whether NPM1 and

NPMC+ have effects on *Hox* expression and *Hox*-mediated leukemic

transformation. Preliminary experiments show that MLL-AF9 loses its ability to

form leukemic colonies from hematopoietic progenitor cells in the presence of

NPM1 (Fig. 3.32). Whether this is due to NPM1's direct antagonism of MLL-AF9

remains to be seen.
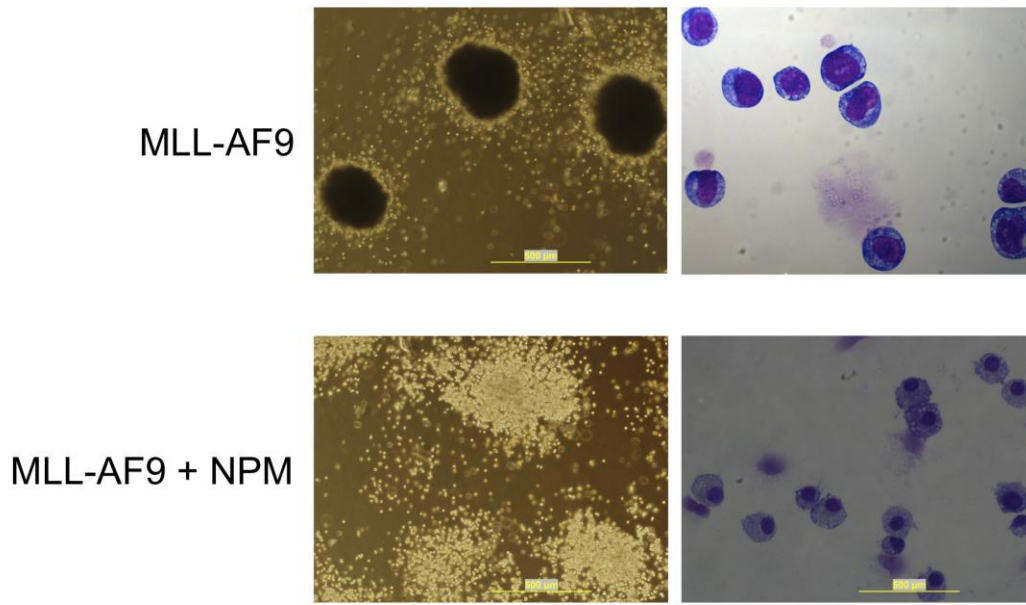
Figure 3.32 NPM1 inhibition of MLL-AF9-mediated leukemogenesis Methyl cellulose cultures (left) showing MLL-AF9 loses its ability to form large, compact colonies in the presence of NPM (lower panel). Wright-Giemsa staining shows myeloblast that form after MLL-AF9 transduction and monocytic cells when NPM is co-transduced with MLL-AF9 (bottom right).

Further, we tested whether the cytoplasmic mutant, NPMC+ could lead to leukemic transformation alone or in cooperation with another oncoprotein, FLT3-ITD, which is commonly found in leukemias with NPMC+ [139]. The expression of NPMC+ alone in hematopoietic cells does lead to the activation of *Hoxa9* (Fig. 3.33), and this effect is enhanced by co-transduction with FLT3-ITD (Fig. 3.33). However, NPMC+ alone was not sufficient to lead to leukemic colony formation in methyl cellulose.
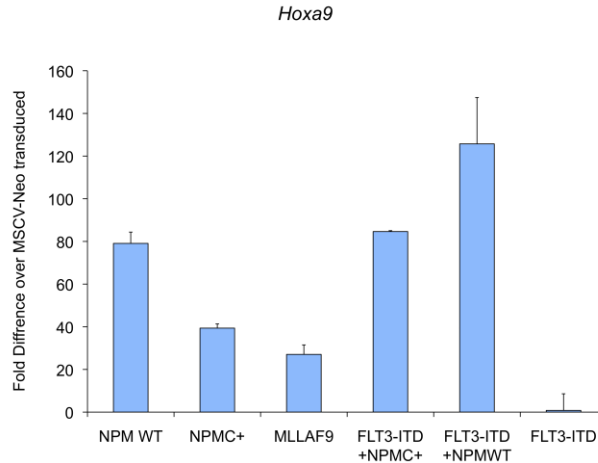
Hoxa9

Figure 3.33 FLT3-ITD and NPM1 effects on *Hoxa9* expression qPCR detection of *Hoxa9* expression after one week of retroviral transduction with the constructs indicated along the x-axis. Results are expressed as fold difference over MSCV-transduced cells. Data are normalized to *Gapdh*.

Transduction with NPMC+ and FLT3-ITD did lead to the formation of very large, atypical colonies that exhibit high levels of *Hoxa9* expression and uncontrolled cell growth. However, this phenotype does not appear to be due to the loss of NPM's nuclear function as the phenotype was greatly potentiated by the combination of wild-type NPM1 and FLT3-ITD (Fig. 3.34)
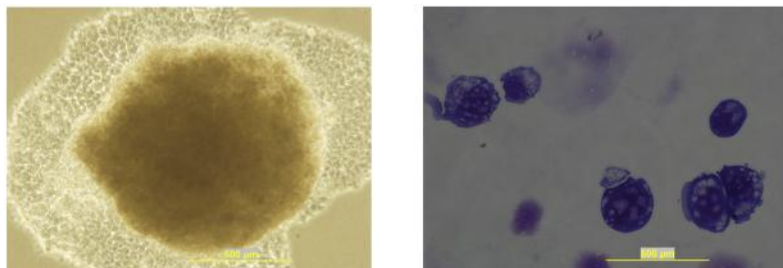
Figure 3.34 Morphology of hematopoietic cells co-transduced with FLT3-ITD and NPM1 Methyl cellulose colonies (left) show cohesive cells that develop after co-transduction of NPM1 and FLT3-ITD. Wright-Giemsa staining reveals high nuclear to cytoplasmic ratio indicating that they may be neoplastic.

These cells do not appear to express hematopoietic lineage markers. It is possible that a non-hematopoietic cell was transformed to yield these colonies, or more provocatively, that a hematopoietic cell trans-differentiated into another cell type in response to the combination of FLT3-ITD and NPM1. These phenomena require more investigation to identify the cell type and the cell that it originated from.

Redundancy in EAP

Many of the interactions identified with AF9 raise the possibility of redundancy between subunits. There is structural and functional homology among, LAF4, AF5q31, and AF4, CYCLIN T1 and CYCLIN T2, and AF9 and ENL. One possibility is that they exist in distinct complexes, potentially at different target genes. The fact that we were never able to observe Cyclin T1 at *Hoxa9* in murine or human leukemia cells may indicate that Cyclin T2 is the primary regulator of *Hox* genes.

Similarly, relatively low levels of Af9 were detected at *Hoxa9* and *Meis1* in MLL-ENL transformed cells (Fig. 3.7), possibly suggesting that MLL-ENL does not require Af9 for transcriptional activation. Furthermore, Enl and AF9 were weakly identified as interacting proteins with AF9$^{C\text{-term}}$ and ENL, respectively (Table 3.3, [105]). It should be noted that, in these experiments, MLL-AF9 appears to be a weaker oncogene than MLL-ENL with regards to *Hoxa9* and *Meis1* expression (Fig. 3.6) and RNA polymerase II-associated factors (Fig. 3.9). This may be due to the fact that MLL-AF9 is expressed at 25% the levels of MLL-ENL (Fig. 3.35).
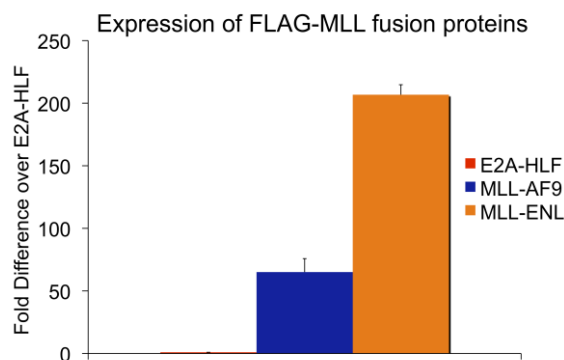
Figure 3.35 Expression of FLAG-MLL fusion proteins in MLL fusion transformed cells qPCR detection of MLL fusion proteins in fusion transformed cell lines priming FLAG sequence and N-terminal MLL sequence. Data are normalized to *Gapdh*.

However, another possibility is that MLL-ENL, which contains most of the ENL protein, has a greater capacity to interact with positive regulators of transcription than the 90 C-terminal residues of AF9 found in the MLL-AF9 used in these experiments. For instance, MLL-ENL contains the histone binding YEATS domain that possibly aids in efficient targeting to loci, while MLL-AF9 lacks this domain. MLL-AF9 does recruit Enl to *Hoxa9* and *Meis1* (Fig. 3.7). Thus, in cases of *MLL*-rearranged leukemias, where much of AF9 or ENL may be lost from the translocation, there may be advantages to having both AF9 and ENL at target loci, and the importance of these proteins to each other, even given the weak association, has not been ruled out.

A preliminary ChIP experiment indicates that both AF4 and AF5q31 are present at the *Hoxa9* locus (Fig. 3.36). Thus, two or more of the FMR2 proteins may function together. In support of this, AF4 and AF5q31 were shown to preferentially heterodimerize through their C-terminal domains [100]. The precise role of these proteins remains to be defined. They do not appear to differ greatly

in their levels at *Hoxa9* between the E2A-HLF and MLL fusion transformed cells.

Thus, there may be differences in their ability to stimulate pTEFb activity [119]

through some yet to be discovered mechanism that regulates FMR2 protein

activity or associations.
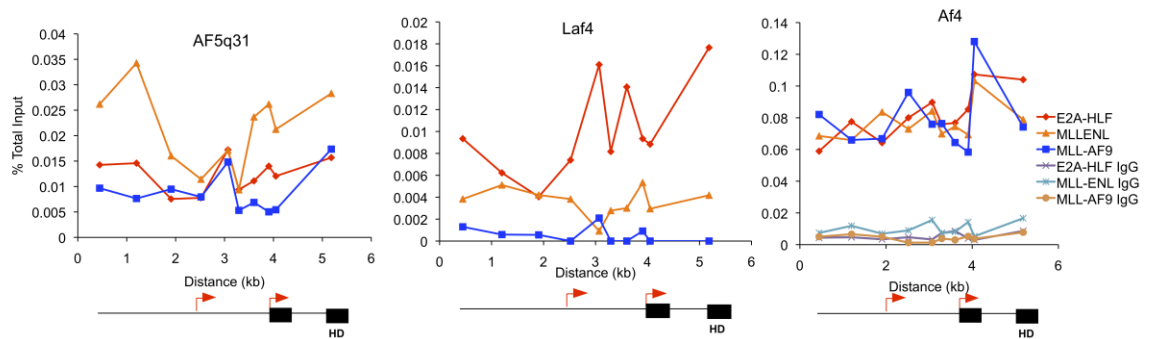
Figure 3.36 FMR2 family member binding at *Hoxa9* Schematics of *Hoxa9* are depicted below the graphs, with red arrows indicating transcription start sites and black boxes indicating exons. HD is the homeodomain-encoding exon.

Hierarchy of EAP

The hierarchy in EAP remains unclear. Thus far, data have been

presented suggesting that pTEFb, in association with AF4 members and ENL, is

sufficient for MLL fusion protein-mediated leukemogenesis, with other events

such as Dot1L activity occurring downstream. Our differentiation experiments,

which show the earliest and most dramatic dissociation of AF9, ENL, and Cyclin

T2, lend support to this idea (Fig. 3.15). However, the order of downstream

events that are critical to *Hox* activation and the different EAP subunits involved

are unclear and require more experimentation.

Chapter 4

Concluding Remarks

MLL fusion proteins are multi-potent proteins that form a sophisticated transcriptional network,which leads to leukemia. Although there are many other aspects to the mechanism of MLL fusion protein-mediated leukemogenesis, several lines of evidence show that the fusion partner and its associating factors are critical. The work presented in this dissertation show the following:

- The transforming domain of AF9 associates with other MLL fusion partners and enzymes associated with transcriptional elongation, including the CTD kinase pTEFb, and the HMT Dot1L, and this complex has been named Elongation Assisting Proteins (EAP).

- EAP dissociates from target loci early in response to differentiation cues.

- EAP remains bound at loci in the presence of MLL fusion proteins in spite of cues to differentiation.

EAP components have also been identified in association with other MLL fusion partners, including AF4 and ENL, in independent studies [100,101,105,119]. A fascinating finding is that many of the nuclear fusion partners associate with each other, suggesting that they share a common mechanism of transformation. Even the cytoplasmic partners have been shown to recruit some of the same machinery as the nuclear partners albeit through an alternative mechanism [100]. This may greatly simplify therapeutic strategies of targeting MLL fusion protein

associated leukemias, which are heterogeneous due to the variety of possible fusion partners.

The most effective therapeutic targets will be the proteins or associations that present the least amount of harm to normal cells. Unfortunately, MLL fusion proteins exploit transcription factors that are needed for the transcription of most genes. Thus, from the data presented to date, targeting aberrant protein-protein interactions in the MLL fusion protein-associated complexes, such as those with Dot1L and pTEFb, show the most promise. Another interesting approach would be to exploit the dual nature of EAP, which appears to be a bi-functional complex that contains transcriptional activators and repressors. Identifying signaling pathways that control its transcriptional mode may reveal therapeutic targets as well.

References

1. (2009) Leukemia, Lymphoma, Myeloma Facts 2009-2010.

2. Chowdhury T, Brady HJ (2008) Insights from clinical studies into the role of the MLL gene in infant and childhood leukemia. Blood Cells Mol Dis 40: 192-199.

3. Jenuwein T, Allis CD (2001) Translating the histone code. Science 293: 1074-1080.

4. Wang GG, Allis CD, Chi P (2007) Chromatin remodeling and cancer, Part II: ATP-dependent chromatin remodeling. Trends Mol Med 13: 373-380.

5. Wang GG, Allis CD, Chi P (2007) Chromatin remodeling and cancer, Part I: Covalent histone modifications. Trends Mol Med 13: 363-372.

6. Villeneuve LM, Natarajan R (2010) The role of epigenetics in the pathology of diabetic complications. Am J Physiol Renal Physiol 299: F14-25.

7. Urdinguio RG, Sanchez-Mut JV, Esteller M (2009) Epigenetic mechanisms in neurological diseases: genes, syndromes, and therapies. Lancet Neurol 8: 1056-1072.

8. Barnes PJ (2009) Targeting the epigenome in the treatment of asthma and chronic obstructive pulmonary disease. Proc Am Thorac Soc 6: 693-696.

9. Gluckman PD, Hanson MA, Buklijas T, Low FM, Beedle AS (2009) Epigenetic mechanisms that underpin metabolic and cardiovascular diseases. Nat Rev Endocrinol 5: 401-408.

10. Turunen MP, Aavik E, Yla-Herttuala S (2009) Epigenetics and atherosclerosis. Biochim Biophys Acta 1790: 886-891.

11. Chi P, Allis CD, Wang GG (2010) Covalent histone modifications--miswritten, misinterpreted and mis-erased in human cancers. Nat Rev Cancer 10: 457-469.

12. Birke M, Schreiner S, Garcia-Cuellar MP, Mahr K, Titgemeyer F, et al. (2002) The MT domain of the proto-oncoprotein MLL binds to CpG-containing DNA and discriminates against methylation. Nucleic Acids Res 30: 958-965.

13. Erfurth FE, Popovic R, Grembecka J, Cierpicki T, Theisler C, et al. (2008) MLL protects CpG clusters from methylation within the Hoxa9 gene, maintaining transcript expression. Proc Natl Acad Sci U S A 105: 7517-7522.

14. Xia ZB, Anderson M, Diaz MO, Zeleznik-Le NJ (2003) MLL repression domain interacts with histone deacetylases, the polycomb group proteins HPC2 and BMI-1, and the corepressor C-terminal-binding protein. Proc Natl Acad Sci U S A 100: 8342-8347.

15. Chang PY, Hom RA, Musselman CA, Zhu L, Kuo A, et al. (2010) Binding of the MLL PHD3 finger to histone H3K4me3 is required for MLL-dependent gene transcription. J Mol Biol 400: 137-144.

16. Fair K, Anderson M, Bulanova E, Mi H, Tropschug M, et al. (2001) Protein interactions of the MLL PHD fingers modulate MLL target gene regulation in human cells. Mol Cell Biol 21: 3589-3597.

17. Mi H, Kops O, Zimmermann E, Jaschke A, Tropschug M (1996) A nuclear RNA-binding cyclophilin in human T cells. FEBS Lett 398: 201-205.

18. Ernst P, Wang J, Huang M, Goodman RH, Korsmeyer SJ (2001) MLL and CREB bind cooperatively to the nuclear coactivator CREB-binding protein. Mol Cell Biol 21: 2249-2258.

19. Dou Y, Milne TA, Tackett AJ, Smith ER, Fukuda A, et al. (2005) Physical association and coordinate function of the H3 K4 methyltransferase MLL1 and the H4 K16 acetyltransferase MOF. Cell 121: 873-885.

20. Milne TA, Briggs SD, Brock HW, Martin ME, Gibbs D, et al. (2002) MLL targets SET domain methyltransferase activity to Hox gene promoters. Mol Cell 10: 1107-1117.

21. Rozenblatt-Rosen O, Rozovskaia T, Burakov D, Sedkov Y, Tillib S, et al. (1998) The C-terminal SET domains of ALL-1 and TRITHORAX interact with the INI1 and SNR1 proteins, components of the SWI/SNF complex. Proc Natl Acad Sci U S A 95: 4152-4157.

22. Stojanova A, Penn LZ (2009) The role of INI1/hSNF5 in gene regulation and cancer. Biochem Cell Biol 87: 163-177.

23. Chen J, Santillan DA, Koonce M, Wei W, Luo R, et al. (2008) Loss of MLL PHD finger 3 is necessary for MLL-ENL-induced hematopoietic stem cell immortalization. Cancer Res 68: 6199-6207.

24. Park S, Osmers U, Raman G, Schwantes RH, Diaz MO, et al. (2010) The PHD3 Domain of MLL Acts as a CYP33-Regulated Switch between MLL-Mediated Activation and Repression. Biochemistry 49: 6576-6586.

25. Wang Z, Song J, Milne TA, Wang GG, Li H, et al. (2010) Pro isomerization in MLL1 PHD3-bromo cassette connects H3K4me readout to CyP33 and HDAC-mediated repression. Cell 141: 1183-1194.

26. Zeleznik-Le NJ, Harden AM, Rowley JD (1994) 11q23 translocations split the "AT-hook" cruciform DNA-binding region and the transcriptional repression domain from the activation domain of the mixed-lineage leukemia (MLL) gene. Proc Natl Acad Sci U S A 91: 10610-10614.

27. Ernst P, Mabon M, Davidson AJ, Zon LI, Korsmeyer SJ (2004) An Mll-dependent Hox program drives hematopoietic progenitor expansion. Curr Biol 14: 2063-2069.

28. Yu BD, Hess JL, Horning SE, Brown GA, Korsmeyer SJ (1995) Altered Hox expression and segmental identity in Mll-mutant mice. Nature 378: 505-508.

29. Argiropoulos B, Humphries RK (2007) Hox genes in hematopoiesis and leukemogenesis. Oncogene 26: 6766-6776.

30. Mann RS, Lelli KM, Joshi R (2009) Hox specificity unique roles for cofactors and collaborators. Curr Top Dev Biol 88: 63-101.

31. Falaschi A, Abdurashidova G, Biamonti G (2010) DNA replication, development and cancer: a homeotic connection? Crit Rev Biochem Mol Biol 45: 14-22.

32. Golub TR, Slonim DK, Tamayo P, Huard C, Gaasenbeek M, et al. (1999) Molecular classification of cancer: class discovery and class prediction by gene expression monitoring. Science 286: 531-537.

33. Drabkin HA, Parsy C, Ferguson K, Guilhot F, Lacotte L, et al. (2002) Quantitative HOX expression in chromosomally defined subsets of acute myelogenous leukemia. Leukemia 16: 186-195.

34. Sitwala KV, Dandekar MN, Hess JL (2008) HOX Proteins and Leukemia. Int J Clin Exp Pathol 1: 461-474.

35. Yekta S, Tabin CJ, Bartel DP (2008) MicroRNAs in the Hox network: an apparent link to posterior prevalence. Nat Rev Genet 9: 789-796.

36. Zhang Y, Morrone G, Zhang J, Chen X, Lu X, et al. (2003) CUL-4A stimulates ubiquitylation and degradation of the HOXA9 homeodomain protein. EMBO J 22: 6057-6067.

37. Wang N, Kim HG, Cotta CV, Wan M, Tang Y, et al. (2006) TGFbeta/BMP inhibits the bone marrow transformation capability of Hoxa9 by repressing its DNA-binding ability. EMBO J 25: 1469-1480.

38. Vijapurkar U, Fischbach N, Shen W, Brandts C, Stokoe D, et al. (2004) Protein kinase C-mediated phosphorylation of the leukemia-associated HOXA9 protein impairs its DNA binding ability and induces myeloid differentiation. Mol Cell Biol 24: 3827-3837.

39. Kroon E, Krosl J, Thorsteinsdottir U, Baban S, Buchberg AM, et al. (1998) Hoxa9 transforms primary bone marrow cells through specific collaboration with Meis1a but not Pbx1b. EMBO J 17: 3714-3725.

40. Faber J, Krivtsov AV, Stubbs MC, Wright R, Davis TN, et al. (2009) HOXA9 is required for survival in human MLL-rearranged acute leukemias. Blood 113: 2375-2385.

41. Ferrell CM, Dorsam ST, Ohta H, Humphries RK, Derynck MK, et al. (2005) Activation of stem-cell specific genes by HOXA9 and HOXA10 homeodomain proteins in CD34+ human cord blood cells. Stem Cells 23: 644-655.

42. Terranova R, Agherbi H, Boned A, Meresse S, Djabali M (2006) Histone and DNA methylation defects at Hox genes in mice expressing a SET domain-truncated form of Mll. Proc Natl Acad Sci U S A 103: 6629-6634.

43. Mitterbauer-Hohendanner G, Mannhalter C (2004) The biological and clinical significance of MLL abnormalities in haematological malignancies. Eur J Clin Invest 34 Suppl 2: 12-24.

44. Corral J, Lavenir I, Impey H, Warren AJ, Forster A, et al. (1996) An Mll-AF9 fusion gene made by homologous recombination causes acute leukemia in chimeric mice: a method to create fusion oncogenes. Cell 85: 853-861.

45. Chen W, Li Q, Hudson WA, Kumar A, Kirchhof N, et al. (2006) A murine Mll-AF4 knock-in model results in lymphoid and myeloid deregulation and hematologic malignancy. Blood 108: 669-677.

46. Forster A, Pannell R, Drynan LF, McCormack M, Collins EC, et al. (2003) Engineering de novo reciprocal chromosomal translocations associated with Mll to replicate primary events of human cancer. Cancer Cell 3: 449-458.

47. Zeisig BB, Milne T, Garcia-Cuellar MP, Schreiner S, Martin ME, et al. (2004) Hoxa9 and Meis1 are key targets for MLL-ENL-mediated cellular immortalization. Mol Cell Biol 24: 617-628.

48. Krivtsov AV, Twomey D, Feng Z, Stubbs MC, Wang Y, et al. (2006) Transformation from committed progenitor to leukaemia stem cell initiated by MLL-AF9. Nature 442: 818-822.

49. Hess JL, Bittner CB, Zeisig DT, Bach C, Fuchs U, et al. (2006) c-Myb is an essential downstream target for homeobox-mediated transformation of hematopoietic cells. Blood 108: 297-304.

50. Krivtsov AV, Feng Z, Lemieux ME, Faber J, Vempati S, et al. (2008) H3K79 methylation profiles define murine and human MLL-AF4 leukemias. Cancer Cell 14: 355-368.

51. Armstrong SA, Staunton JE, Silverman LB, Pieters R, den Boer ML, et al. (2002) MLL translocations specify a distinct gene expression profile that distinguishes a unique leukemia. Nat Genet 30: 41-47.

52. Ayton PM, Cleary ML (2003) Transformation of myeloid progenitors by MLL oncoproteins is dependent on Hoxa7 and Hoxa9. Genes Dev 17: 2298-2307.

53. Yokoyama A, Somervaille TC, Smith KS, Rozenblatt-Rosen O, Meyerson M, et al. (2005) The menin tumor suppressor protein is an essential oncogenic cofactor for MLL-associated leukemogenesis. Cell 123: 207-218.

54. Yokoyama A, Cleary ML (2008) Menin critically links MLL proteins with LEDGF on cancer-associated target genes. Cancer Cell 14: 36-46.

55. Muntean AG, Tan J, Sitwala K, Huang Y, Bronstein J, et al. (2010) The PAF complex synergizes with MLL fusion proteins at HOX loci to promote leukemogenesis. Cancer Cell 17: 609-621.

56. Caslini C, Yang Z, El-Osta M, Milne TA, Slany RK, et al. (2007) Interaction of MLL amino terminal sequences with menin is required for transformation. Cancer Res 67: 7275-7283.

57. Thiel AT, Blessington P, Zou T, Feather D, Wu X, et al. (2010) MLL-AF9-induced leukemogenesis requires coexpression of the wild-type Mll allele. Cancer Cell 17: 148-159.

58. Wu X, Hua X (2008) Menin, histone h3 methyltransferases, and regulation of cell proliferation: current knowledge and perspective. Curr Mol Med 8: 805-815.

59. Chaudhary K, Deb S, Moniaux N, Ponnusamy MP, Batra SK (2007) Human RNA polymerase II-associated factor complex: dysregulation in cancer. Oncogene 26: 7499-7507.

60. Krogan NJ, Dover J, Wood A, Schneider J, Heidt J, et al. (2003) The Paf1 complex is required for histone H3 methylation by COMPASS and Dot1p: linking transcriptional elongation to histone methylation. Mol Cell 11: 721-729.

61. Pavri R, Zhu B, Li G, Trojer P, Mandal S, et al. (2006) Histone H2B monoubiquitination functions cooperatively with FACT to regulate elongation by RNA polymerase II. Cell 125: 703-717.

62. Zhu B, Zheng Y, Pham AD, Mandal SS, Erdjument-Bromage H, et al. (2005) Monoubiquitination of human histone H2B: the factors involved and their roles in HOX gene regulation. Mol Cell 20: 601-611.

63. So CW, Lin M, Ayton PM, Chen EH, Cleary ML (2003) Dimerization contributes to oncogenic activation of MLL chimeras in acute leukemias. Cancer Cell 4: 99-110.

64. Martin ME, Milne TA, Bloyer S, Galoian K, Shen W, et al. (2003) Dimerization of MLL fusion proteins immortalizes hematopoietic cells. Cancer Cell 4: 197-207.

65. Dobson CL, Warren AJ, Pannell R, Forster A, Rabbitts TH (2000) Tumorigenesis in mice with a fusion of the leukaemia oncogene Mll and the bacterial lacZ gene. EMBO J 19: 843-851.

66. Slany RK, Lavau C, Cleary ML (1998) The oncogenic capacity of HRX-ENL requires the transcriptional transactivation activity of ENL and the DNA binding motifs of HRX. Mol Cell Biol 18: 122-129.

67. Prasad R, Yano T, Sorio C, Nakamura T, Rallapalli R, et al. (1995) Domains with transcriptional regulatory activity within the ALL1 and AF4 proteins involved in acute leukemia. Proc Natl Acad Sci U S A 92: 12160-12164.

68. Meyer C, Schneider B, Jakob S, Strehl S, Attarbaschi A, et al. (2006) The MLL recombinome of acute leukemias. Leukemia 20: 777-784.

69. Milne TA, Martin ME, Brock HW, Slany RK, Hess JL (2005) Leukemogenic MLL fusion proteins bind across a broad region of the Hox a9 locus,

promoting transcription and multiple histone modifications. Cancer Res 65: 11367-11374.

70. Schmittgen TD, Livak KJ (2008) Analyzing real-time PCR data by the comparative C(T) method. Nat Protoc 3: 1101-1108.

71. Milne TA, Zhao K, Hess JL (2009) Chromatin immunoprecipitation (ChIP) for analysis of histone modifications and chromatin-associated proteins. Methods Mol Biol 538: 409-423.

72. Ernst P, Fisher JK, Avery W, Wade S, Foy D, et al. (2004) Definitive hematopoiesis requires the mixed-lineage leukemia gene. Dev Cell 6: 437-443.

73. Milne TA, Kim J, Wang GG, Stadler SC, Basrur V, et al. (2010) Multiple interactions recruit MLL1 and MLL1 fusion proteins to the HOXA9 locus in leukemogenesis. Mol Cell 38: 853-863.

74. Liu H, Cheng EH, Hsieh JJ (2007) Bimodal degradation of MLL by SCFSkp2 and APCCdc20 assures cell cycle execution: a critical regulatory circuit lost in leukemogenic MLL fusions. Genes Dev 21: 2385-2398.

75. Hsieh JJ, Ernst P, Erdjument-Bromage H, Tempst P, Korsmeyer SJ (2003) Proteolytic cleavage of MLL generates a complex of N- and C-terminal fragments that confers protein stability and subnuclear localization. Mol Cell Biol 23: 186-194.

76. Tanabe S, Zeleznik-Le NJ, Kobayashi H, Vignon C, Espinosa R, 3rd, et al. (1996) Analysis of the t(6;11)(q27;q23) in leukemia shows a consistent

breakpoint in AF6 in three patients and in the ML-2 cell line. Genes

Chromosomes Cancer 15: 206-216.

77. Zeisig DT, Bittner CB, Zeisig BB, Garcia-Cuellar MP, Hess JL, et al. (2005)

The eleven-nineteen-leukemia protein ENL connects nuclear MLL fusion

partners with chromatin. Oncogene 24: 5525-5532.

78. Hemenway CS, de Erkenez AC, Gould GC (2001) The polycomb protein

MPc3 interacts with AF9, an MLL fusion partner in t(9;11)(p22;q23) acute

leukemias. Oncogene 20: 3798-3805.

79. Garcia-Cuellar MP, Zilles O, Schreiner SA, Birke M, Winkler TH, et al. (2001)

The ENL moiety of the childhood leukemia-associated MLL-ENL

oncoprotein recruits human Polycomb 3. Oncogene 20: 411-419.

80. Ayton PM, Cleary ML (2001) Molecular mechanisms of leukemogenesis

mediated by MLL fusion proteins. Oncogene 20: 5695-5707.

81. Erfurth F, Hemenway CS, de Erkenez AC, Domer PH (2004) MLL fusion

partners AF4 and AF9 interact at subnuclear foci. Leukemia 18: 92-102.

82. Rubnitz JE, Morrissey J, Savage PA, Cleary ML (1994) ENL, the gene fused

with HRX in t(11;19) leukemias, encodes a nuclear protein with

transcriptional activation potential in lymphoid and myeloid cells. Blood 84:

1747-1752.

83. Morita S, Kojima T, Kitamura T (2000) Plat-E: an efficient and stable system

for transient packaging of retroviruses. Gene Ther 7: 1063-1066.

84. Keller A, Nesvizhskii AI, Kolker E, Aebersold R (2002) Empirical statistical model to estimate the accuracy of peptide identifications made by MS/MS and database search. Anal Chem 74: 5383-5392.

85. Nesvizhskii AI, Keller A, Kolker E, Aebersold R (2003) A statistical model for identifying proteins by tandem mass spectrometry. Anal Chem 75: 4646-4658.

86. Medlin J, Scurry A, Taylor A, Zhang F, Peterlin BM, et al. (2005) P-TEFb is not an essential elongation factor for the intronless human U2 snRNA and histone H2b genes. EMBO J 24: 4154-4165.

87. Gamble MJ, Erdjument-Bromage H, Tempst P, Freedman LP, Fisher RP (2005) The histone chaperone TAF-I/SET/INHAT is required for transcription in vitro of chromatin templates. Mol Cell Biol 25: 797-807.

88. Karetsou Z, Martic G, Sflomos G, Papamarcaki T (2005) The histone chaperone SET/TAF-Ibeta interacts functionally with the CREB-binding protein. Biochem Biophys Res Commun 335: 322-327.

89. Van Vlierberghe P, van Grotel M, Tchinda J, Lee C, Beverloo HB, et al. (2008) The recurrent SET-NUP214 fusion as a new HOXA activation mechanism in pediatric T-cell acute lymphoblastic leukemia. Blood 111: 4668-4680.

90. Seki Y, Kurisaki A, Watanabe-Susaki K, Nakajima Y, Nakanishi M, et al. (2010) TIF1beta regulates the pluripotency of embryonic stem cells in a phosphorylation-dependent manner. Proc Natl Acad Sci U S A 107: 10926-10931.

91. Ho L, Crabtree GR (2010) Chromatin remodelling during development. Nature 463: 474-484.

92. Verreault A, Kaufman PD, Kobayashi R, Stillman B (1998) Nucleosomal DNA regulates the core-histone-binding subunit of the human Hat1 acetyltransferase. Curr Biol 8: 96-108.

93. Friedman JR, Fredericks WJ, Jensen DE, Speicher DW, Huang XP, et al. (1996) KAP-1, a novel corepressor for the highly conserved KRAB repression domain. Genes Dev 10: 2067-2078.

94. Kutney SN, Hong R, Macfarlan T, Chakravarti D (2004) A signaling role of histone-binding proteins and INHAT subunits pp32 and Set/TAF-Ibeta in integrating chromatin hypoacetylation and transcriptional repression. J Biol Chem 279: 30850-30855.

95. Kato JY, Yoneda-Kato N (2009) Mammalian COP9 signalosome. Genes Cells 14: 1209-1225.

96. Steger DJ, Lefterova MI, Ying L, Stonestrom AJ, Schupp M, et al. (2008) DOT1L/KMT4 recruitment and H3K79 methylation are ubiquitously coupled with gene transcription in mammalian cells. Mol Cell Biol 28: 2825-2839.

97. Bres V, Yoh SM, Jones KA (2008) The multi-tasking P-TEFb complex. Curr Opin Cell Biol 20: 334-340.

98. Okada Y, Feng Q, Lin Y, Jiang Q, Li Y, et al. (2005) hDOT1L links histone methylation to leukemogenesis. Cell 121: 167-178.

99. Mueller D, Garcia-Cuellar MP, Bach C, Buhl S, Maethner E, et al. (2009) Misguided transcriptional elongation causes mixed lineage leukemia. PLoS Biol 7: e1000249.

100. Yokoyama A, Lin M, Naresh A, Kitabayashi I, Cleary ML (2010) A higher-order complex containing AF4 and ENL family proteins with P-TEFb facilitates oncogenic and physiologic MLL-dependent transcription. Cancer Cell 17: 198-212.

101. Mohan M, Herz HM, Takahashi YH, Lin C, Lai KC, et al. (2010) Linking H3K79 trimethylation to Wnt signaling through a novel Dot1-containing complex (DotCom). Genes Dev 24: 574-589.

102. Guenther MG, Lawton LN, Rozovskaia T, Frampton GM, Levine SS, et al. (2008) Aberrant chromatin at genes encoding stem cell regulators in human mixed-lineage leukemia. Genes Dev 22: 3403-3408.

103. Zhou Q, Yik JH (2006) The Yin and Yang of P-TEFb regulation: implications for human immunodeficiency virus gene expression and global control of cell growth and differentiation. Microbiol Mol Biol Rev 70: 646-659.

104. Yamada T, Yamaguchi Y, Inukai N, Okamoto S, Mura T, et al. (2006) P-TEFb-mediated phosphorylation of hSpt5 C-terminal repeats is critical for processive transcription elongation. Mol Cell 21: 227-237.

105. Mueller D, Bach C, Zeisig D, Garcia-Cuellar MP, Monroe S, et al. (2007) A role for the MLL fusion partner ENL in transcriptional elongation and chromatin modification. Blood 110: 4445-4454.

106. Chao SH, Fujinaga K, Marion JE, Taube R, Sausville EA, et al. (2000) Flavopiridol inhibits P-TEFb and blocks HIV-1 replication. J Biol Chem 275: 28345-28348.

107. Lam LT, Pickeral OK, Peng AC, Rosenwald A, Hurt EM, et al. (2001) Genomic-scale measurement of mRNA turnover and the mechanisms of action of the anti-cancer drug flavopiridol. Genome Biol 2: RESEARCH0041.

108. Lu X, Burgan WE, Cerra MA, Chuang EY, Tsai MH, et al. (2004) Transcriptional signature of flavopiridol-induced tumor cell death. Mol Cancer Ther 3: 861-872.

109. Fathi AT, Grant S, Karp JE (2010) Exploiting cellular pathways to develop new treatment strategies for AML. Cancer Treat Rev 36: 142-150.

110. Karp JE, Ross DD, Yang W, Tidwell ML, Wei Y, et al. (2003) Timed sequential therapy of acute leukemia with flavopiridol: in vitro model for a phase I clinical trial. Clin Cancer Res 9: 307-315.

111. Blum W, Phelps MA, Klisovic RB, Rozewski DM, Ni W, et al. (2010) Phase I clinical and pharmacokinetic study of a novel schedule of flavopiridol in relapsed or refractory acute leukemias. Haematologica 95: 1098-1105.

112. Feng Q, Wang H, Ng HH, Erdjument-Bromage H, Tempst P, et al. (2002) Methylation of H3-lysine 79 is mediated by a new family of HMTases without a SET domain. Curr Biol 12: 1052-1058.

113. Jones B, Su H, Bhat A, Lei H, Bajko J, et al. (2008) The histone H3K79 methyltransferase Dot1L is essential for mammalian development and heterochromatin structure. PLoS Genet 4: e1000190.

114. Chiu CP, Lee F (1989) IL-6 is a differentiation factor for M1 and WEHI-3B myeloid leukemic cells. J Immunol 142: 1909-1915.

115. Collins EC, Appert A, Ariza-McNaughton L, Pannell R, Yamada Y, et al. (2002) Mouse Af9 is a controller of embryo patterning, like Mll, whose human homologue fuses with Af9 after chromosomal translocation in leukemia. Mol Cell Biol 22: 7313-7324.

116. Ichikawa Y (1969) Differentiation of a cell line of myeloid leukemia. J Cell Physiol 74: 223-234.

117. Copeland NG, Jenkins NA (1999) Myeloid leukemia: disease genes and mouse models. Prog Exp Tumor Res 35: 53-63.

118. Kurata S, Matsumoto M, Tsuji Y, Nakajima H (1996) Lipopolysaccharide activates transcription of the heme oxygenase gene in mouse M1 cells through oxidative activation of nuclear factor kappa B. Eur J Biochem 239: 566-571.

119. Bitoun E, Oliver PL, Davies KE (2007) The mixed-lineage leukemia fusion partner AF4 stimulates RNA polymerase II transcriptional elongation and mediates coordinated chromatin remodeling. Hum Mol Genet 16: 92-106.

120. Estable MC, Naghavi MH, Kato H, Xiao H, Qin J, et al. (2002) MCEF, the newest member of the AF4 family of transcription factors involved in

leukemia, is a positive transcription elongation factor-b-associated protein. J Biomed Sci 9: 234-245.

121. Zeitlinger J, Stark A, Kellis M, Hong JW, Nechaev S, et al. (2007) RNA polymerase stalling at developmental control genes in the Drosophila melanogaster embryo. Nat Genet 39: 1512-1516.

122. Margaritis T, Holstege FC (2008) Poised RNA polymerase II gives pause for thought. Cell 133: 581-584.

123. Chopra VS, Hong JW, Levine M (2009) Regulation of Hox gene activity by transcriptional elongation in Drosophila. Curr Biol 19: 688-693.

124. Romano G, Giordano A (2008) Role of the cyclin-dependent kinase 9-related pathway in mammalian gene expression and human diseases. Cell Cycle 7: 3664-3668.

125. Wysocka J, Swigut T, Xiao H, Milne TA, Kwon SY, et al. (2006) A PHD finger of NURF couples histone H3 lysine 4 trimethylation with chromatin remodelling. Nature 442: 86-90.

126. Wittwer F, van der Straten A, Keleman K, Dickson BJ, Hafen E (2001) Lilliputian: an AF4/FMR2-related protein that controls cell identity and cell growth. Development 128: 791-800.

127. Wang Y, Krivtsov AV, Sinha AU, North TE, Goessling W, et al. (2010) The Wnt/beta-catenin pathway is required for the development of leukemia stem cells in AML. Science 327: 1650-1653.

128. Takeda DY, Wohlschlegel JA, Dutta A (2001) A bipartite substrate recognition motif for cyclin-dependent kinases. J Biol Chem 276: 1993-1997.

129. Ubersax JA, Woodbury EL, Quang PN, Paraz M, Blethrow JD, et al. (2003) Targets of the cyclin-dependent kinase Cdk1. Nature 425: 859-864.

130. Minami M, Inoue M, Wei S, Takeda K, Matsumoto M, et al. (1996) STAT3 activation is a critical step in gp130-mediated terminal differentiation and growth arrest of a myeloid cell line. Proc Natl Acad Sci U S A 93: 3963-3966.

131. Srinivasan RS, de Erkenez AC, Hemenway CS (2003) The mixed lineage leukemia fusion partner AF9 binds specific isoforms of the BCL-6 corepressor. Oncogene 22: 3395-3406.

132. Fujimura Y, Isono K, Vidal M, Endoh M, Kajita H, et al. (2006) Distinct roles of Polycomb group gene products in transcriptionally repressed and active domains of Hoxb8. Development 133: 2371-2381.

133. d Graaff W, Tomotsune D, Oosterveen T, Takihara Y, Koseki H, et al. (2003) Randomly inserted and targeted Hox/reporter fusions transcriptionally silenced in Polycomb mutants. Proc Natl Acad Sci U S A 100: 13362-13367.

134. Gurumurthy M, Tan CH, Ng R, Zeiger L, Lau J, et al. (2008) Nucleophosmin interacts with HEXIM1 and regulates RNA polymerase II transcription. J Mol Biol 378: 302-317.

135. Frehlick LJ, Eirin-Lopez JM, Ausio J (2007) New insights into the nucleophosmin/nucleoplasmin family of nuclear chaperones. Bioessays 29: 49-59.

136. Koeffler HP (1983) Induction of differentiation of human acute myelogenous leukemia cells: therapeutic implications. Blood 62: 709-721.

137. Mullighan CG, Kennedy A, Zhou X, Radtke I, Phillips LA, et al. (2007) Pediatric acute myeloid leukemia with NPM1 mutations is characterized by a gene expression profile with dysregulated HOX gene expression distinct from MLL-rearranged leukemias. Leukemia 21: 2000-2009.

138. Falini B, Mecucci C, Tiacci E, Alcalay M, Rosati R, et al. (2005) Cytoplasmic nucleophosmin in acute myelogenous leukemia with a normal karyotype. N Engl J Med 352: 254-266.

139. Falini B, Nicoletti I, Martelli MF, Mecucci C (2007) Acute myeloid leukemia carrying cytoplasmic/mutated nucleophosmin (NPMc+ AML): biologic and clinical features. Blood 109: 874-885.